ADSORPTION AND REACTION KINETICS OF THIOPHENE IN n-PENTANE IN A BATCH RECIRCULATED CATALYTIC REACTOR

by

E. RUSSELL LAMBERT, III

A thesis submitted to the Faculty and Board of Trustees of the Colorado School of Mines in partial fulfillment of the requirements for the degree of Doctor of Philosophy (Chemical and Petroleum Refining Engineering).

Signed: E. Russell Lambert, III
E. Russell Lambert, III

Golden, Colorado
Date: March 31, 1978

Approved:
Thesis Advisor and
Head of Department

Golden, Colorado
Date: APRIL 10, 1978

DEDICATION

To all my girls: Betsy, Lindsey, and Katherine.

ABSTRACT

A batch reactor technique is used to examine the kinetics of thiophene hydrogenolysis under conditions of high n-pentane and hydrogen sulfide concentration. Hydrogen sulfide exhibits an enhancement effect at low concentrations, and an inhibiting effect at high concentrations.

ACKNOWLEDGMENTS

The batch recirculated reactor used in this study was constructed entirely of equipment donated to or already on hand at Colorado School of Mines, and was built for a total equipment expenditure of less than two hundred dollars. The mass spectrometer was donated to the department by Marathon Oil Company. The diaphragm pump, tubular reactor, furnace and controller, other instrumentation, reactants, tubing and fittings were on hand or were obtained through the Chemical and Petroleum Refining Engineering Department with the help of Dr. P.F. Dickson and of Dr. J.H. Gary.

The help and patience of fellow graduate student R.M. Baldwin and of a succession of thesis committee members, especially Mssrs. P.F. Dickson, W.R. Astle, V.F. Yesavage, D.W. Dickerhoof, J.O. Golden, and E. Shimoda, is gratefully acknowledged. The advice of Professor Astle in the areas of statistics and regression analysis was indispensible, as was the technical advice of Dr. Yesavage. The financial support of Colorado School of Mines and the CSM Foundation, through teaching and research assistantships, and of Gulf Oil Foundation through a fellowship, is greatly appreciated.

But for the guidance of F.C. Maseles of the University of Texas in my beginning years of acquaintance with mass spectrometry, and of Dr. Karl J. Sladek who first guided me in my work with chemical reactor equipment, this study might never have begun. Without the encouragement of J. L. Young, J. L. Price, and R. T. Eby of Monsanto, it would never have been completed. However, the majority of the credit for motivation, financing, and moral support goes to my wife, Betsy, and daughters, Lindsey and Katherine, to whom much more than this work is dedicated. The contributions of my parents, Eleanor and Russell Lambert, Jr., and of my parents-in-law, Ann and the late Charles A. Holaday, are immeasurable, and the presence of my Father-in-law is greatly missed.

CONTENTS

LIST OF TABLES

LIST OF ILLUSTRATIONS

INTRODUCTION AND LITERATURE SURVEY

Introduction

It is desirable to remove sulfur from oil to reduce both air pollution and catalyst poisoning during refining. Much of the more difficult-to-remove sulfur in crude oil, coal, and shale oils occurs in the form of thiophenic compounds (1, 2). Removal or reduction of the amount of this form of sulfur may be accomplished by hydrogen treating of the sulfur to more readily removable hydrogen sulfide, or by deposition as a poison in a "guard" reactor. Published studies of sulfur removal have concentrated mainly on hydrogen treating and on the effects of sulfur compounds on reforming catalysts. Much of the available desulfurization is concerned with cobalt-molybdate catalysts. Nickel-molybdate catalysts have not been studied in detail (1), and the role of hydrogen sulfide in catalyst activation, deactivation, and poisoning is not well understood.

The Catalyst

The most extensively-investigated hydrodesulfurization (HDS) catalyst is the cobalt-molybdate, or $CoO-MoO_3-Al_2O_3$, catalyst (5, 9, 13-17, 83-89). Typical catalysts of this type contain 8%

to 15% MoO_3 and 2% to 4% CoO supported on γ-Al_2O_3. Preparation method affects the activity of the catalyst: alumina impregnated with solutions of ammonium molybdate and a cobalt salt, then dried and calcined, is more active than precipitated cobalt molybdate on alumina. Catalysts prepared by pelletization of the compounds, or mechanical mixtures of CoO and MoO_3 are less active still (9, 10, 84). Several excellent discussions of physical and mechanical properties of HDS catalysts, and methods for their preparation, are available in the literature (83-85, 87, 88, 90).

Other catalysts for the hydrodesulfurization (hydrogenolysis) of thiophene reported in the literature include vanadium oxide (93), vanadium molybdate (23), molybdenum oxide/sulfide (22, 80, 94), cobalt oxide/sulfide (94); nickel sulfide (91), sulfided chromia (6, 11, 15, 18, 95), platinum (19-21), and tungsten sulfide (80), often supported on alumina. Catalytic HDS activity of γ-alumina impregnated with oxides of various metals decreases (104) in the order

$$Pt>Pd>Ru>Co>Ni>Fe.$$

For a MoO_3-γ-alumina catalyst impregnated with different metal oxides, activity decreased in the order

$$Ni>Co>Pd>Pt.$$

<u>The Reaction</u>

Thiophene, C_4H_4S, a ring-structured sulfur-containing compound, has been used in recent years in evaluating the ability of various

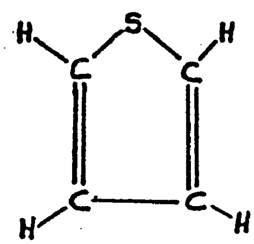

Figure 1

THIOPHENE

catalysts to desulfurize petroleum fractions (1, 2). Most investigators of the hydrogenolysis reaction have reached similar conclusions about the mechanism: that 1) two-point adsorption of thiophene takes place (84, 91, 93), that 2) conversion to a half-hydrogenated state takes place, that 3) rupture of C-S bonds is favored over rupture of C-C bonds, and that 4) conversion of the adsorbed molecule to butene or butane takes place (91). Compounds such as tetrahydrothiophene (91, 95) and mercaptans (3, 80) have not been identified as intermediates or reaction products, although there is some argument for their existence (80).

The order in which these steps take place is still in dispute, however. The above order, due to work in 1949 by Griffith, Marsh, and Newling (91), has been slightly changed by Owens and Amberg (95), who proposed that, following two-point adsorption, C-S bond cleavage occurs. Conversion to the half-hydrogenated step is represented by production of butadiene, which can be observed as a gas-phase product over sulfided chromia (93). Butadiene is rapidly hydrogenated, and is observed over molybdenum sulfide or cobalt molybdate (6) only at very low thiophene conversions. The rate-limiting step is considered (3) to be C-S bond cleavage.

Hydrogenation and hydrodesulfurization occur at two types of catalytic sites (95). Satterfield and Roberts (4) suggest that thiophene hydrogenolysis follows a sequence whereby butene hydrogenation occurs at different sites than does the desulfurization step. Mann (8) investigated fifteen combinations of supported and unsupported oxides and sulfides of cobalt and molybdenum, and found that the best activity was obtained at a 1:1 ratio of the two compounds. Differences were explained by two types of sites, one converting thiophene to butene and hydrogen sulfide, and the other converting butenes to butane. If cobalt and molybdenum compounds were mechanically, rather than chemically, mixed, lessened activity (9, 10) resulted. With a chromia catalyst, butenes appeared to be found only at the first reaction site, and H_2S was a less effective poison (11). Where two sites are thought to be present, both appear to be acid sites (3), and have been blocked in several studies by sodium (deposited as sodium carbonate) (3), pyridine (7, 89), or H_2S.

Although butadiene adsorption from the gas phase and hydrogenation is rapid, butenes produced as intermediates and desorbed (or butenes added to the mixture) appear not to undergo further hydrogenation over chromia (6, 102). Satterfield and Roberts, however, found otherwise, and fitted a kinetic equation to butene disappearance (4). Butene reaction appears to be a function of catalyst type and/or reaction conditions. Hydrogenation occurs predominately on the more strongly acidic sites, with hydrodesulfurization occurring on the weaker acidic sites (7). These sites may be less acidic due to the presence of the sulfur as sulfided catalyst or as H_2S.

A recent proposal by Kolboe (102), that hydrogen atoms required to produce H_2S are provided by rearrangement of thiophene to H_2S and diacetylene which then hydrogenates to butadiene has been tested by using deuterium in place of hydrogen during the hydrodesulfurization reaction (101). The amount of D_2S was low, indicating splitting out of H_2S from thiophene as the desulfurization step. (Some hydrogen/deuterium exchange in thiophene did take place, accounting for the small amount of D_2S produced late in the reaction.)

Reaction Rate

The hydrogenolysis of thiophene is approximately first-order in thiophene in an excess of hydrogen. Both rate and order decrease with an increasing concentration of sulfur compounds (16, 84). At high concentrations, rate becomes inversely proportional to concentration (84, 91). As early as 1933, the reaction was recognized to be retarded by reactant and products (94).

Hydrogen sulfide has been observed to retard hydrodesulfurization (HDS) rate in many studies (4-7, 91-95). Butene hydrogenation is hindered by H_2S, but butadiene hydrogenation and isomerization of butenes are not (11, 18, 95). The presence of H_2S appears to be necessary as a sulfiding agent in nickel-based catalysts (103) to increase desulfurization selectivity,even though it inhibits adsorption of thiophene and hydrocarbons (106). On cobalt-molybdate catalysts, the role of sulfiding is disputed. Though some references indicate that sulfiding is necessary (11, 13, 14, 105), Mann (107) activated catalyst by reduction with hydrogen. Lipsch (83) compared activation of a cobalt-molybdate catalyst with H_2S with activation with hydrogen, and could find no difference in activity.

Intermediate compounds are thought not to interfere with the HDS reaction (4, 95); butene adsorption is 10 to 15 times weaker than thiophene adsorption (95). A heat of adsorption of 11.6 to 8.3 kcal/gm mole was obtained on cobalt-molybdate catalyst (3,95,100) (on "clean" catalyst in adsorption apparatus or in pulsed-flow reactors). Van Looy and Limodo (96) report a value of 17 kcal/gm mole, and Roberts (4, 25) reports a value of 24 kcal/gm mole, both obtained under reaction conditions.

Reaction rate is first-order in hydrogen (18, 96). The reaction appears to occur with gas-phase, rather than chemisorbed, hydrogen (98).

The activation energy for the HDS reaction of thiophene is approximately 25 kcal/gm mole (6, 11, 95, 96); other studies report values from 21.6 to 26.5 kcal/gm mole (3, 6, 20, 98). As Roberts (4) states, the above values were probably obtained by an Arrhenius type of relationship for overall reaction rate (a plot of logarithm of thiophene conversion versus reciprocal temperature). This method is misapplied, as the resulting activation energy then includes effects of adsorption as well as reaction velocity, Roberts obtained a value of 3.7 kcal/gm mole, based on reaction rate constants obtained from a Langmuir-Hinshelwood type of rate model (discussed below). By a similar argument, his thiophene heat of adsorption value (and that of Van Looy and Limodo) disagrees with those values previously published.

Effect of Other Species

Compounds other than reactants and products also influence the hydrogenolysis of thiophene. Cyclopentadiene has a structure similar to thiophene, and retards reaction rate (91) by adsorbing, blocking reaction sites, and subsequently polymerizing. Steric effects are suspected of reducing the HDS rate of oils with sulfur compounds of various molecular weights. With increasing molecular weight, reaction rate decreases (92), leading to the conclusion that bulky hydrocarbon groups on the higher molecular weight compounds shield the sulfur atom attached to the surface from neighboring hydrogen atoms.

Blocking effects of hydrocarbons seem to be caused by steric inhibition rather than adsorption strength. Studies with thiophene in n-heptane/n-heptene (97), with thiophene in hexane/hexene (95), and with thiophene in cyclohexane/cyclohexene (18), indicate only a slight reduction in reaction rate when olefin content is increased to as much as 50% of the hydrocarbon mixture.

Other compounds, such as pyridine (7, 89, 108), carbon disulfide, and coal gas constituents (103) also retard the reaction. With the exception of pyridine, compounds other than H_2S have not been extensively studied.

Modeling the Reaction

Most studies of thiophene hydrogenolysis have involved varying flowrates of compounds through a reactor and noting the conversion obtained. Few investigators have attempted to mathematically model the reaction. Van Looy and Limodo (96), and later, Roberts (4, 25), modeled the reaction with equations of the Langmuir-Hinshelwood (also referred to as Hougen-Watson) type, to account for adsorption effects. More recently, Satterfield, Modell, and Mayer (108) used this type of equation to qualitatively explain competition between thiophene and pyridine for catalytic sites in simultaneous hydrodesulfurization/hydrodenitrification. Morooka and Hamrin (109) used Langmuir-Hinshelwood kinetics to model HDS over cobalt-molybdate catalyst as well as over coal mineral matter. (The coal mineral matter, while catalytic, was several orders of magnitude less so than the cobalt-molybdate.)

A Langmuir-Hinshelwood kinetic equation takes the general form: *

$$-r_T = kP_T^{n1}P_H^{n2}/(1+K_TP_T+K_SP_S)^{n3} \tag{1}$$

for thiophene hydrogenolysis, where k is an overall rate constant, P_i is the partial pressure of component i, K_i is the adsorption coefficient for component i, and n1, n2, and n3 are integer constants. The value of n3 corresponds to the number of adsorption sites participating in the reaction. Derivation of models of this type is discussed at length in a number of references, and was first summarized by Hougen and Watson (52). For given values of n1-n3, coefficients k, K_T, and K_S are estimated by either non-linear regression analysis or by linearizing equation 1) to the form:

$$(P_T^{n1}P_H^{n2}/(-r_T))^{1/n3} = 1/k^{1/n3}+(K_T/k^{1/n3})P_T+(K_S/k^{1/n3})P_S \tag{2}$$

Linearization has the drawback that the right side (independent)

* -see Nomenclature section beginning page 125.

variables are used to construct a response, which is then used to estimate the coefficients of the equation, rather than using the actual response, $-r_T$. This can sometimes lead to erroneous results (4, 41, 68, 110). Remedies available include careful statistical design of experiments, and the use of either weighted linear regression or non-linear regression.

Reactor Type

Flow reactors such as have been used in many laboratory studies have the drawback that they yield integral conversion data. Elimination of temperature and concentration gradients greatly simplifies analysis of the data. This may be accomplished by using a continuous stirred-tank reactor (CSTR), in which the composition and temperature are uniform throughout due to complete mixing (and intra-particle mass transfer limitations (24) are absent if proper reaction conditions are chosen). Another method, the differential reactor, contains a small enough reaction zone that only a small change in composition (approximately differential), and thus, only a small change in temperature, is produced. If the effluent from a differential reactor is recycled at a large rate compared with feed rate, operation approaches the CSTR manner (4, 25, 35). Care must be taken that the recirculation rate is sufficient to cause all reactions to be differential in nature (111).

If feed rate and produce rate are reduced to zero, the gradientless nature of both differential and CSTR reactor types is retained but the reactor operates in the unsteady state. The reactor, termed a batch-recirculated reactor or loop reactor, is well suited (26, 112) for assessing the properties of catalytic reactions. Data analysis is simplified, since the design equation for the batch reactor, derived from a material balance with the "in" and "out" terms equal to zero, is simply the accumulation term (kinetic expression describing the reaction).

Limitations

Batch operation does impose limitations, however. Elimination of temperature and concentration gradients in a batch catalytic reactor at other than relatively low temperatures or pressures requires not only a very small amount of catalyst, but also mixing enhanced by outside means in addition to the natural convective and diffusive processes. The highest mixing rates presently obtainable are provided by mechanical agitation in the "spinning basket", or Carberry, reactor (27) in which the catalyst is suspended in a rapidly rotating basket, and in reactors in which the catalyst is stationary and the bulk phase is mixed rapidly (28). The main drawbacks to these reactors are the expense of special fabrication (in the case of Berty et al (28)) and mechanical difficulties such as bearing and packing failure under elevated conditions of temperature and pressure (29). Batch reactors are also unsuitable when data analysis requires sampling methods which remove more than a small fraction of the total reactant/product mixture; a large-sized reactor of the above types may be prohibitively expensive. An alternative is to use a standard reaction vessel such as a tubular reactor and furnace, and to use an external pump for recirculation.

Reactor Design Considerations

Design of batch reaction equipment usually requires a compromise between large volume (to minimize effects of sample removal on the material balance) and capability of high recirculation rate (to insure minimal concentration differences in the bulk fluid phase). Smith (30) briefly describes a batch recycle reactor system used in the study of vapor-phase decomposition of acetone (a homogeneous reaction) in which he suggests that the validity of the assumption of uniform composition throughout the reactor depends on the degree of mixing in the reservoir containing the catalyst, the volume of the reservoir compared to that of the rest of the system (important only in homogeneous reaction systems), and the conversion per pass through the catalyst. Several studies have been conducted in recent years using externally-recirculated reactors. Butt et al (35) studied dehydration of ethanol and diethyl ether over alumina at 274^{o} to $314^{o}C$ and approximately one atmosphere pressure. Korback and Stewart (36) conducted benzene hydrogenation experiments over platinum-alumina catalyst at 500^{o} to $600^{o}F$ at pressures of up to 14 atmospheres. Both studies used commercially available external diaphragm pumps for recirculation. Diaphragm pumps avoid the necessity for rotating shafts with packing and bearing surfaces subjected to extremes of pressure, temperature, or chemical atmospheres.

Adsorption Measurements During Catalysis

Concurrent adsorption/reaction studies have been undertaken in recent years in stirred flow and batch reactors (113-117). Tamaru (115) reviews several studies which use the techniques of:

1) Gravimetric method -- measuring catalyst weight during reaction.

2) Volumetric method -- monitoring pressure, gas composition, and rate of introduction of reaction components.

3) Chromatographic method -- pulsed-flow reactor method as presented by Amberg et al (3, 6, 7, 11, 18, 95)..

4) Infra-red analysis -- monitoring spectra of surface species during the reaction.

These methods seek to either determine the type and concentration of surface species directly, or to measure surface concentrations by material balance relationships.

In an unpublished work by Siddiqui and Amberg, mentioned by Amberg in a separate paper (113), observation of the surface of a cobalt-molybdate catalyst was attempted via infra-red spectroscopy in a closed-loop reactor. Unfortunately, the observed spectra were too complex to be interpreted unambiguously. The reaction mixture was circulated by a magnetically-operated rotary vane pump, and could be operated as high as 275^{o}C. Whether or not this reactor was operated as a batch reactor was not mentioned.

Additional studies have concerned formic acid decomposition (continuous IR spectroscopy in a closed circulation system with occasional samples withdrawn for analysis) (116), benzene hydrogenation (continuous stirred-tank reactor with a microbalance incorporated to monitor catalyst weight) (114), and dehydration of ethanol (batch reactor with a microbalance) (117).

PURPOSE, EXPERIMENTAL DESIGN,
EQUIPMENT DESIGN OBJECTIVE

Purpose of Study

This study was undertaken to demonstrate the capability of a batch recirculated reactor to obtain useful kinetic and adsorption information, and to contribute information to the literature on the hydrogenolysis of thiophene over a nickel-molybdate catalyst outside the usual range of hydrogen sulfide and hydrocarbon concentrations. The reactor is designed to operate under conditions free of the masking effects of incomplete mixing and diffusion, at pressures and temperatures approaching those found in commercial refining operations.

Experimental Design

A typical approach to an experimental design is to carry out a replicated multi-level investigation of parameters considered to influence the process under study. The levels, or quantitative values, of each variable investigated are selected so as to emphasize effects of that variable (i.e., condition the resulting data). Previous studies of thiophene hydrogenolysis, cited above, identified temperature, flowrates, and concentrations of hydrogen, thiophene, hydrogen sulfide, and unsaturated hydrocarbons as being significant variables. An additional factor which may influence operation of a batch recirculated reactor is recirculation rate.

In this study, two temperatures (275^o and 256^oC) and two levels each of hydrogen sulfide starting concentration, starting thiophene-to-pentane (diluent) ratio, and circulation rate are used. Composition data are obtained as a function of time, and are used to determine kinetic parameters in Langmuir-Hinshelwood reaction rate models by linear regression analysis. The experimental design is a five-factor design, two-level in temperature, recirculation rate, and both H_2S and thiophene/pentane initial concentrations, and four- to six-level in time (varying from run to run).

In order for an experimental design to be a replicated factorial design, the experimenter must be able to set operating levels of the independent variables. In a flow reactor, flowrates, reactant concentrations, and temperature are controllable. However, in a batch reactor, only initial concentrations, temperature, mixing rate, and elapsed time between samples are controllable.

In order to obtain a desired combination of concentrations at a desired time, a knowledge of the stoichiometry and kinetics, and manipulation of initial concentrations is necessary. Since the stoichiometry and/or kinetics are usually under investigation, samples at desired concentration levels are difficult to obtain and replicate. This problem may be partially alleviated by providing means of adding or removing material selectively during reaction (such as reaction with iron packing as used in this study). Removal of material has the added advantage of reducing covariance between reactant and product compositions due to material balance relationships. A batch recirculated reactor has the advantage of obtaining kinetic information rapidly, compared with flow reactors. The ability to test the dependent variable directly for significance of the independent variables (and their interactions) is not sacrificed, so long as either the material balance relationship between reactants and products is modified, or only independent species are considered in the kinetic model.

Equipment Design Considerations

In addition to safety considerations, the reactor equipment was designed to yield kinetic data for reactions of 30 minute half-life or longer. This restriction insures negligible temperature and concentration gradients, due to adequate mixing, as well as allowing a sufficient number of data points to be obtained during an experimental run. (A 20-minute sequence of valve manipulation is required to reduce the sample pressure to the proper level with the present mass spectrometer inlet design.) All equipment exposed to the reaction atmosphere, except for the steel ball packing used in a portion of this study, is of teflon or 316 stainless steel to avoid corrosion, and the recirculation circuit is electrically heated to avoid reactant condensation.

EQUIPMENT AND INSTRUMENTATION

Description

The reaction and recirculation system was designed to obtain kinetic data for hydrogenolysis of two-percent sulfur-containing mixtures (thiophene in n-pentane) at pressures found in commercial hydrodesulfurization equipment, during experimental runs of approximately four hours. The relatively low reaction temperature of 275°C was chosen so that most of the apparatus could operate safely below the melting point of the teflon gaskets required by the tubular reactor.

The reaction apparatus with associated recirculation equipment is shown in Figure 2. Reactions occur on the surface of the catalyst within the tubular reactor heated by a Lindberg, Heviduty, 3000 watt, three-zone furnace and proportional controller. Temperature within the reactor is monitored by four type J, shielded thermocouples, two of which are positioned immediately above and below the catalyst. For all except the blank runs (when no catalyst was used), American Cyanamid, Aero HDS-3A, nickel-molybdate catalyst was present. Properties of the catalyst are listed in Appendix II. The catalyst was presulfided prior to the experimental study using procedures outlined by the manufacturer, in a hydrogen-hydrogen sulfide atmosphere. Air was excluded at all times after catalyst activation.

FIGURE 2

REACTION APPARATUS

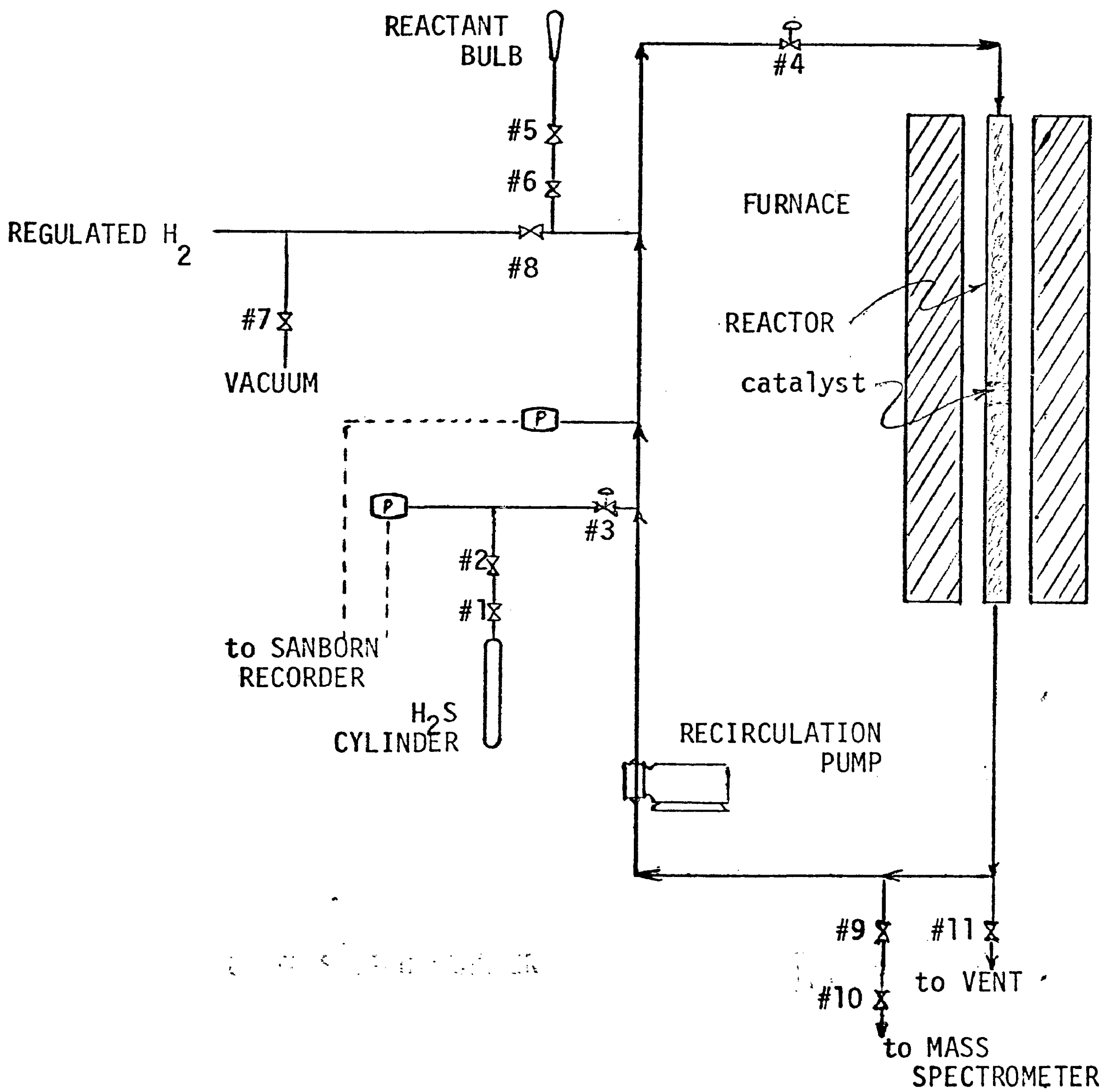

Reactants are circulated downward through the catalyst, which is supported by glass wool and held in place by either 1 mm diameter glass beads or 3/16-inch-diameter steel ball bearings which facilitate heat transfer and mixing. Circulation is provided by a Lapp Pulsafeeder, model LS-20, diaphragm pump, rated at 900 cm^3 per hour. Back pressure on the check valves built into the pump is provided by valve #4 (see Figure 2), and monitored by magnitude of the cyclic disturbance in pressure caused by the pump. All tubing (¼-inch-diameter 316 stainless steel) is electrically heated and monitored by an eight point Brown temperature recorder using type K thermocouples mounted on the outside surfaces of the tubing. The lowest temperature in the recirculation circuit during an experimental run is typically 175°F; temperatures in peripheral equipment such as the total pressure transducer are approximately 150°F. Pressure is monitored with a Wiancko Engineering Company transducer capable of operation to 1000 psig; read-out of the electrical signal is done on channel "D" of a four-channel Sanborn model 150 recorder. The recorder is modified to include a galvanometer in a parallel with the chart pen driver; read-out is accomplished by adjusting the zero suppression so as to null the galvanometer. Further details may be found in Appendix VI.

Reactor Startup

Before reactor operation, liquid and gaseous reactants must be added. A volumetric flask is evacuated, weighed, filled to a mark on its neck with liquid, and the valve on its stem (#5) is attached to valve #6 of the reactant inlet. Hydrogen sulfide is added by manipulating valves 1, 2, and 3 of the gas addition inlet and monitoring the pressure by means of a CED, Model 4-015, 0-500 psia pressure transducer connected to Sanborn recorder channel "B". Details of gas addition inlet operation may be found in Appendix VI. The H_2S and liquids are added to the reactor system, and hydrogen is introduced through valve #8 to the desired pressure. With valves 6 and 8 closed, the pump, heating tapes and furnace are started, and steady temperature and pressure conditions are reached in approximately 45 minutes.

Sampling Procedure

Samples of the reaction mixture are obtained by opening and closing valve #9, which traps a small quantity of vapor in the volume between valves 9 and 10. The mass spectrometer inlet system is maintained by a mechanical vacuum pump at an indicated pressure of below 50 microns. With the three-way valve closed (Figure 3), and all valves except Nos. 13 and 16 open, valve #10 is opened for approximately 15 seconds to introduce the sample to the inlet. Contamination of the sample by any leakage past valve #9 from the reaction in progress in the reactor and recirculation equipment is avoided by re-closing valve #10. Pressure in the inlet is now above the 1000 micron range of the thermal conductivity vacuum gauge. The sample is allowed to equilibrate for five minutes to insure no composition gradients due to flow at low pressure are present. Valve #15 is now closed and valves #11 and #13 to the mechanical vacuum pump are opened, evacuating the inlet of all sample except that amount trapped between valves 15 and 16.

After the pressure has been reduced to or below 50 microns for three minutes, valves #11, #12 and #13 are closed and valve #15 opened.

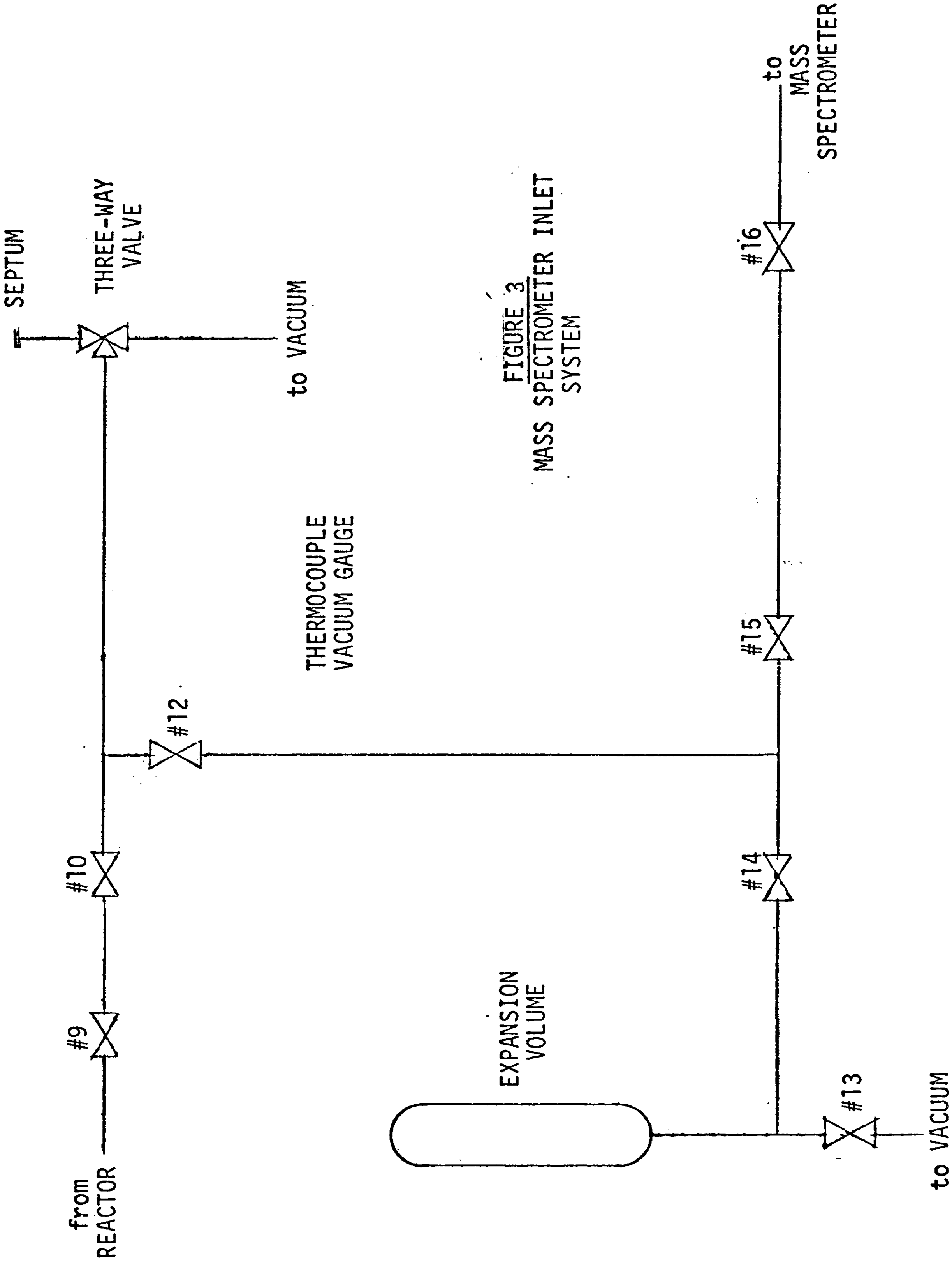

FIGURE 3
MASS SPECTROMETER INLET SYSTEM

The sample expands into the larger available volume, reducing sample pressure to about 600 microns. A five-minute waiting period allows concentration gradients to be reduced (see Appendix VI for further discussion). A mass spectrum may now be obtained by opening valve #16, which introduces the sample to the mass spectrometer through a small opening in the disc of gold foil. The pressure in the instrument's cycloid tube is approximately 1.2×10^{-5} mm Hg, which is excessive for most samples. This is remedied by closing valve #14 prior to opening valve #16, which results in a pressure of about 6×10^{-6} mm. It becomes necessary to use the higher pressure procedure toward the end of a reaction run, due to the small amount of thiophene present.

Each sample obtained reduces the pressure of the reactor/recirculation circuit by approximately 2 psi at 700 psia operating pressure. The maximum number of samples withdrawn, 6, reduces the amount of reacting mixture by approximately 2%.

CHEMICAL ANALYSIS

The Mass Spectrum

Each chemical compound has a unique mass spectrum, which may be described by the sensitivity of the highest (or base) peak, mass number at which it occurs, and heights of peaks at other mass numbers. Base peak sensitivity, measured in scale divisions per micron of pressure, varies among spectrometers, but is approximately the same under similar conditions of amplifier gain and ionization (all measurements in this study are made at standard ionization potential of 68 volts and current of 20 microamperes). In order to compare results from different spectrometers, the base peak sensitivity of normal-butane is reported in pure-compound mass spectral data, and the base peak sensitivity of the compound under consideration is ratioed to it. Peak heights at mass numbers other than that of the base peak are reported as fractions of base peak height. Tabulated mass spectra, such as those of API Project 44 (39), enable approximate identification of compounds, but calibration at periodic intervals is necessary to insure accuracy in quantitative measurement of mixtures. Table 1 lists API mass spectral data for high-contrast mass numbers of the C_4's, n-C_5, i-C_5, H_2S, and thiophene.

Mixture Composition Determination

Molecules of a compound introduced into the mass spectrometer are

TABLE 1

API MASS SPECTRAL DATA
FOR HIGH CONTRAST PEAKS

Mass	1-Butene	Cis-2-$C_4^=$	Trans 2 $C_4^=$	nC_5	H_2S	Thiophene	nC_4	iC_5*
29	.1080	.1310	.1670	.2330	-	.0012	.4420	.4433
33	-	-	-	-	.4200	.0097	-	-
34	-	-	-	-	1.0000	.0039	-	-
39	.2830	.2960	.2970	.1090	-	.0007	.1250	.1509
42	.0349	.0339	.0333	.5021	-	.0443	.1220	.7930
47	-	-	-	-	-	.0255	-	-
55	.2160	.2690	.2660	.0232	-	-	.0093	.0375
56	.4420	.5650	.5410	.0173	-	.0162	.0072	.1263
57	.0197	.0245	.0234	.1032	-	.1290	.0242	.4532
58	.0007	.0004	.0004	.0045	-	.6480	.1230	.0209
72	-	-	-	.0531	-	-	-	.0301
84	-	-	-	-	-	1.0000	-	-
Base Peak Sensitivity Relative to n-Butane	1.04536	.71316	.70947	1.25	.75388	.81395	1.0	.82

*Reference - Consolidated Electrodynamics Corp. Mass Spectrometer, Model 21-130, Operating Manual (74).
All other data: API Project 44 (39).

ionized and fragmented by a hot filament. The charged fragments are accelerated by an electric field, and injected into a magnetic field. During passage through the magnetic field, each fragment follows a curved trajectory whose shape depends on the mass of the fragment. By varying the electrical potential, and thus the velocity of the fragments, fragments of different mass are caused to impact and discharge on a metal collector. The resulting current, amplified, drives galvanometers, whose deflection is proportional to the rate at which ions of the particular mass focused on the collector are arriving. A larger concentration of fragments of a particular mass results in a greater arrival rate (larger current). For a mixture, the peak height corresponding to a given mass, j, represents the sum of contributions from fragments of all compounds, i, present, and is related to composition by:

$$(\text{pk.ht.})_j = \sum_i (\text{b.p.s.})_i (\text{frac.pk.ht.}_j)_i (\text{concentration})_i \qquad (3)$$

where b.p.s. is the base peak sensitivity. For a mixture containing N compounds, with base peak sensitivities and fractional peak height data available for all compounds present, N peak heights may be used (N equations to N unknowns, equation (3) at N different mass numbers) to determine the composition of the mixture.

Peak heights used in equation (3) must be corrected for background, i.e. residual gas in the spectrometer and inlet. This is accomplished by obtaining a mass spectrum with no material added to the spectrometer, and subtracting the resulting peak heights from the appropriate peaks in the spectrum of the mixture under study. Typical compounds represented in the background are water, nitrogen, oxygen, and small amounts of hydrocarbon if a hydrocarbon diffusion pump oil is used. If the time between samples is relatively short or the inlet pump oil is contaminated, a small amount of the previous sample may be present.

Mass Spectrometer Inlet Effects

The material in the inlet system of the mass spectrometer may be different in composition from that in the spectrometer if Knudsen (molecular) flow takes place, due to differing diffusion rates through the gold leak (pressure-reducing orifice). As a result, some mixture components may appear in greater relative amounts in the analyzer of the spectrometer than in the inlet. Diffusion rates in molecular flow are related to molecular weight and structural properties through gaseous diffusion theory at low densities (37):

$$D_{AA} \propto (mw_A)^{-\frac{1}{2}}(d_A)^{-2} \tag{4}$$

where D_{AA} is the self-diffusivity of a compound, A, mw_A is its molecular weight, and d_A is the molecular diameter. Compounds differing radically in molecular weight and/or structure can be expected to diffuse at differing rates, so calibration using known mixtures is necessary. If, however, flow is precominately viscous in nature (79), fractionation will not occur. As is shown in Appendix VI, viscous flow was present in the apparatus and no fractionation occurred.

Concentration Determination

Mass spectrometers operate at 10^{-5} mm Hg of pressure or below, and are sensitive to very small amounts of sampled material. It is ordinarily necessary to introduce samples of uniform size in order to relate peak height information to absolute amounts of material in the system being sampled. This is accomplished with an inlet system, consisting of a gas metering system and pressure gauge. This equipment was not included with the mass spectrometer, so an inlet had to be constructed. An accurate vacuum gauge was not available, so an alternate means of determining sample size was necessary.

The use of peak height ratios to determine composition is helpful in eliminating errors due to varying sample size, if the concentration of the reference compound is not changed in any way by the process under study (78). In this case, n-pentane is added to the reactor as a diluent, and is assumed to undergo negligible change in concentration due to reaction (6, 26, 80, 84). See Appendix III for thermodynamic verification of this assumption. Absolute peak height data at mass 72, the "parent" peak for pentane, are plotted in Figure 4 for runs 9-30. Data for each experimental run are connected with straight lines. There is no significant trend toward declining pentane concentration (which would be indicated by peak height data decreasing with time).

The concentration of thiophene relative to that of n-pentane can be predicted, using tabulated mass spectral data, by using equation (3) at mass 84 (thiophene parent peak) and again at mass 72 (pentane parent peak). A ratio of peak height 84 to peak height 72 is proportional to the ratio of thiophene concentration to pentane concentration. The proportionality constant is the base-peak-sensitivity-times-

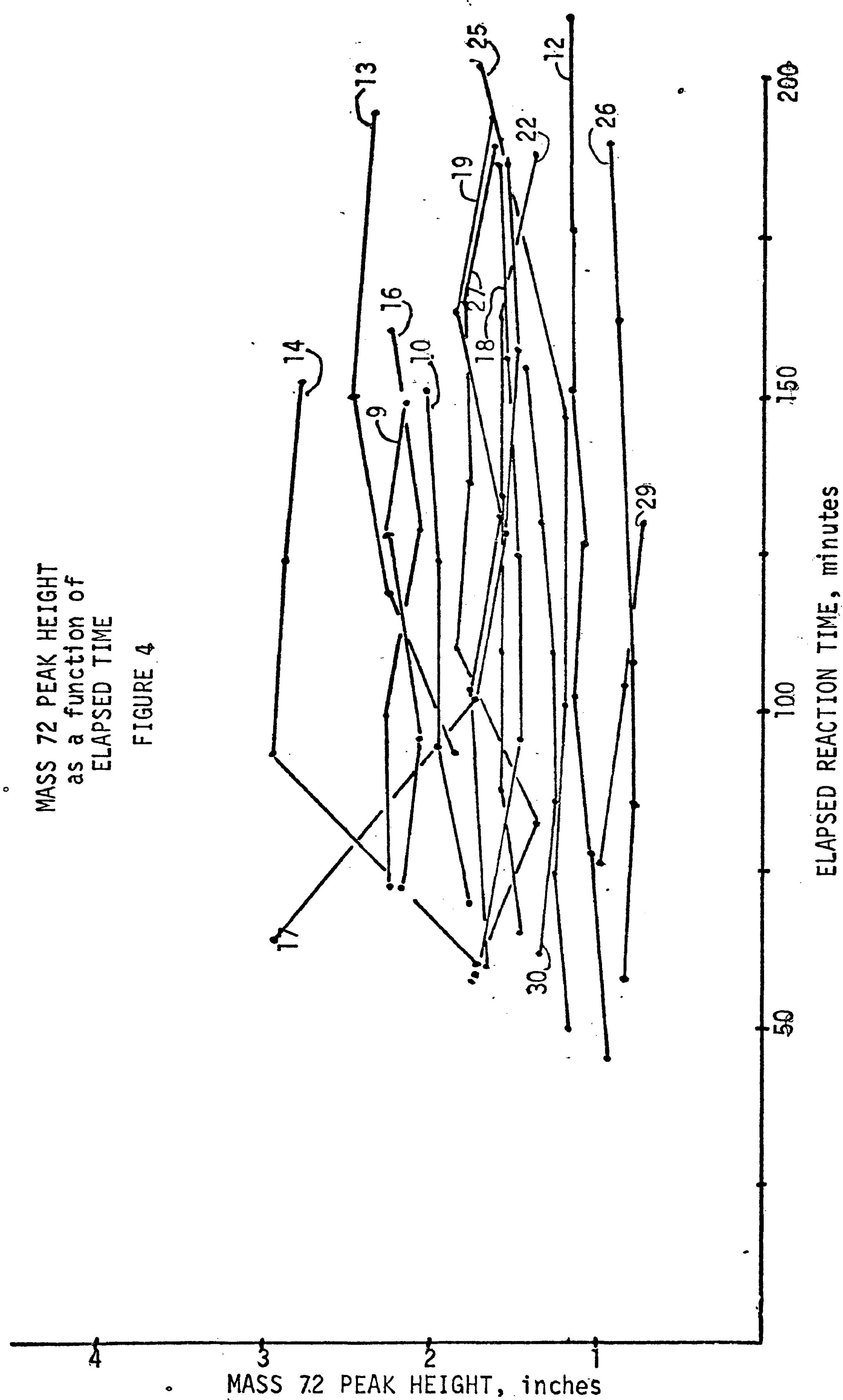

MASS 72 PEAK HEIGHT
as a function of
ELAPSED TIME

FIGURE 4

fractional-peak-height for thiophene at mass 84, ratioed to the similar product for pentane at mass 72. Thiophene does not exhibit a peak at mass 72, nor does n-pentane exhibit a peak at mass 84, so the summation in equation (3) is not necessary.

Calibration of the spectrometer on a known mixture of thiophene and n-pentane gives a proportionality factor slightly different from that predicted by the tabulated data. The value obtained by using tabulated data is .0815; the equation used for predicting thiophene concentration from a known amount of n-pentane, based on calibration data is:

$$C_T = a(h_{84}/h_{72})C_5 \tag{5}$$

where C_T and C_5 are concentrations of thiophene and n-pentane respectively, and where a is 0.0840 for runs with H_2S added and 0.0968 for runs without H_2S addition. The reason for the differing calibrations is not known, but is suspected to be due to interaction of H_2S with the rhenium mass spectrometer filament. Since results at both high and low H_2S concentrations are reproducible, this difference is not considered serious. Calibration is summarized in Appendix VI.

The amount of hydrogen sulfide in the vapor phase is calculated from mass spectra via:

$$C_S = .0510\ (h_{34}/h_{72})C_5 \tag{6}$$

which was determined by calibration using known mixtures of H_2S and n-pentane. This factor was estimated, using tabulated data, as .0880. This discrepancy can be explained largely by a discrepancy between tabulated and measured values of mass 72 peak height data (see Appendix VI).

The amount of butane (as n-butane) present relative to the concentration of n-pentane is predicted with equation (3) as follows. The peak height at mass 58 divided by the peak height at mass 72 is equal to:

$$\begin{aligned} h_{58}/h_{72} = \{&(\text{b.p.s.})_T(\text{frac.pk.ht.}_{58})_T(\text{conc.})_T \\ &+(\text{b.p.s.})_5(\text{frac.pk.ht.}_{58})_5(\text{conc.})_5 \\ &+(\text{b.p.s.})_4(\text{frac.pk.ht.}_{58})_4(\text{conc.})_4\} \\ &/\{(\text{b.p.s.})_5(\text{frac.pk.ht.}_{72})_5(\text{conc.})_5\} \end{aligned} \tag{7}$$

Substitution of base peak sensitivities and fractional peak height data into equation (7) and algebraic rearrangement yeilds an approximate expression for butane concentration. Calibration, using known amounts of thiophene, butane, and pentane, gave the expression:

$$C_4 = \{.2506(h_{58}/h_{72}) - .1624(h_{84}/h_{72}) - .0015\}C_5 \tag{8}$$

Details of the calibration may be found in Appendix VI. These factors were estimated, using tabulated data, as .5396, -.3808, and -.0457. These discrepancies also are due in large part to the higher-than-expected ratio of mass 72 to mass 43 peak height ratio for the internal standard, n-pentane (see Appendix VI).

The amount of butenes present in the reaction mixture represents only a small amount of the thiophene-and C_4 carbon balance, due to the fact that butenes are reaction intermediates. Calibration runs were not made on samples of the different C_4 olefins. If all the butene material is assumed to be represented by the same spectrum (as seen below, the spectra are very similar), concentration can be calculated (using tabulated API data, and substituting experimental values for thiophene and n-butane calibrations) as:

(trans-2-butene)

$$C_4^-/C_5 = .2703(h_{56}/h_{72})-.0047(h_{58}/h_{72})-.0733\text{, or} \tag{9}$$

(cis-2-butene)

$$C_4^-/C_5 = .2575(h_{56}/h_{72})-.0045(h_{58}/h_{72})-.0698\text{, or} \tag{10}$$

(1-butene)

$$C_4^-/C_5 = .2247(h_{56}/h_{72})-.0039(h_{58}/h_{72})-.0609. \tag{11}$$

where the thiophene and n-butane expressions were substituted into equation (3) and algebraic rearrangement was performed. Since there is a peak correction term for thiophene in both the butane and butene expressions, the mass 84/72 peak height ratio terms cancel.

MODEL DEVELOPMENT

Introduction

Satterfield and Roberts (4), in their models of thiophene hydrogenolysis and butene hydrogenation, could not test kinetic models incorporating both thiophene and butene partial pressure due to a material balance relationship that made the two interrelated. The problem was circumvented for thiophene/hydrogen sulfide by continuously adding both thiophene and H_2S to the reactor at independently-controlled rates.

This cannot be done in batch reactors. The effects of covariance due to material balance relationships can, however, be minimized by a combination of:

1) varying the amount of initially-charged reactants and products, and
2) removing a portion of the reactants or products by secondary reaction(s) during the course of the main reaction.

In this study, both methods are utilized. By varying the amount of thiophene/pentane mixture initially charged to the reactor, different thiophene/pentane ratios are achieved over the desired range of thiophene concentrations. Also, hydrogen sulfide is charged to the initial reaction mixture in some experimental runs to raise the H_2S concentration to levels significantly higher than those produced by the thiophene hydrogenolysis reaction. Additionally, use of iron packing in a portion of the experimental work removes hydrogen sulfide during the course of the reaction. This allows effects of both reactant and product to be examined by reducing the degree of statistical confounding caused by the material balance relationship.

The use of iron packing to remove a portion of the H_2S, while statistically advantageous for the kinetic model, prevents obtaining hydrogen sulfide adsorption data during the reaction. At low pressures (i.e. low coverage of the catalyst surface) this would be of little consequence, but at high surface coverages in multi-component systems, both gas-phase and surface concentrations of all species must be known. Glass packing, used in place of iron packing, allows both thiophene and H_2S adsorption data to be obtained, but due to the material balance relationship, makes the data less desireable for use in regression fitting of kinetic models.

Both sets of data (iron packing, glass packing) are generated by the same reaction kinetics, however. Thus a kinetic model derived from iron packing data should (in the absence of catalytic effects from the iron) fit data gathered over glass packing. This is discussed below, and is verified in Appendix IV.

<u>Adsorption Derivation</u>

In the Langmuir adsorption isotherm (Smith (30), chapters eight and nine), expressed in terms of concentration, the rate of adsorption of a species, A, is proportional to the concentration of A in the gas phase and the number of vacant sites on the catalyst:

$$r_A = k_a C_A(\bar{C}_m - \bar{C}_A), \tag{12}$$

where the k_a is the adsorption rate constant, C_A is the gas-phase concentration of A, $\bar{C}_m$ is the surface concentration of total available adsorption sites, and $\bar{C}_A$ is the surface concentration of adsorbed A. Note that the quantity in parentheses is the number of vacant sites. This expression is valid for single-component adsorption only.

The desorption rate is proportional to the concentration of adsorbed A,

$$r_d = k_d \bar{C}_A \tag{13}$$

At equilibrium the adsorption and desorption rates are equal, and

$$K_A C_A(\bar{C}_m - \bar{C}_A) = \bar{C}_A, \tag{14}$$

where K_A equals k_a/k_d for species A. For a multi-component system, this equation can be written

$$K_A C_A(\bar{C}_m - \bar{C}_A - \bar{C}_B - \bar{C}_O) = \bar{C}_A, \tag{15}$$

where $\bar{C}_B$ represents the adsorbed concentration of species B and $\bar{C}_O$ represents adsorbed concentrations of all species other than A or B.

Reaction Kinetic Derivation

A first-order reaction,

$$A \rightarrow \text{Products} \tag{16}$$

may be modeled as either single-site

$$-r_s = k_s\bar{C}_A \tag{17}$$

or dual-site

$$-r_s = k_s\bar{C}_A\bar{C}_v \tag{18}$$

on the surface of a catalyst, where $\bar{C}_v$ represents the concentration of vacant sites (33). There are instances, however, when such a model can be disguised. If a large enough excess of species A is present, the surface of the catalyst will be almost completely occupied and further addition of A to the bulk phase will have little observable effect, i.e. zero-order kinetics will be seen (115). If sufficient other species are present to interfere with adsorption of A onto two or more adjacent sites (assuming that the reaction mechanism requires adsorption onto adjacent sites and that steric hinderance or blocking prevents either proper orientation or adsorption on the second site), the reaction will be slower as more interference occurs. As noted in the literature, thiophene hydrogenolysis is generally believed to be a first-order reaction in thiophene concentration, inhibited by both reactant and product adsorption, of dual-site character, with the surface reaction (C-S bond fission) considered the limiting step. An adequate kinetic model must include these characteristics, but also describe interference effects properly.

A popular means of describing kinetic behavior is attributed to Hinshelwood (Kinetics of Chemical Change, Oxford University Press, London, 1940), and was developed in detail in a work by Hougen and

Watson (52). The resulting models, called variously Hougen-Watson or Langmuir-Hinshelwood kinetic models, express surface concentrations in terms of bulk-phase concentrations and adsorption coefficients. For equations (17) and (18), the derivation is as follows.

The total number of available sites per weight of catalyst, $\bar{C}_m$, is equal to the total number of sites occupied by all species plus the number of vacant sites:

$$\bar{C}_m = \bar{C}_A+\bar{C}_B+\bar{C}_O+\bar{C}_v \tag{19}$$

Rearrangement gives

$$1 = \bar{C}_m/(\bar{C}_v+\bar{C}_A+\bar{C}_B+\bar{C}_O) \tag{20}$$

Each component can be described by its Langmuir isotherm:

$$\bar{C}_A = K_A C_A \bar{C}_v, \tag{21}$$

etc. Substitution gives, after rearrangement,

$$\bar{C}_v = \bar{C}_m/(1+K_A C_A+K_B C_B+K\ldots\ldots) \tag{22}$$

with an adsorption term in the denominator for each species present (some of which are usually assumed to be zero). Substitution of equation (21) into equation (17) or (18), followed by substitution of equation (22), gives either the single- or dual-site adsorption-inhibited model,

$$-r = kC_A/(1+K_A C_A+K_B C_B+K\ldots.)^m, \tag{23}$$

where m is 1 for the single-site model and 2 for the dual-site model.

Enhancement

Carberry (125) discusses briefly models representing reaction with adsorption enhancement. In Langmuir-Hinshelwood models, this condition results in one of the adsorption coefficients being negative:

$$-r = kC_A/(1 + K_AC_A - K_BC_B)^m \quad . \qquad (24)$$

Models with negative adsorption coefficients are generally considered physically impossible.

Two alternate means of considering enhancement are available (125): a single-type-of-site competitive model

$$-r = kC_AC_B/((1 + K_AC_A)(1 + K_BC_B)) \qquad (25)$$

and a model with A and B adsorbing independently on two types of sites:

$$-r = kC_AC_B/(1 + K_AC_A + K_BC_B)^2 \quad . \qquad (26)$$

EXPERIMENTAL RESULTS

Introduction

There are two types of experimental evidence considered here: 1) graphs of concentration-versus-time data, and 2) kinetic rate data analyzed by linear regression analysis. The interaction between thiophene and hydrogen sulfide on the catalyst surface is complicated by the presence of n-pentane and reaction products.

Concentration-Time Data

Figure 5 is a compilation of thiophene composition data as a function of time for a number of experimental runs. The starting time for each run has been shifted slightly, as noted in the legend, so as to group together those runs with high initial hydrogen sulfide concentration and those with no additional H_2S added. The purpose of this grouping is qualitative only. Two features are apparent:

1) The rate of change of thiophene concentration in the low H_2S runs is generally lower than that of the high-H_2S runs, and tends to decrease with time.

2) The rate of change of thiophene concentration in the high H_2S data, particularly at high thiophene concentrations, appears constant, implying a zero-order reaction.

FIGURE 5
COMPOSITE THIOPHENE
CONCENTRATION-TIME
DATA

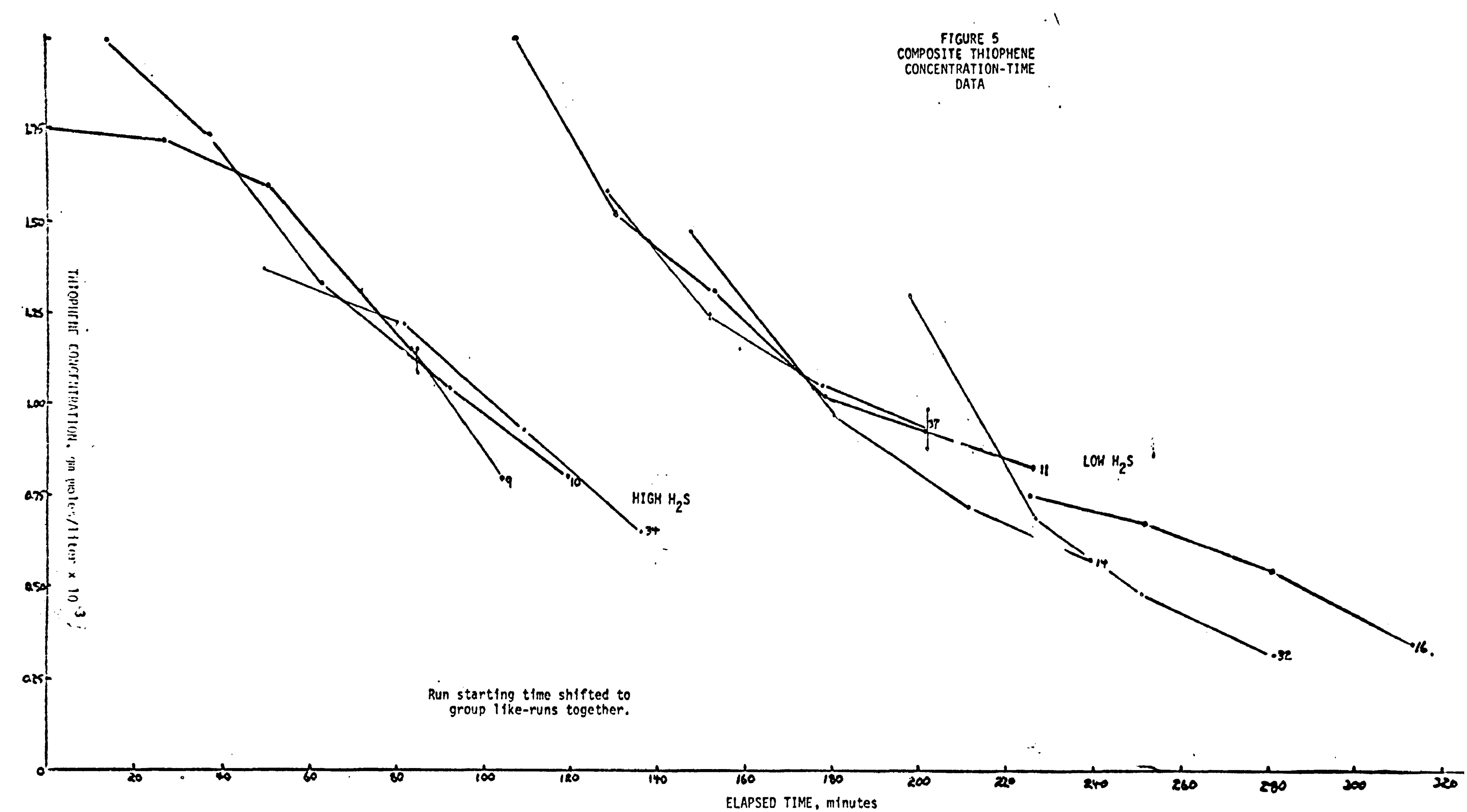

Apparently some property of hydrogen sulfide is exhibited that accelerates the thiophene reaction rate under these reaction conditions. At the same time, the zero-order reaction suggests that the surface available to thiophene is very nearly saturated with that compound.

Studies cited in the Literature Survey have indicated that the hydrogenolysis of thiophene is retarded by both thiophene and hydrogen sulfide. However, in only one (92) of those studies were large amounts of chemical species present other than reactants and products. Thus it is possible that the increased activity experienced by adding H_2S to the reactor is due to preferential adsorption of H_2S in place of the more bulky n-pentane. This could lead to an enhancement effect, indicated by what appears to be a negative adsorption coefficient for H_2S in Langmuir-Hinshelwood models.

Within the high or low H_2S treatments, H_2S may serve to enhance or retard the reaction rate. Overall, it appears to keep the rate high. The shift from 1st order toward zero order with increasing H_2S concentration is probably due to the increased H_2S concentration reducing the number of vacant sites available for adsorption of thiophene, causing the surface to become more saturated.

Plots of composition-time data are included as Figures 6 through 15. The numerical data are tabulated in Appendix VII.

Relative Adsorption Data

Using initial concentrations of reactants and products, and measuring these concentrations relative to an unreactive reference compound (n-pentane), concentrations of both bulk-phase and adsorbed

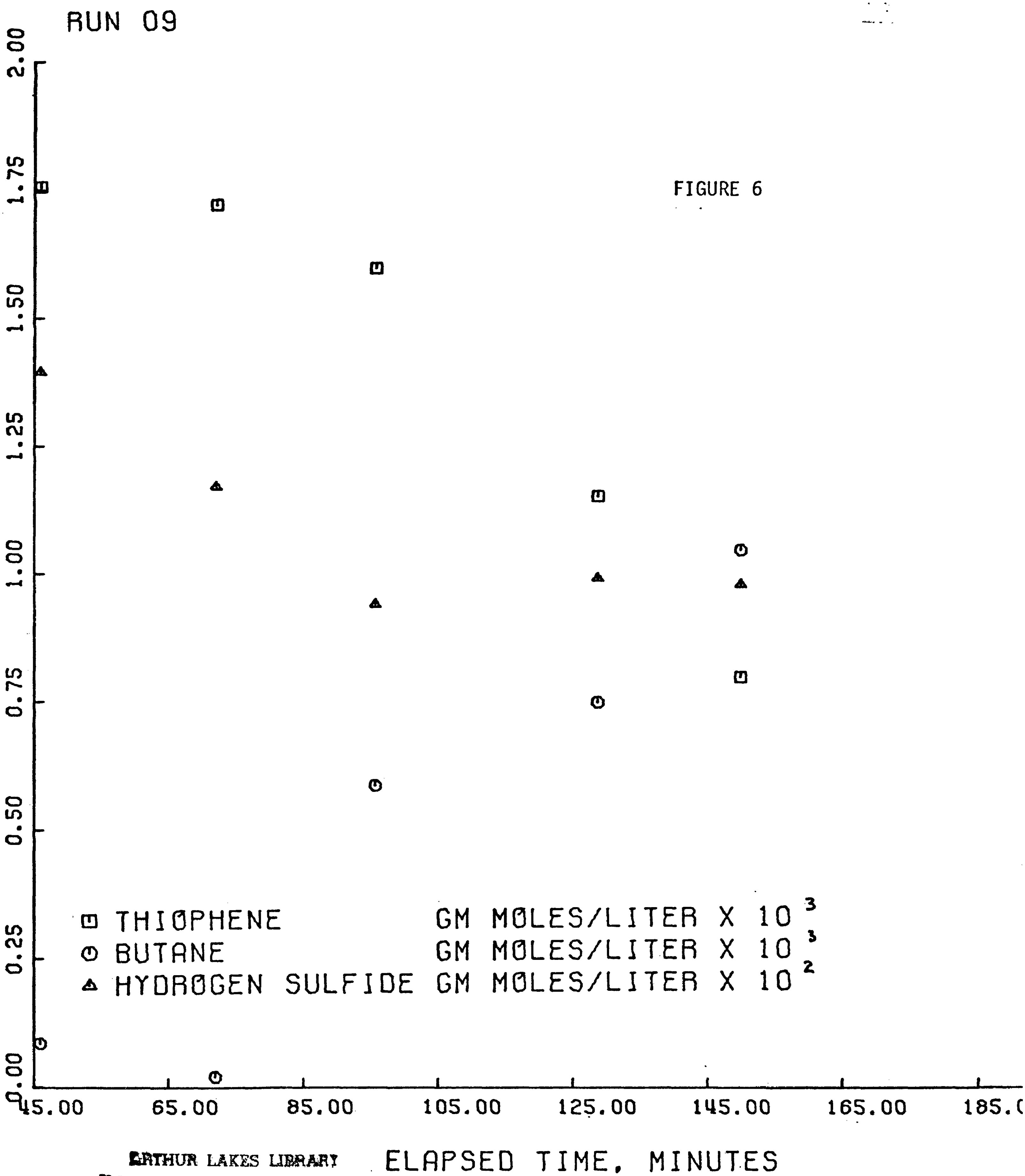
RUN 09
FIGURE 6
2.00
1.75
1.50
1.25
1.00
0.75
0.50
0.25
0.00
45.00
65.00
85.00
105.00
125.00
145.00
165.00
185.0
THIOPHENE GM MOLES/LITER X 10 3
BUTANE GM MOLES/LITER X 10 3
HYDROGEN SULFIDE GM MOLES/LITER X 10 2
ELAPSED TIME, MINUTES

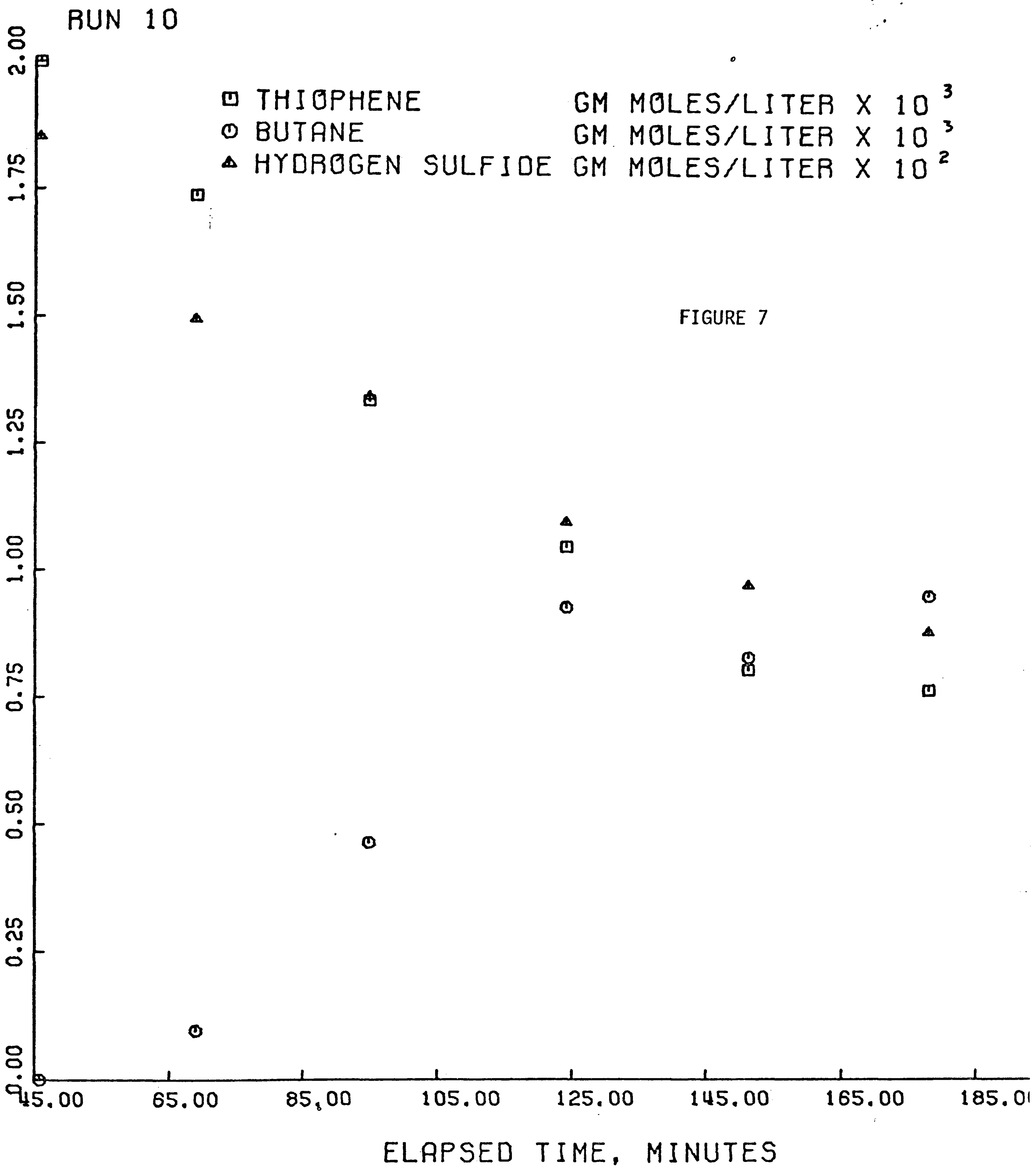
RUN 10
THIOPHENE GM MOLES/LITER X 10^3
BUTANE GM MOLES/LITER X 10^3
HYDROGEN SULFIDE GM MOLES/LITER X 10^2
0.00
0.25
0.50
0.75
1.00
1.25
1.50
1.75
2.00
45.00
65.00
85.00
105.00
125.00
145.00
165.00
185.00
ELAPSED TIME, MINUTES

FIGURE 7

FIGURE 8

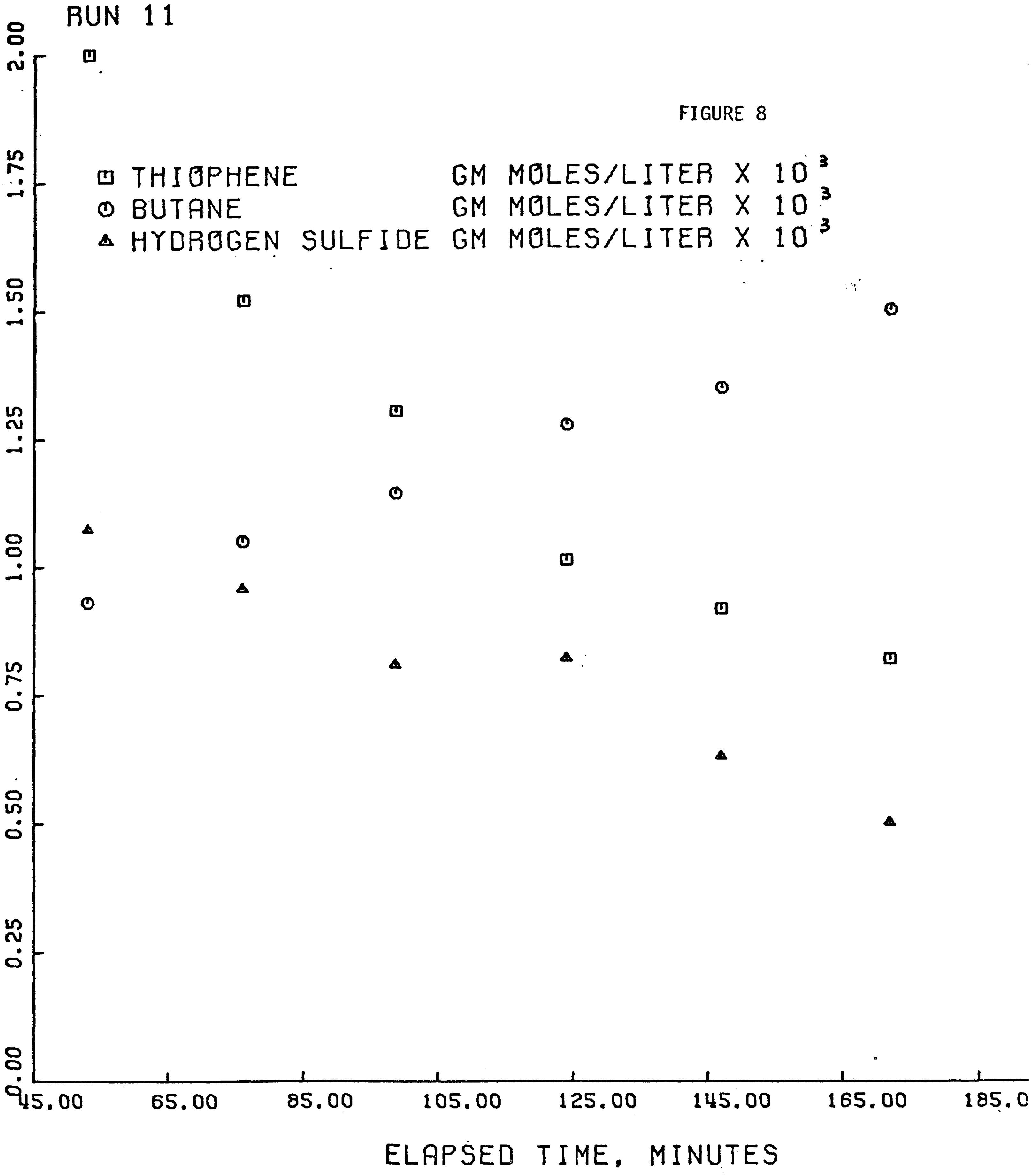
RUN 11
THIØPHENE GM MØLES/LITER X 10 3
BUTANE GM MØLES/LITER X 10 3
HYDRØGEN SULFIDE GM MØLES/LITER X 10 3
0.00
0.25
0.50
0.75
1.00
1.25
1.50
1.75
2.00
45.00
65.00
85.00
105.00
125.00
145.00
165.00
185.0
ELAPSED TIME, MINUTES

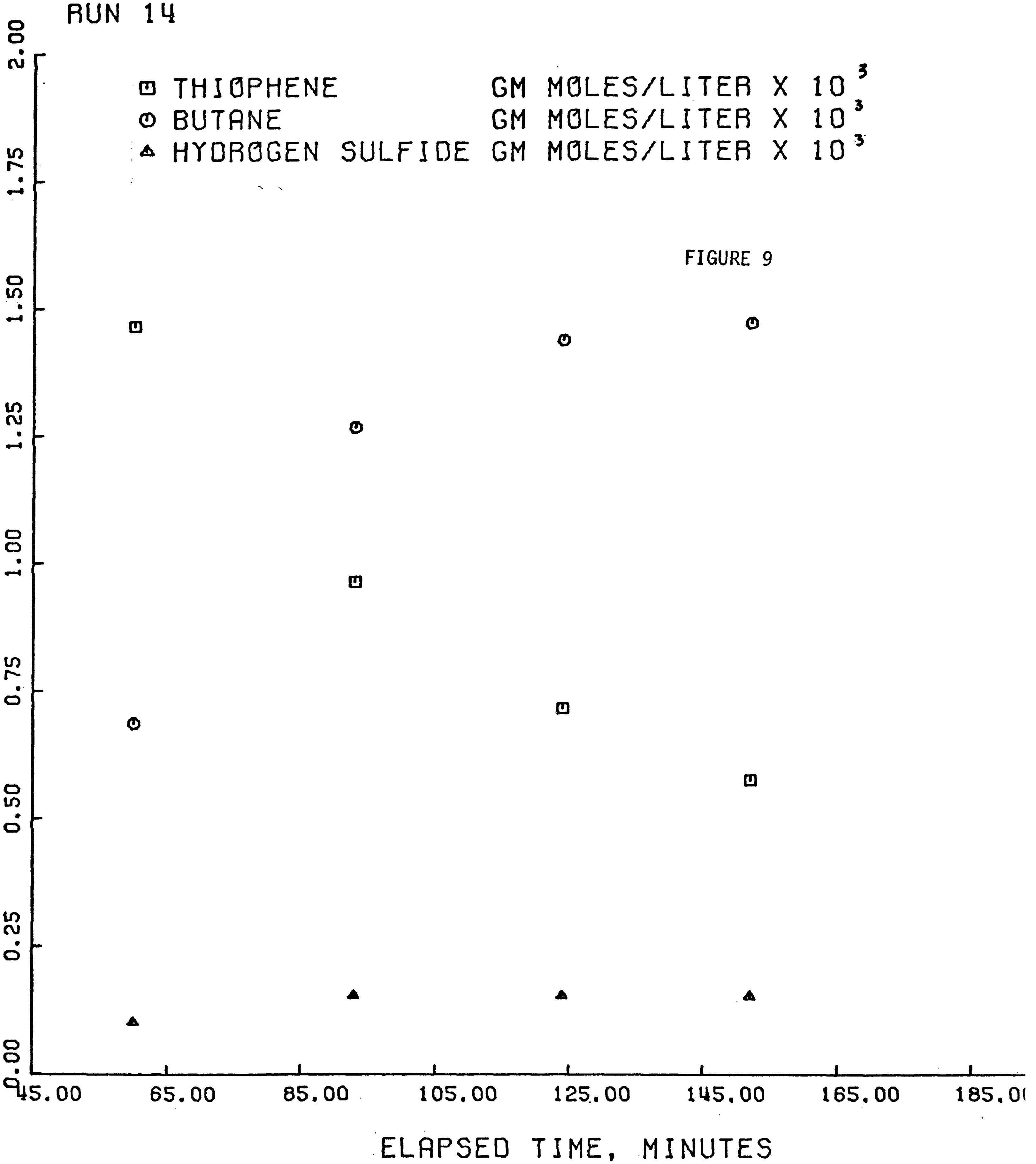
RUN 14
THIOPHENE GM MOLES/LITER X 10^3
BUTANE GM MOLES/LITER X 10^3
HYDROGEN SULFIDE GM MOLES/LITER X 10^3
0.00
0.25
0.50
0.75
1.00
1.25
1.50
1.75
2.00
45.00
65.00
85.00
105.00
125.00
145.00
165.00
185.00
ELAPSED TIME, MINUTES

FIGURE 9

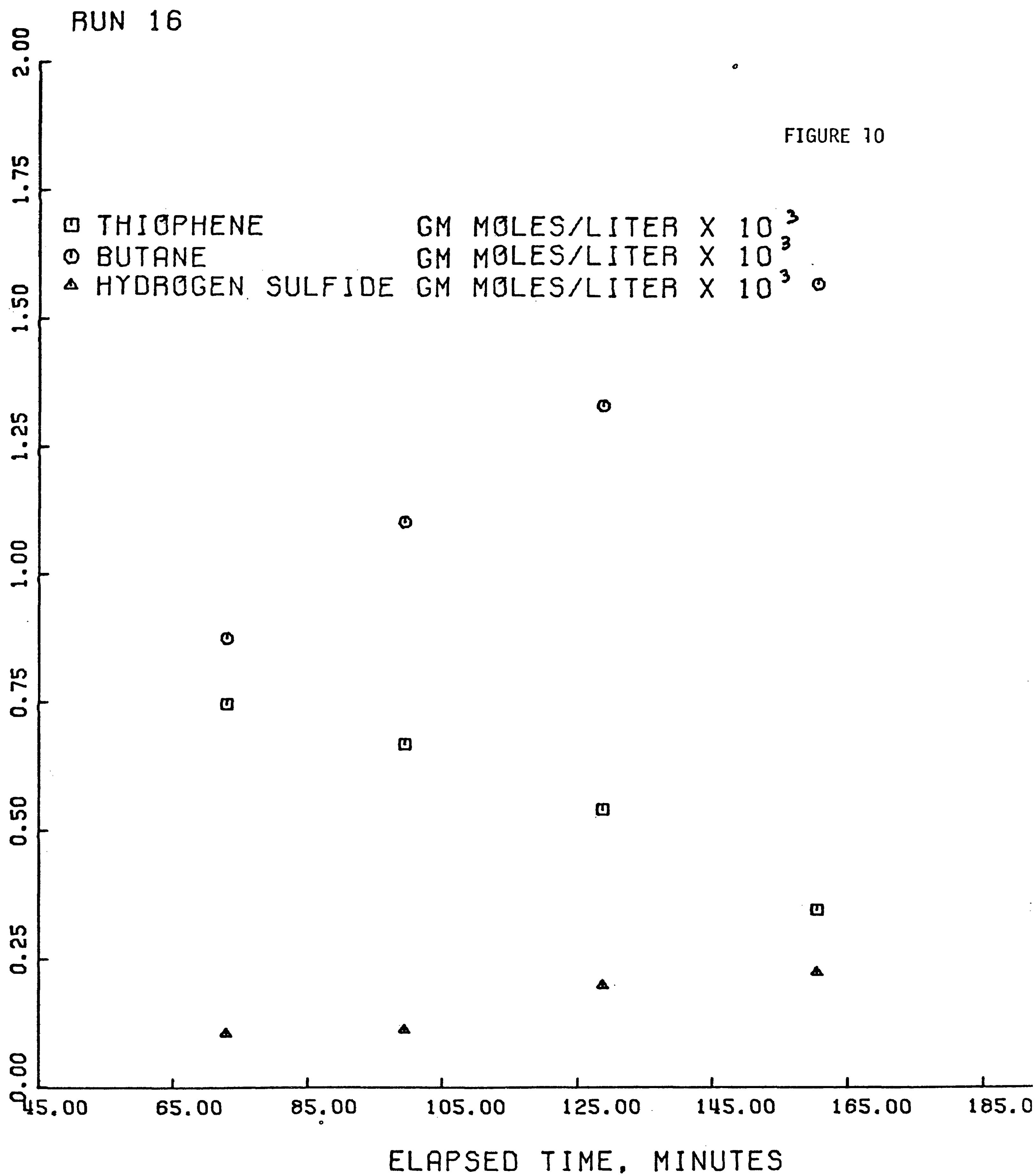
RUN 16
FIGURE 10
THIØPHENE GM MØLES/LITER X 10^3
BUTANE GM MØLES/LITER X 10^3
HYDRØGEN SULFIDE GM MØLES/LITER X 10^3
0.00
0.25
0.50
0.75
1.00
1.25
1.50
1.75
2.00
45.00
65.00
85.00
105.00
125.00
145.00
165.00
185.0
ELAPSED TIME, MINUTES

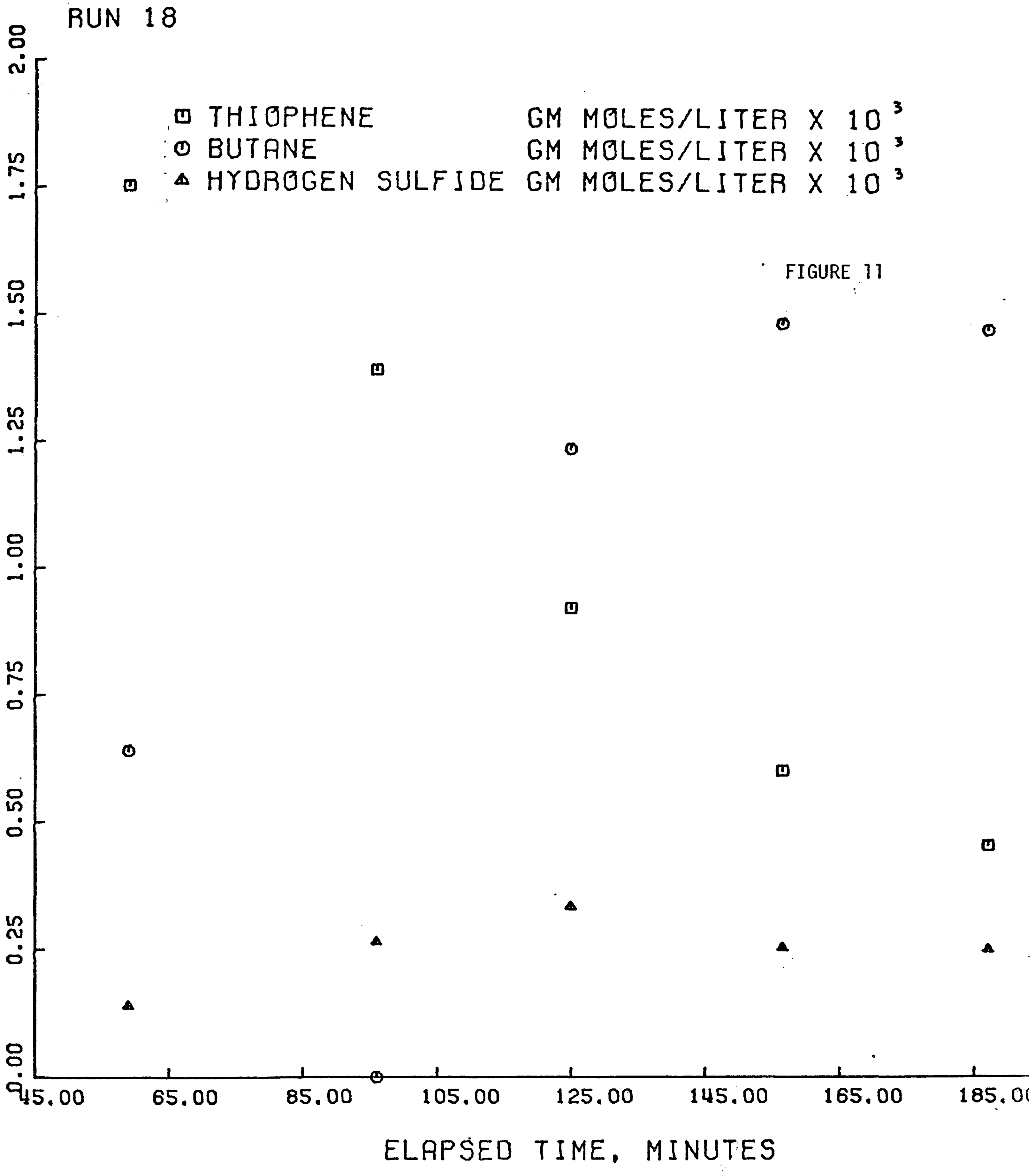
RUN 18
THIOPHENE GM MOLES/LITER X 10^3
BUTANE GM MOLES/LITER X 10^3
HYDROGEN SULFIDE GM MOLES/LITER X 10^3
0.00
0.25
0.50
0.75
1.00
1.25
1.50
1.75
2.00
45.00
65.00
85.00
105.00
125.00
145.00
165.00
185.00
ELAPSED TIME, MINUTES

FIGURE 11

FIGURE 12

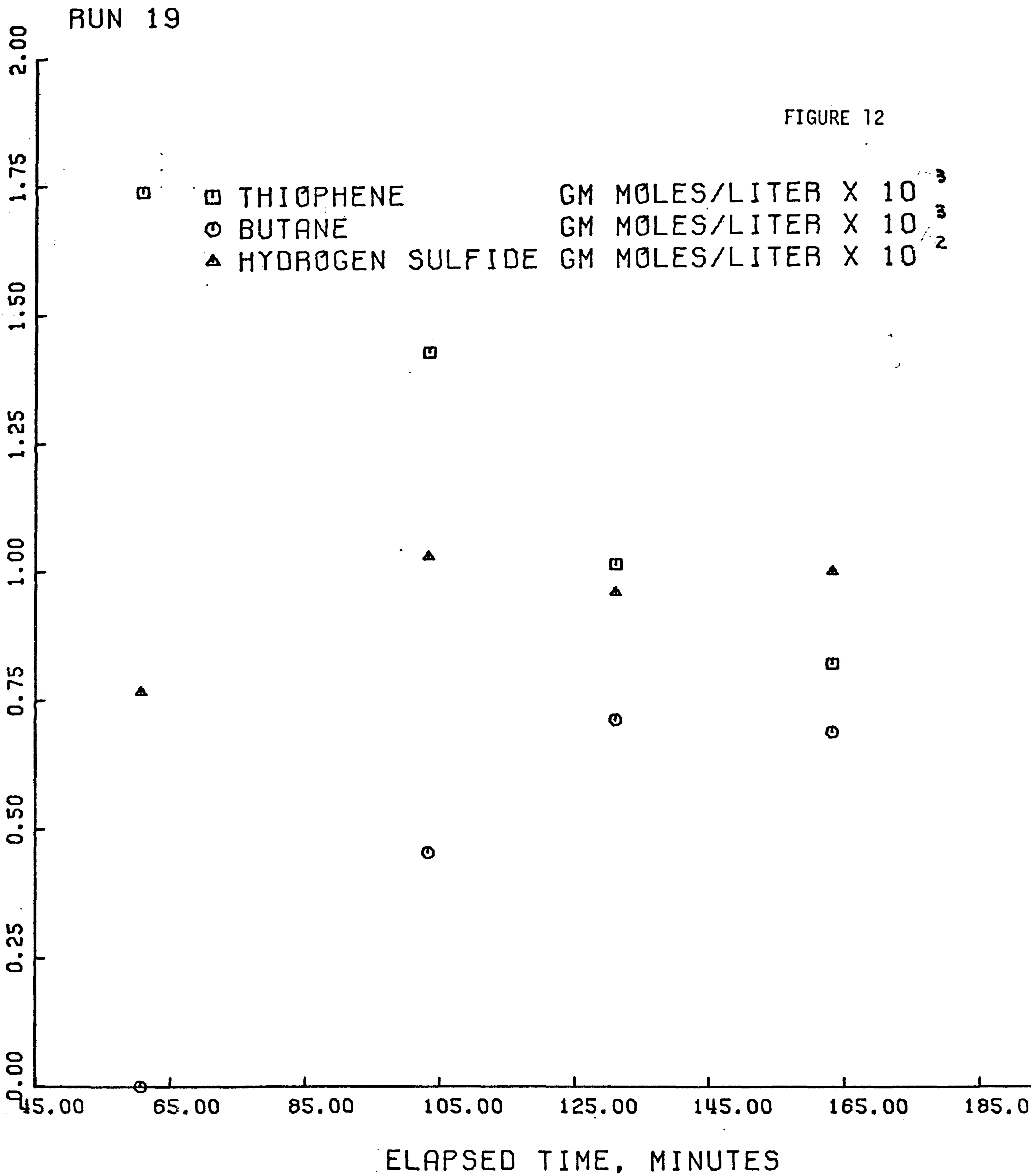
RUN 19
THIOPHENE GM MOLES/LITER X 10^3
BUTANE GM MOLES/LITER X 10^3
HYDROGEN SULFIDE GM MOLES/LITER X 10^2
0.00
0.25
0.50
0.75
1.00
1.25
1.50
1.75
2.00
45.00
65.00
85.00
105.00
125.00
145.00
165.00
185.0
ELAPSED TIME, MINUTES

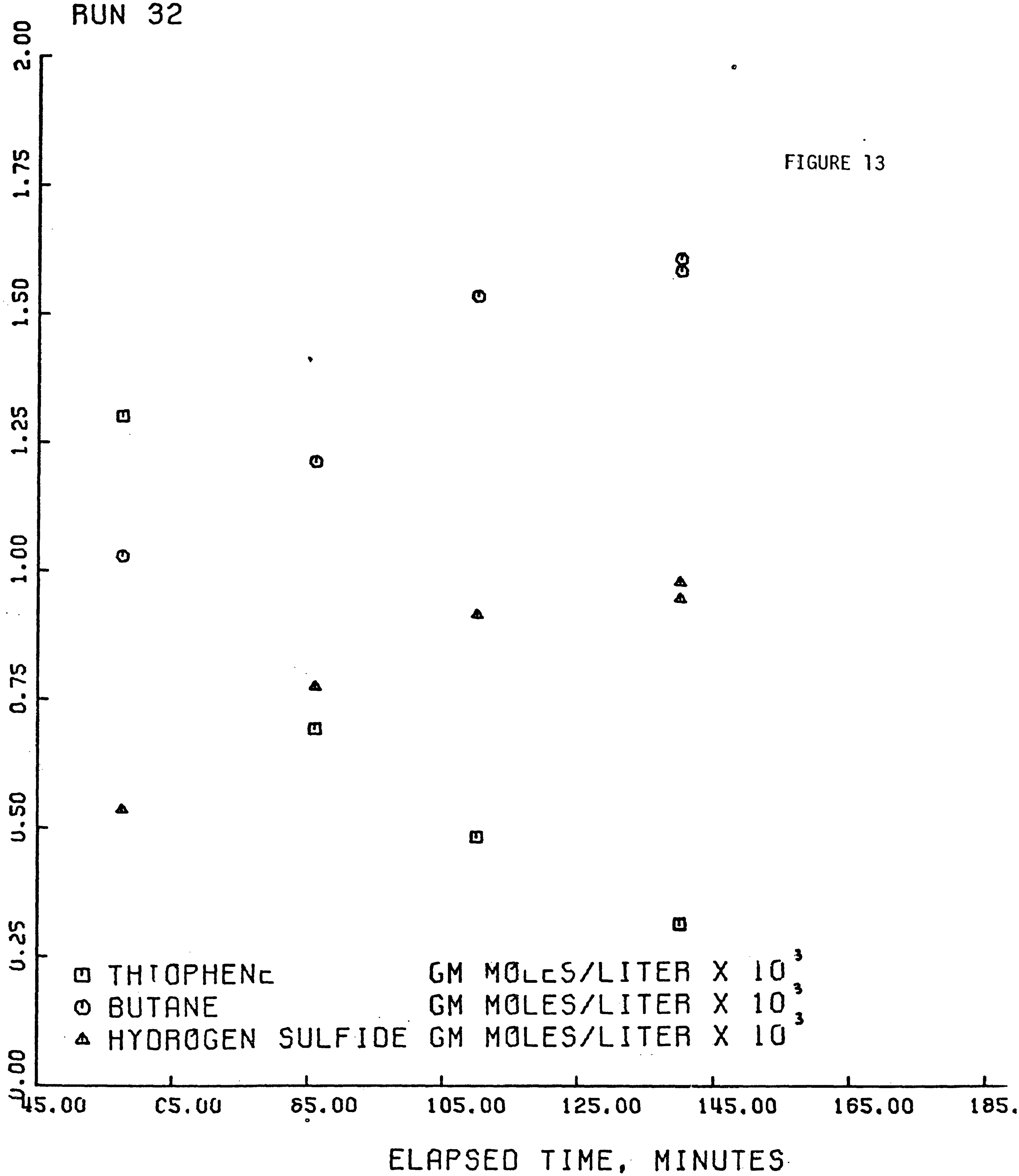
RUN 32
FIGURE 13
□ THIOPHENE GM MOLES/LITER X 10³
○ BUTANE GM MOLES/LITER X 10³
△ HYDROGEN SULFIDE GM MOLES/LITER X 10³
0.00
0.25
0.50
0.75
1.00
1.25
1.50
1.75
2.00
45.00
65.00
85.00
105.00
125.00
145.00
165.00
185.
ELAPSED TIME, MINUTES

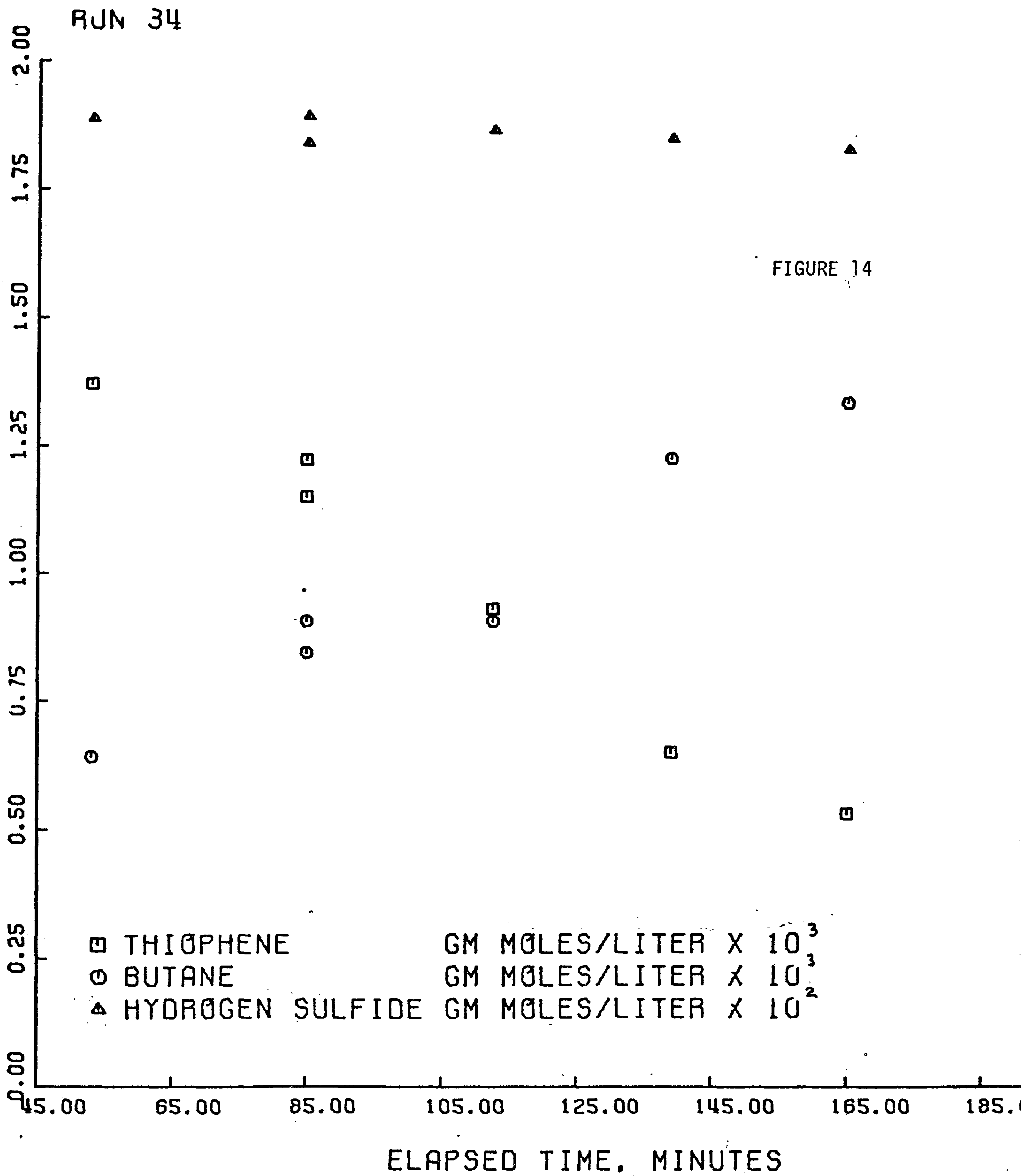
RUN 34
FIGURE 14
2.00
1.75
1.50
1.25
1.00
0.75
0.50
0.25
0.00
45.00
65.00
85.00
105.00
125.00
145.00
165.00
185.
THIOPHENE GM MOLES/LITER X 10^3
BUTANE GM MOLES/LITER X 10^3
HYDROGEN SULFIDE GM MOLES/LITER X 10^2
ELAPSED TIME, MINUTES

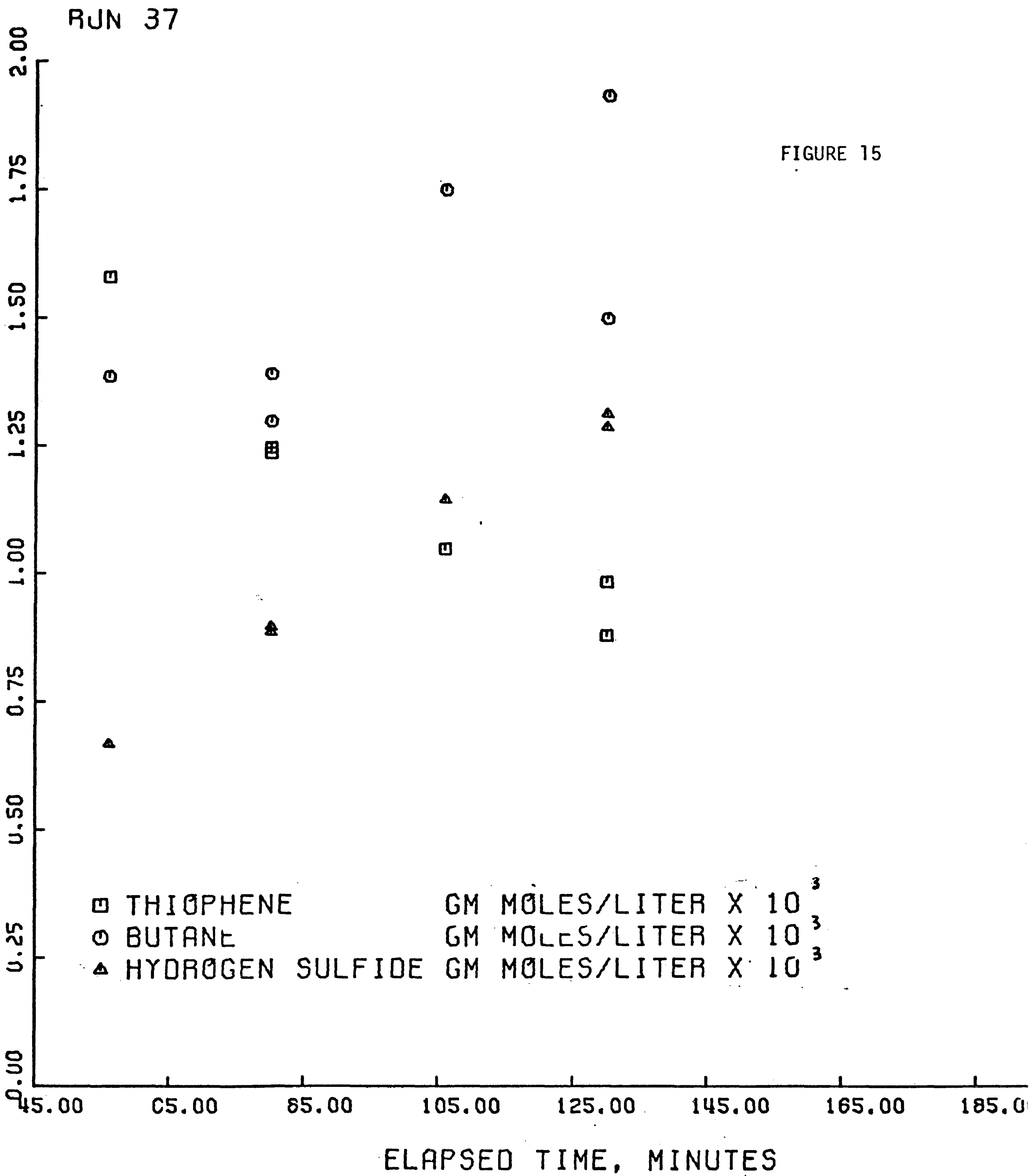
RUN 37
FIGURE 15
2.00
1.75
1.50
1.25
1.00
0.75
0.50
0.25
0.00
45.00
65.00
85.00
105.00
125.00
145.00
165.00
185.00
THIOPHENE GM MOLES/LITER X 10 3
BUTANE GM MOLES/LITER X 10 3
HYDROGEN SULFIDE GM MOLES/LITER X 10 3
ELAPSED TIME, MINUTES

species can be computed. A material balance requires that

$$C_{B,o} + C_{T,o} - C_T = \overline{C}_T + C_{4-} + C_B, \tag{27}$$

where C_B is the butane concentration, C_T is the thiophene concentration, C_{4-} is the concentration of butenes, subscript o denotes an initial concentration, and the superscript bar denotes an adsorbed species. In this case, the adsorbed species is actually the sum of adsorbed thiophene, butenes, and butane. Butane and butene adsorbed amounts are considered small (95); the small amount of butenes in the gas phase suggests that the amount of butenes on the surface would be small even if butene adsorption was strong.

A similar sulfur balance requires that

$$C_{T,o} - C_T - \overline{C}_T = \overline{C}_S + C_S, \tag{28}$$

where subscript S denotes hydrogen sulfide and $\overline{C}_T$ is assumed to be made up entirely of thiophene. Appendix V contains a program written for the Texas Instruments SR-52 programmable calculator which, given initial concentration and catalyst data, converts mass spectrometer peak height ratios to concentrations. Details of composition determination are contained in the Chemical Analysis section and in Appendix VI.

Runs 32, 34, and 37 were conducted at 275 degrees Celsius with glass beads used for packing. Both carbon and sulfur balances were obtained for these runs. A summary of concentration-time data appears in Figures 13, 14, and 15, and in Appendix VII.

Figures 16 through 25 represent the material balance closures for carbon (all runs) and sulfur(runs 32,34, and 37 only). Closure is defined as initial amount reacted minus amount unreacted, times 100, divided by initial amount.

Kinetic Data

Table VII-3 lists all composition-time data for ten experimental runs, a total of 52 data points, with five to six compositions per data point. Runs 9 through 19 were run over the same .1472 gram catalyst sample, with steel ball bearings for reactor packing. Runs 32, 34, and 37 were run over two other catalyst samples, with glass beads for reactor packing.

Numerous authors (see the discussion and references in Hunter and Kittrell (68)) have mentioned the problem of interrelation of measured data. Roberts (4), for example, avoided evaluation of kinetic models containing terms for thiophene, butenes, and butane together, due to the fact that the quantities were related by material balance. In his study and this one, a means of introducing hydrogen sulfide to the reactor is available in addition to the amount generated during the reaction. This partially resolves the

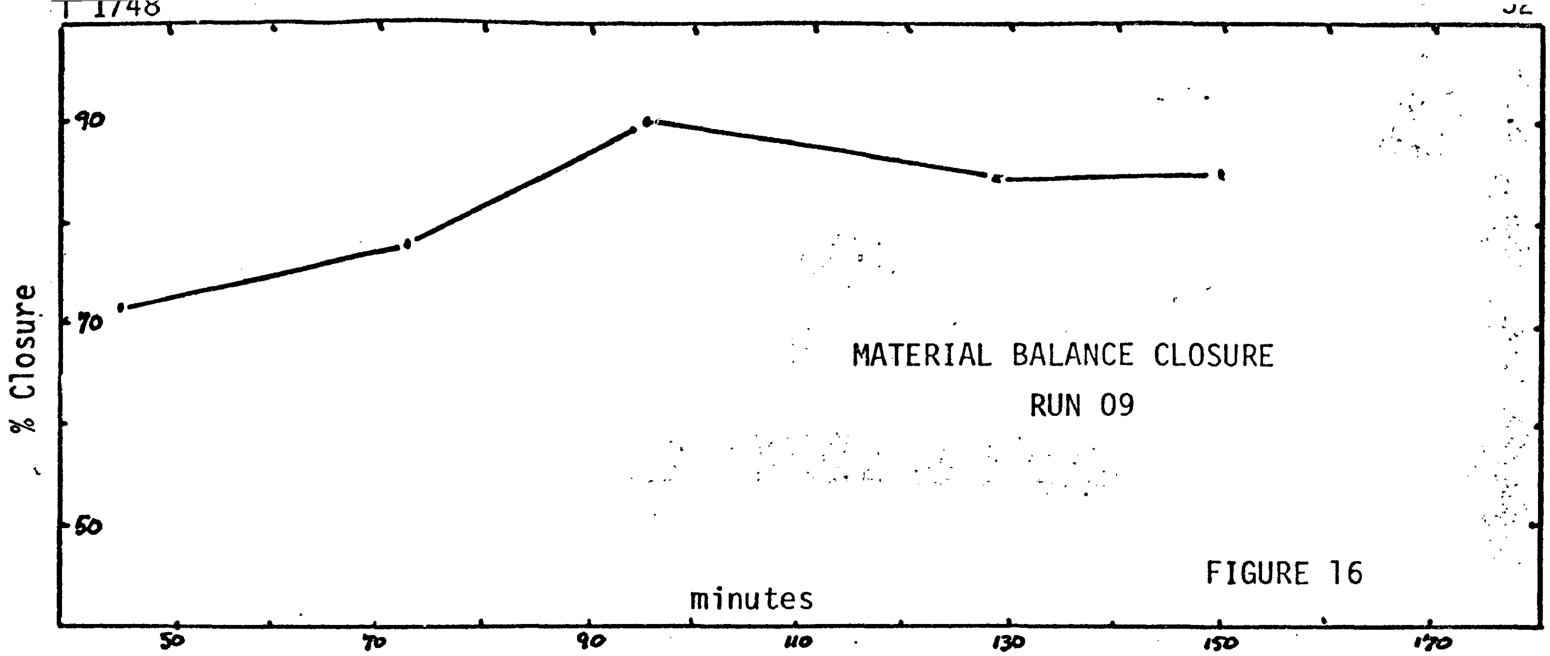

FIGURE 16

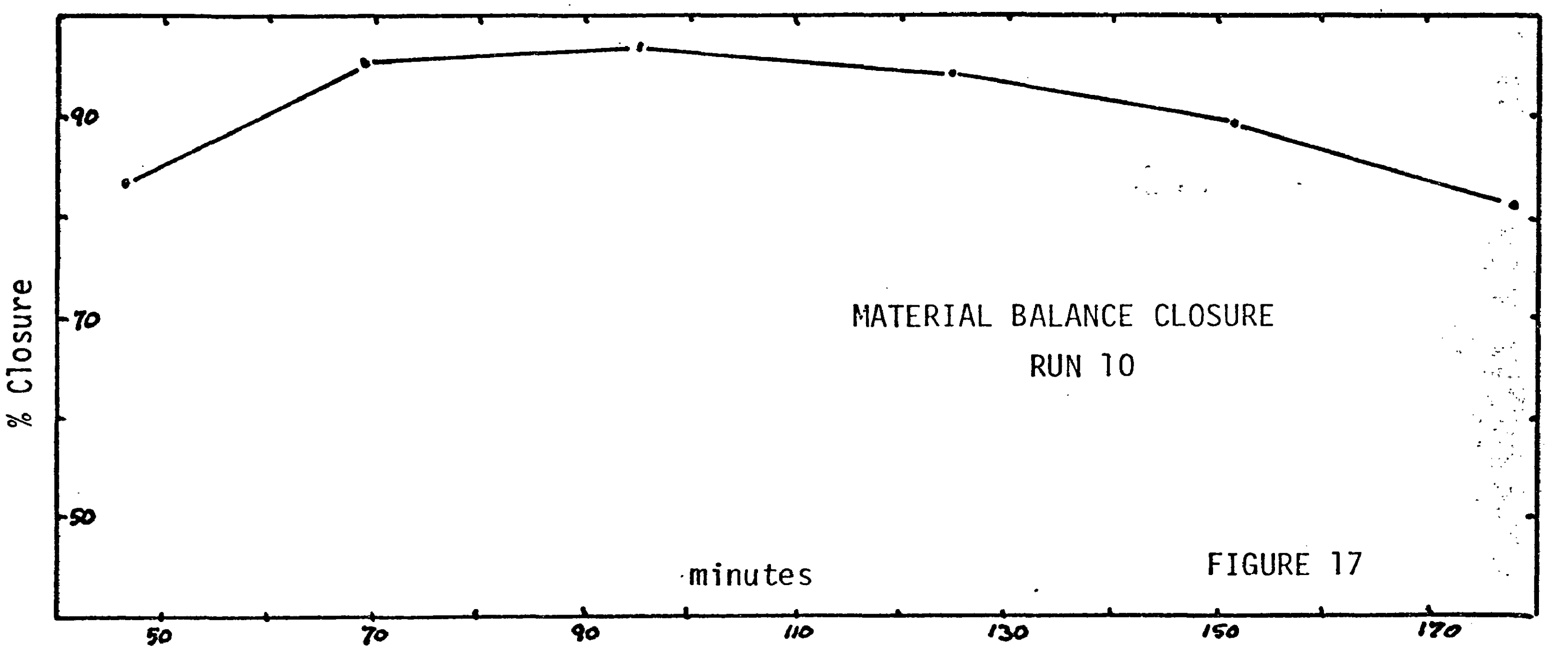

FIGURE 17

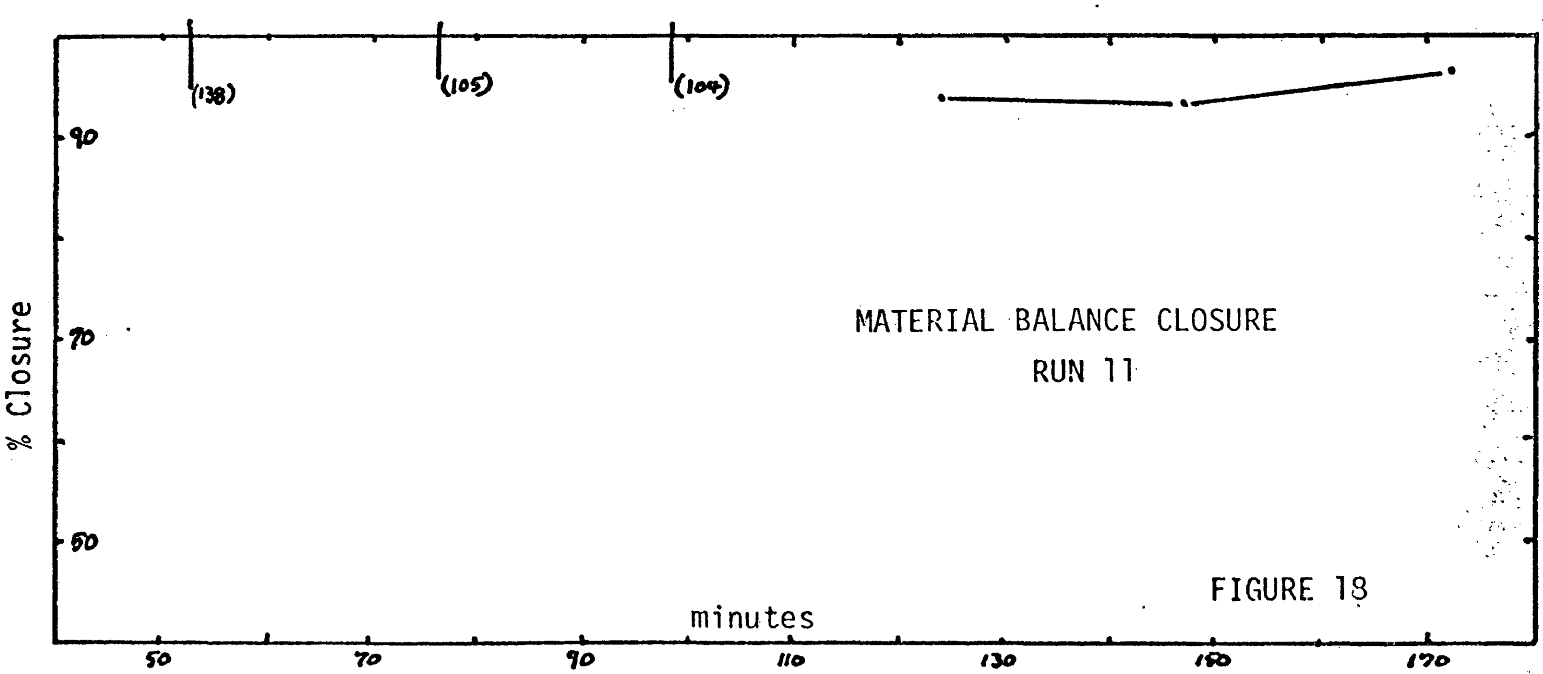

FIGURE 18

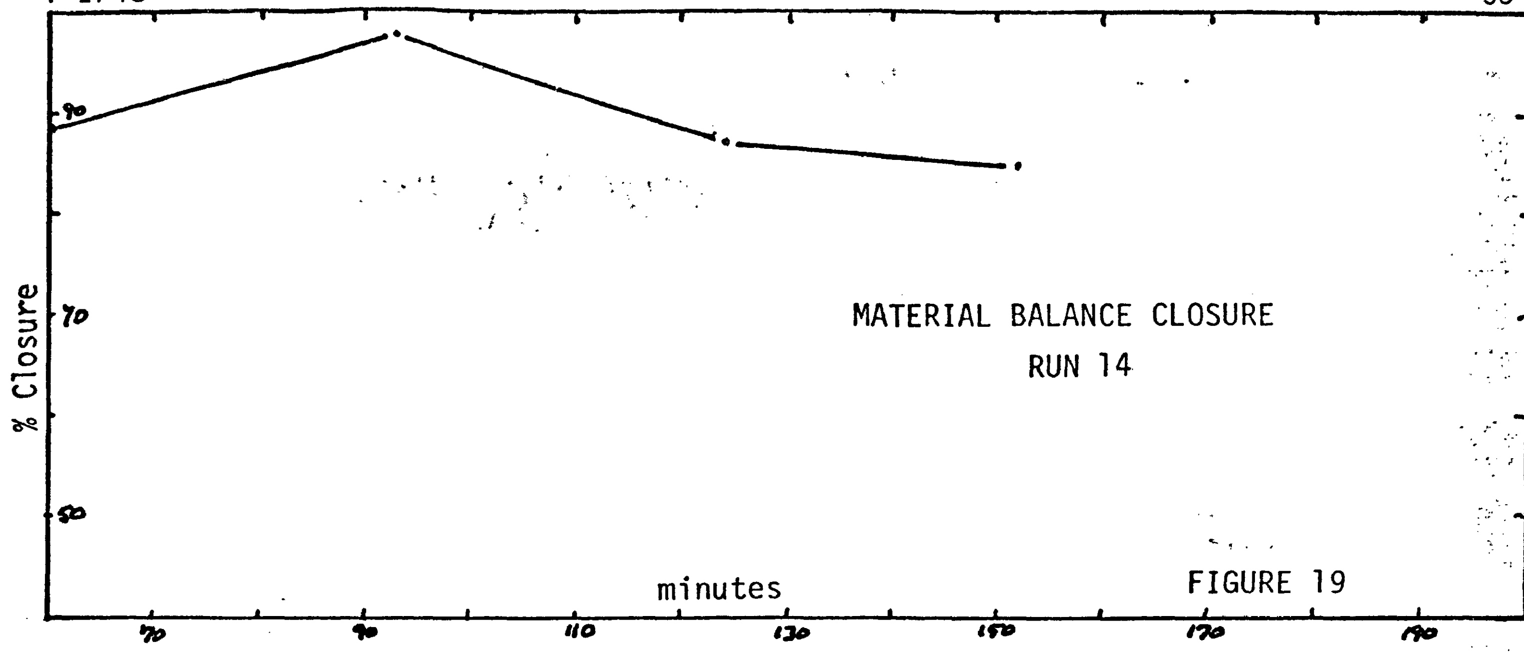

FIGURE 19

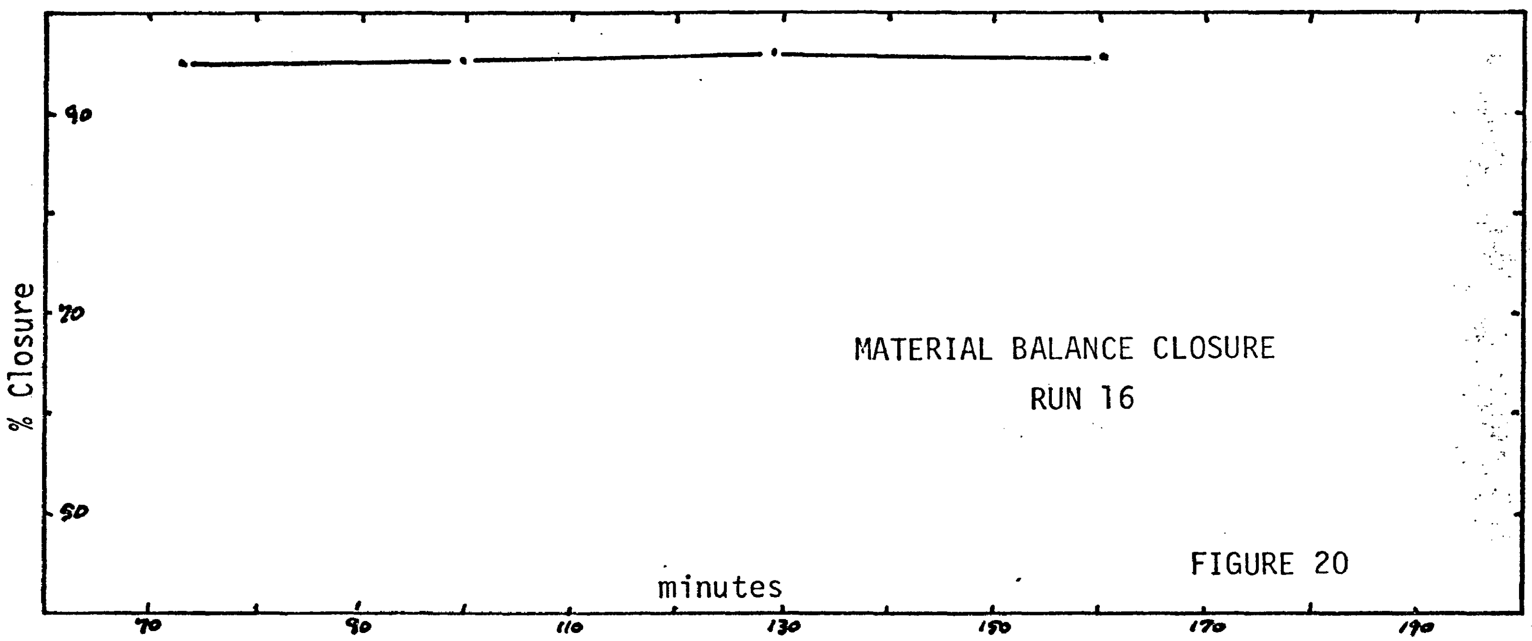

FIGURE 20

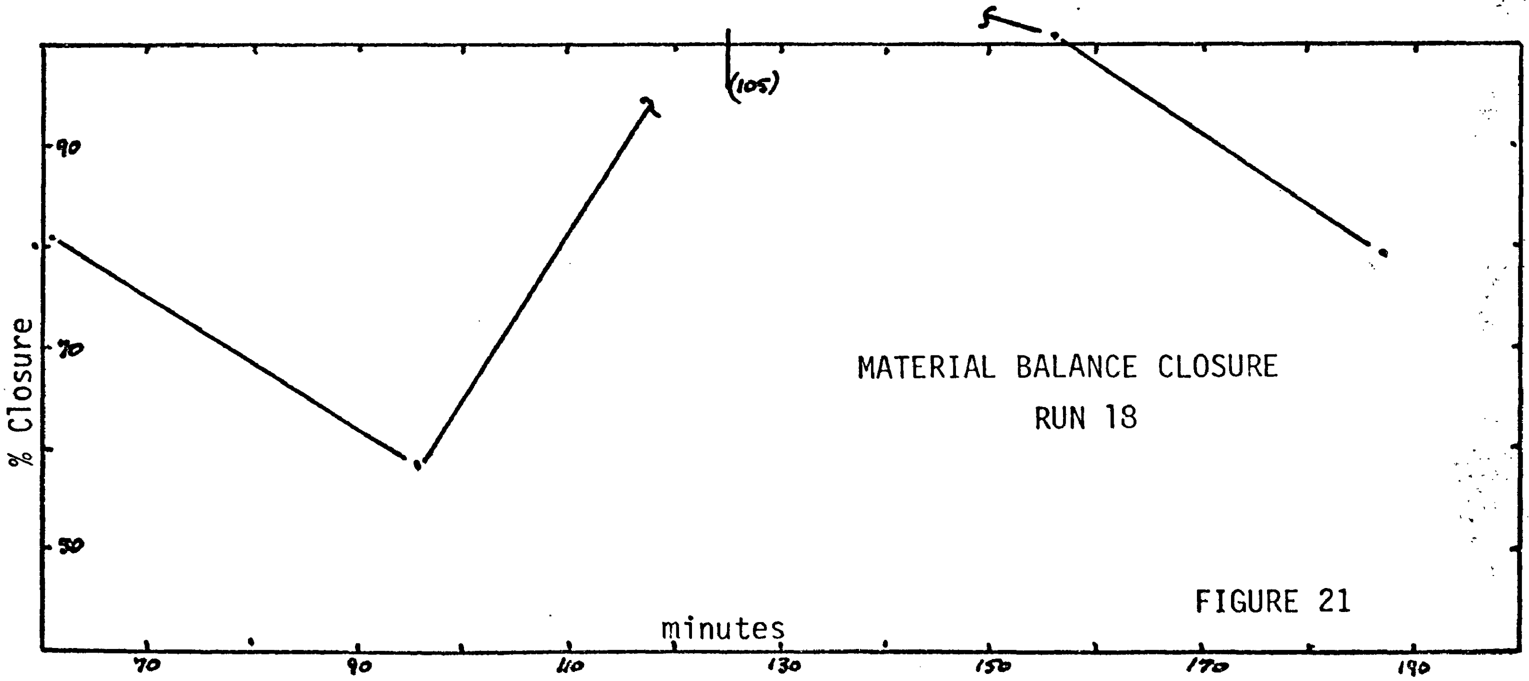

FIGURE 21

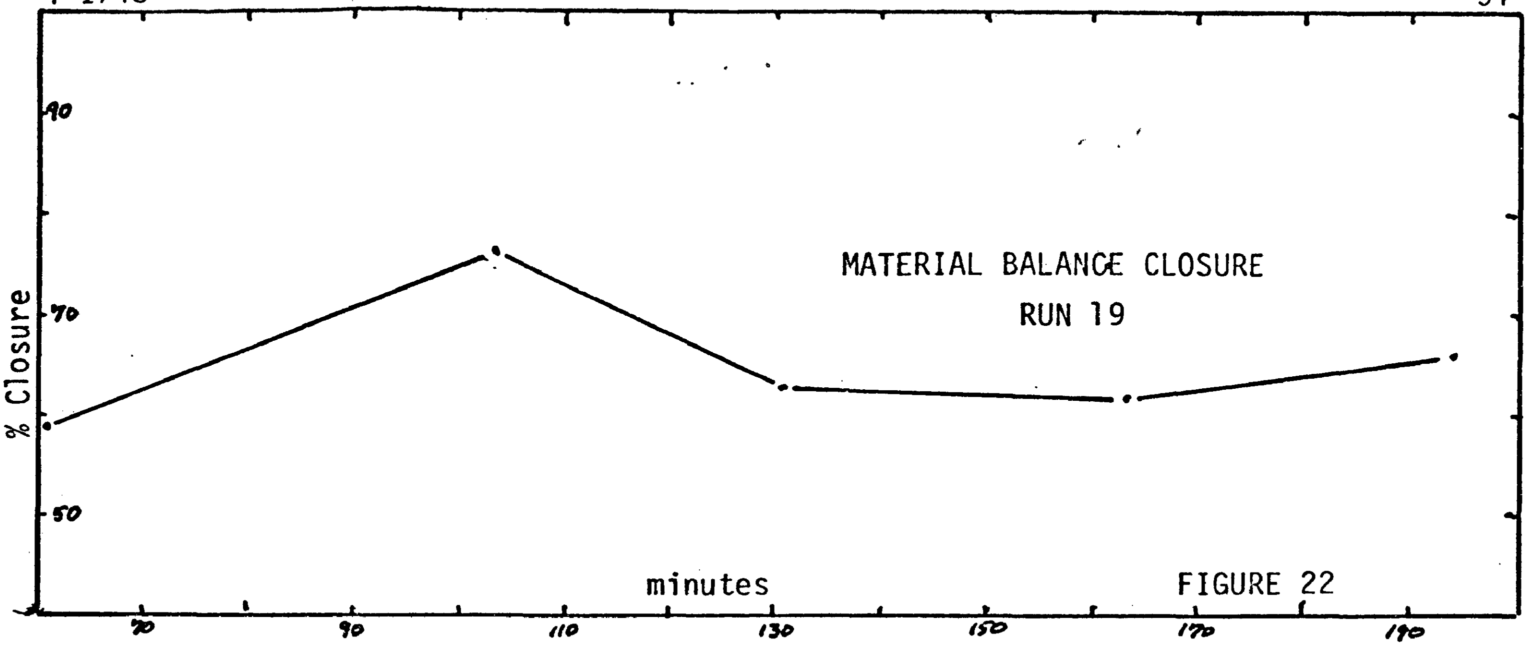

FIGURE 22

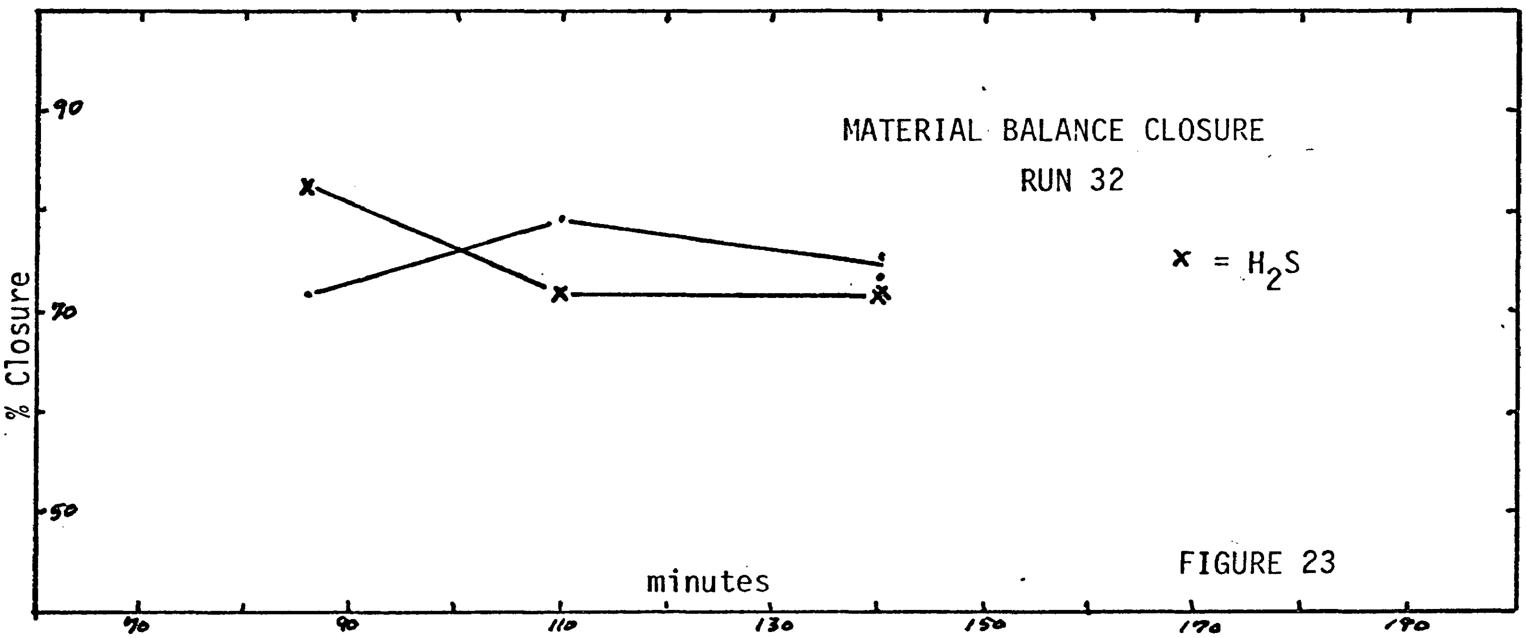

FIGURE 23

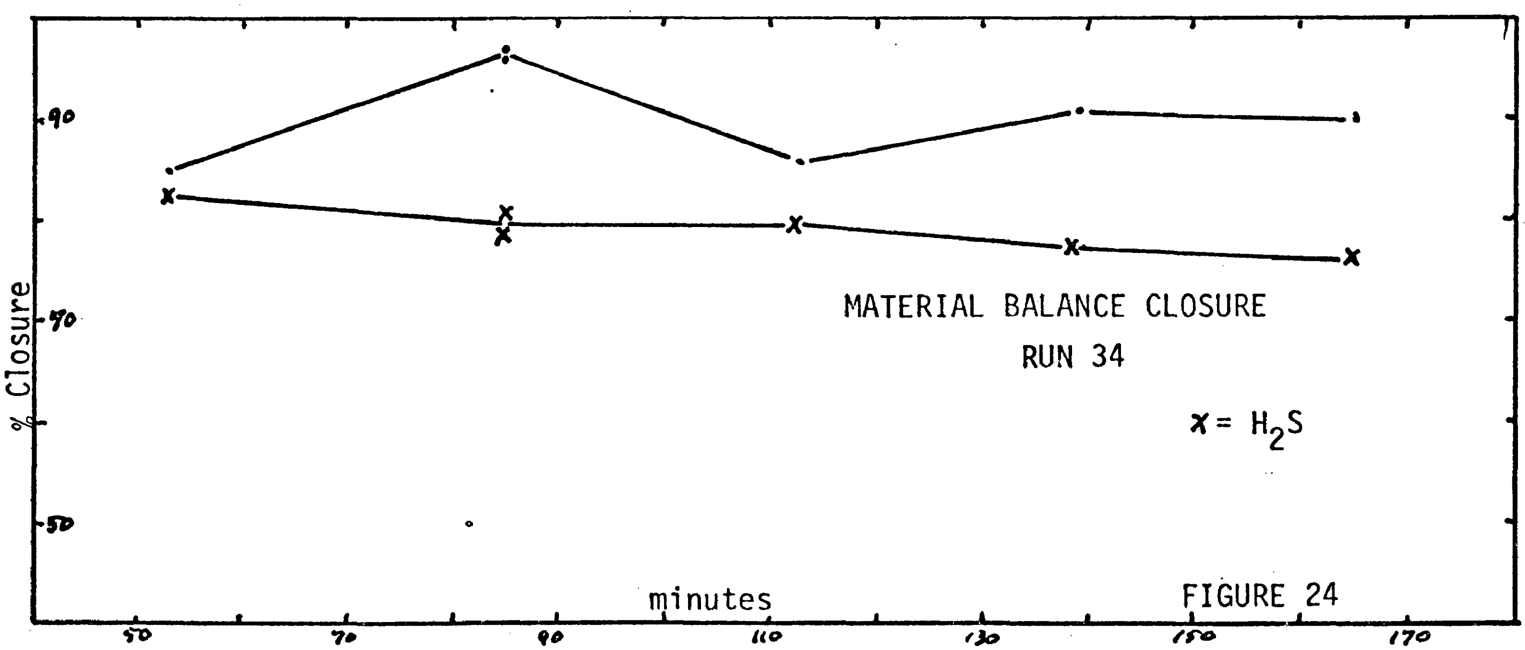

FIGURE 24

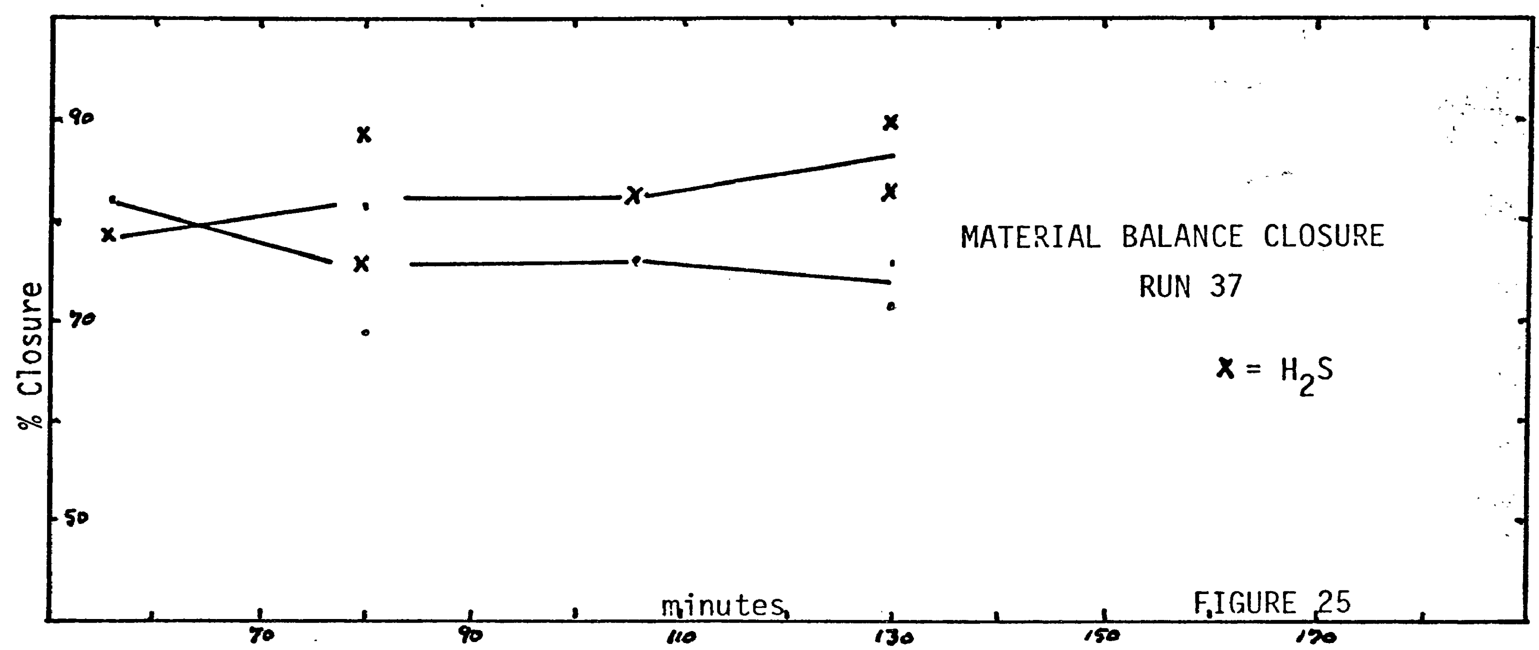
% Closure
90
70
50
MATERIAL BALANCE CLOSURE
RUN 37
X = H_2S
minutes
70
90
110
130
150
170

FIGURE 25

problem of interrelation of thiophene and H_2S concentration, but difficulties are still present in runs 32,34,and 37, since in those runs H_2S still varies directly with thiophene conversion. The steel packing used in runs 9-19, however, reacts with a portion of the H_2S, serving to de-couple the rates of change of thiophene and H_2S.

A linearization of equation (23) by algebraic rearrangement gives

$$(-C_A/r)^{1/n} = 1/k^{1/n}+(K_A/k^{1/n})C_A+(K_B/k^{1/n})C_B \qquad (29)$$

Substitution of thiophene for component A and H_2S for component B yields the linearized model

$$(-C_T/r)^{1/n} = 1/k^{1/n}+(K_T/k^{1/n})C_T+(K_S/k^{1/n})C_S \qquad (30)$$

or,

$$(-C_T/r)^{1/n} = a + bC_T + cC_S \ . \qquad (31)$$

Similarly, equations (25) and (26) linearize to

$$(-C_TC_S/r) = a + bC_T + cC_S + dC_TC_S \qquad (32)$$

where, for equation (25), d is forced to zero. Since d is equal to b times c, equation (26) must be investigated by non-linear regression.

The difficulties cited by many authors (see again the summary by Hunter and Kittrell (68)) stem from the fact that the independent variables are used to generate a dependent variable by computational means, and that several assumptions implicit in linear regression analysis (43) are not always met:

1) Errors in the dependent variable are normally distributed with a mean of zero,
2) These errors have the same variance, independent of the values of the independent variables, and
3) The independent variable values are controlled or observed without error.

These objections can be minimized by a combination of statistical design of experiments and either weighted linear regression analysis or non-linear regression analysis.

In this series of experiments, the following steps were taken to minimize statistical problems:

1) Interdependence of thiophene and hydrogen sulfide concentrations was minimized by
   a. conducting experiments with, and without, extra H_2S addition, and
   b. using iron packing in some runs, which selectively removed a portion of the hydrogen sulfide without affecting the hydrogenolysis reaction sequence. This prevented correlation of H_2S and thiophene concentrations due to the sulfur material balance.
2) Randomized testing was conducted to investigate the importance of these potentially significant factors:
   a. high H_2S concentration
   b. low pump circulation rate
   c. high n-pentane concentration
   d. low temperature.

Table 2 describes the seventeen models investigated. Results are summarized qualitatively in table 2 and, for the statistically significant models with positive adsorption coefficients, quantitatively in table 3. In order to examine low-H_2S data separately, seventeen regression analyses were run on low H_2S data only, seventeen more were run on all data together, and an additional fifteen analyses were run on the high-H_2S data (half-order models were omitted). Models are compared by the ratio of regression sum-square error divided by its degrees of freedom, divided by the error sum-square-error divided by its degrees of freedom. If all assumptions required for linear regression are met, this ratio is F-distributed. Although the assumptions are not strictly true, nonetheless the ratio is a useful means of evaluating goodness of fit of the models.

The negative value for the H_2S adsorption coefficient obtained by regression analysis using equations (30) suggests enhancement. Equation (32) in several forms was successful in fitting the data, furthering the enhancement conclusion.

<u>Temperature Effects</u>

Table 3 also contains linear regression coefficients for low temperature runs 18 and 19. In combination with runs 9-16, these data can be used to estimate Arrhenius activation energy, $-\Delta H$, from the expression

$$k_i = k_0 e^{-H/RT} \quad . \tag{33}$$

Models 5 for low and for high H_2S data, both power-law models, gave activation energies of -10.3 and -10.6 kcal/gm mole respectively. Owens and Amberg (95) report an overall activation energy of -25 kcal/gm mole for clean-surface thiophene hydrogenolysis.

On the basis of having either a negative adsorption coefficient in low temperature runs or an activation energy of the wrong sign, all of the other statistically significant kinetic models investigated except the two mentioned above are rejected. Results are summarized in table 4. Figures 26 and 27 are plots of predicted-versus-actual rate data using the two satisfactory models. In figure 27, variation in slope of the experimental data is small, and the scatter in measured rates is not present in predicted values. As can be seen by plotting both predicted and experimental rate as a function of time (such as in figure 28), predicted and actual rates match well.

Statistically Acceptable Models

The acceptable models are:

$$-r_T = k_{low}\, C_T^{.503}\, C_S^{.227} \qquad \text{(low } H_2S\text{)} \qquad (34)$$

$$-r_T = k_{high}\, C_T^{.108}\, C_S^{-.103} \qquad \text{(high } H_2S\text{)} \qquad (35)$$

with values of k_{low} and k_{high} listed in table 3. Note that thiophene reaction order decreases as the amount of hydrogen sulfide is greatly increased. The role of H_2S within each of the two treatments differs: the positive exponent in the low H_2S treatment indicates enhancement of the reaction rate, but the negative exponent in the high H_2S treatment represents a retarding effect. These results reinforce the statements in the "Concentration-Time Data" section above on the shift from first order to zero order in thiophene, and on the enhancement effect.

TABLE 2

KINETIC MODELS INVESTIGATED

$$-r = \frac{a\, C_T^{N1}\, C_S^{N2}}{(1+bC_T^{N3}+cC_S^{N4})^{N5}}$$

	Model No.	N1	N2	N3	N4	N5	Significance
a		1	1	1	1	1	-
b	1	1	1	1	1	2	**
c	5	Vbl	Vbl	0	0	0	**
d		½	0	1	1	1	-
e		½	0	0	1	1	-
f		0	0	1	1	1	-
g		1	1	1	0	1	-
h	2	1	1	1	0	2	**
i	3	1	1	0	1	1	**
j	4	1	1	0	1	2	**
k		1	1	0	0	0	-
l		1	0	1	1	1	-
m		1	0	1	1	2	-
n	6	1	0	1	0	1	*X
o	7	1	0	1	0	2	*X
p		1	0	0	1	1	-
q		1	0	0	1	2	-

Significance:
- \- Not statistically significant, or adsorption coefficient negative
- ** Statistically significant; all coefficients positive
- * Coefficients positive; not statistically significant
- X High H_2S only, statistically significant

TABLE 3

RESULTS OF REGRESSION ANALYSIS

Model Number	All or Low Sulfur Data	Temp. °C	F-Statistic	a	N1	N2	b	N3	c	N4	N5
1	Low	275	40.28	150.18	1	1	0.9154	1	2.931	1	2
	All		- Coefficient Negative -								
	High		16.67	1268.5			20.959		1.8335		
	Low	256	.422	53.04			0.0749		1.255		
	All		- Skipped -								
	High		3.68	5.019			.5875		.1457		
2	Low	275	5.18	33.432	1	1	0.8842	1	-	0	2
	All		7.20	160.625			7.9134		-		
	High		- Not Significant -								
	Low	256	.009	27.054			- .0097	Negative Coefficient			
	All		.22	3.365			.3934				
	High		- Coefficient Negative -								
3	Low	275	38.80	443.87	1	1	-	0	70.301	1	1
	All		154.72	32.783					4.5719		
	High		- Not Significant -								
	Low	256	.866	40.44					1.9295		
	All		98.58	42.36					8.0529		
	High		- Coefficient Negative -								
4	Low	275	49.40	57.081	1	1	-	0	1.9604	1	2
	All		232.11	13.461					0.2833		
	High		- Not Significant -								
	Low	256	.909	39.664					.8057		
	All		217.5	33.496					.7148		
	High		- Coefficient Negative -								
5	Low	275	13.75	6.5986	.5028	.2265	-	-	-	-	0
	All		21.28	5.8363	.4367	.1129					
	High		16.67	9.7532	.1080	- .1034					
	Low	256	-	4.702	.5028	.2265	Exponents fixed for low temperature data				
	All		-	6.161	.4367	.1129					
	High			6.876	.1080	- .1034					

TABLE 3 (cont'd)

Model Number	All or Low Sulfur Data	Temp. °C	F-Statistic	a	N1	N2	b	N3	c	N4	N5
					1	0		0		1	1
6	Low	275	Not Significant								
	All										
	High		18.57	53.83			-		6.329		
	Low	256	Skipped								
	All										
	High		23.77	9.653					0.8098		
7	Low	275	Not Significant		1	0		0		1	2
	All										
	High		18.84	23.07			-		.7421		
	Low	256	Skipped								
	All										
	High		22.04	2.963			-		.2780		

TABLE 4

ACTIVATION ENERGIES

$$k = k_o e^{k_1/RT}$$

Model No.	Low H_2S or All Data	Overall $l_n k_o$	Overall K_1 Kcal/mole	Thiophene Adsorption $l_n k_o$	Thiophene Adsorption K_1 Kcal/mole	H_2S Adsorption $l_n k_o$	H_2S Adsorption K_1 Kcal/mole	Acceptable ?
1	Low	33.988	- 31.55	-	Negative	-	-	
	All, High	Reject Previously						
2	Low	Reject Previously						
	All	112.70	-117.20	-	Negative	-	-	
	High	Reject Previously						
3	Low	72.80	- 72.64	-	-	-	Negative	
	All	-	Positive	-	-	-14.24	17.165	
	High	Reject Previously						
4	Low	- 3.631	-11.039	-	-	-	Negative	
	All	-	Positive	-	-	-	-	
	High	Reject Previously						
5	Low	11.323	-10.276	-	-	-	-	X
	All	-	Positive	-	-	-	-	
	High	12.009	-10.597					X
6	Low, All	Reject Previously						
	High	51.84	-52.1	-	Negative	-	-	
7	Low, All	Reject Previously						
	High	30.05	-29.3	-	Negative	-	-	

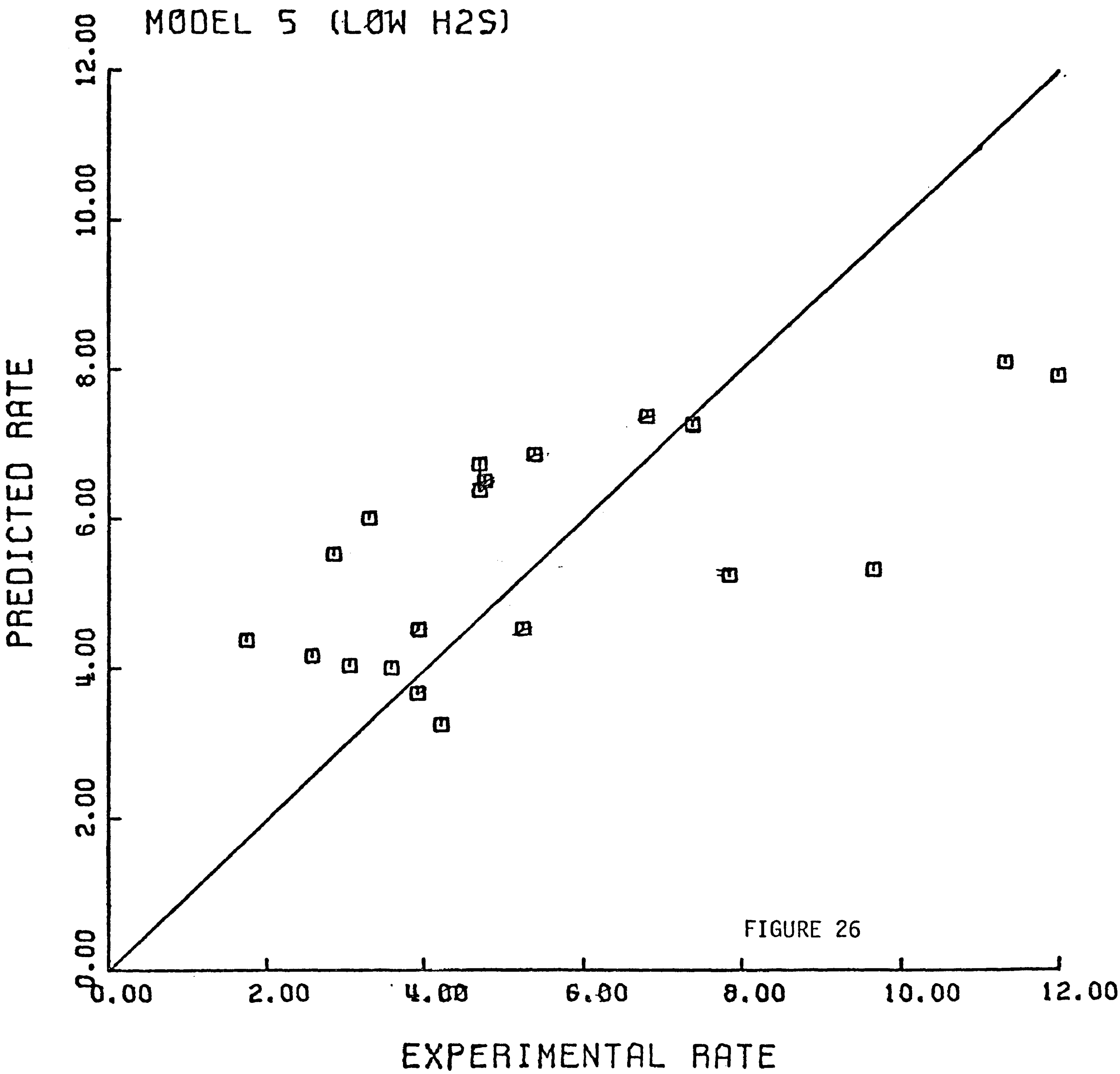
MODEL 5 (LOW H2S)
PREDICTED RATE
EXPERIMENTAL RATE
0.00
2.00
4.00
6.00
8.00
10.00
12.00

FIGURE 26

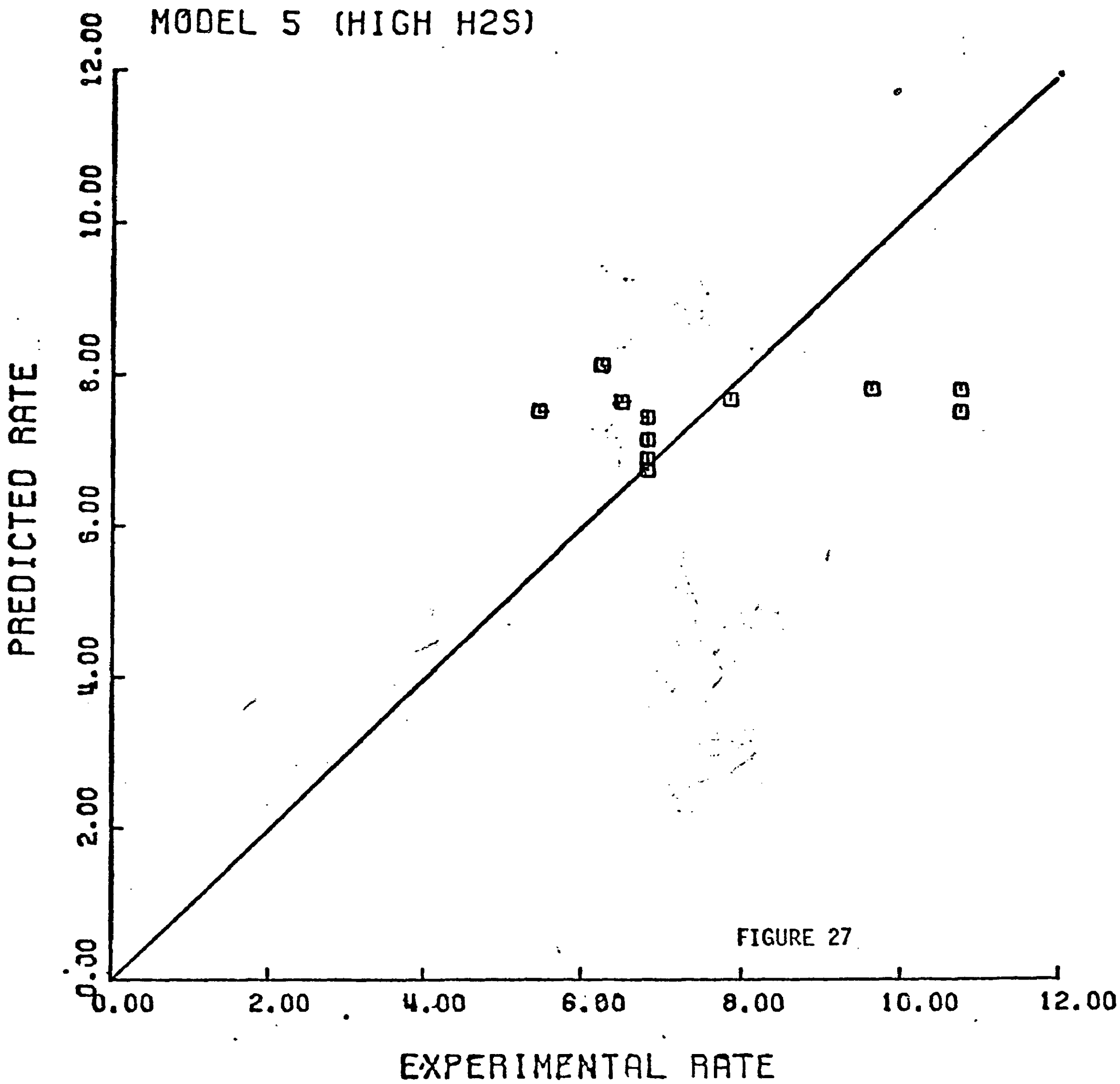

FIGURE 27

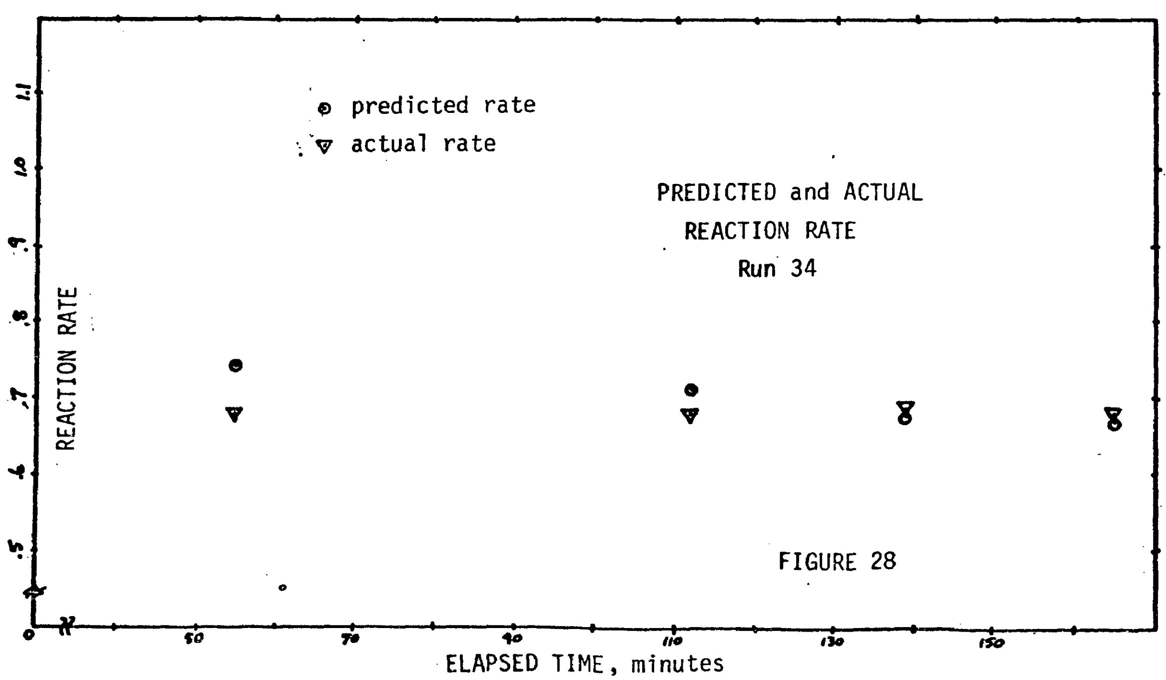

FIGURE 28

CONCLUSIONS

Under conditions of high hydrocarbon concentration, the kinetics of thiophene hydrogenolysis exhibit characteristics different from those examined under usual laboratory conditions. Hydrogen sulfide serves to enhance the hydrogenolysis reaction under conditions of a large concentration of n-pentane. However, the reaction is hindered by high concentrations of hydrogen sulfide, and possibly by thiophene. Activation energies of -10.3 to -10.6 kcal/gm mole are exhibited by power-law fits to thiophene reaction rate.

ERROR ANALYSIS

All compositions are determined relative to the concentration of n-pentane. Peak height 84/72 ratio is reproducible to +/- 4.8%, corresponding to a precision level of +/- 10^{-4} gram moles per liter of thiophene at starting concentration. Calibration on a known mixture of thiophene and n-pentane, compared to spectra predicted by use of API data,showed a significant deviation from the predicted value. Likewise, H_2S calibration deviated significantly from its predicted value. Reproducibility of hydrogen sulfide concentration is +/-3%.

Accuracy of all concentrations is dependent on the accuracy of that of n-pentane, which is determined by weight and reactor volume. With 1.5% uncertainty in reactor volume, the accuracy of n-pentane concentration is approximately +/-2%, or about 10^{-3} gram moles per liter. The accuracy of thiophene and H_2S measurements, then, is +/- 6.8% and +/- 5% respectively.

RECOMMENDATIONS

This study is conducted at low temperatures compared with commercial operation, due to mixing and equipment considerations. Metal gaskets and a larger diaphragm pump, preferably with a stainless steel diaphragm and high temperature hydraulic fluid, would afford greater mixing and more rapid reactions could be studied. With a smaller diameter reactor, turbulent mixing could be obtained. With KEL-F or metal gaskets, higher temperatures could safely be achieved in the equipment.

One possible area of investigation is catalytic reaction in pulsed-flow systems. The diaphragm pump offers a means of varying pulse size and flowrate over a wide range of conditions, and the differential character of the small catalyst charge simplifies the mathematical modelling effort considerably.

Along more traditional lines of investigation, the batch recirculated reactor is well-suited to catalyst evaluation work and mechanistic studies, due to the ability to generate kinetic adsorption and reaction data rapidly in comparison with steady-state methods. The ability to measure adsorbed concentrations of reactants is a benefit not easily obtainable in flow reactors.

APPENDIX I

Reactor Design

Design Conditions

The reaction equipment is designed to obtain kinetic data on the hydrogenolysis of thiophene, using available equipment, through batch operation at commercial pressures and over a typical range of sulfur concentrations. Conditions chosen for the design are:

Temperature- 250°C (limit: teflon melting point)

Pressure- 1000 psia

Feed composition- 2% Thiophene in n-pentane (by weight)

Design hydrogen-to-hydrocarbon ratio is 5:1; the actual ratio is large enough during experimental runs that hydrogen consumption can be ignored. Major available equipment around which the design is formulated includes a Lindberg Heviduty 3000 watt three-zone furnace with the middle zone controlled by a proportional controller manufactured by the same company, a Lapp Pulsafeeder model LS-20 diaphragm pump capable of up to 900 cm^3 per hour pumping rate, and a Consolidated Electrodynamics Corporation model 21-130 mass spectrometer donated by Marathon Oil Company and modified for direct current operation of the filament. The tubular reactor insert for the furnace is 1.85cm in inside diameter and 84cm long.

Amount of Catalyst Required

For design purposes, data and a rate expression for a cobalt-molybdate catalyst determined by Roberts[25] are used. The rate of thiophene disappearance is taken as:

$$-dN_r/dt = kP_TP_4/(1 + K_TP_T + K_SP_S)^2$$

where, at 250°C,

N_r = thiophene concentration, gm moles/gm cat

$k = 0.164 \times 10^{-8}$ gm moles/gm cat-min (mmHg)^2

$K_T = 0.031$ mm^{-1}Hg

$K_S = 0.018$ mm^{-1}Hg

P_T = partial pressure of thiophene, mm Hg

P_S = partial pressure of hydrogen sulfide, mm Hg

P_H = partial pressure of hydrogen, mm Hg

V = volume of reactant, liters

T = 523°K

R = gas constant

t = time, minutes

Assuming this rate expression is good at a total pressure of 1000 psia, and representing H_2S partial pressure by

$$P_S = P_{T,o} - P_T$$

where $P_{T,o}$ is the partial pressure of thiophene at the start of the reaction, the partial pressure of hydrogen (constant throughout the reaction) of 43080 mm Hg may be substituted into the rate expression, to yield:

$$r_T = -7.065_{No}^{-5}P_T/(1 + .013P_T + .018P_{T,o})^2$$

gm moles/gm cat-minute

If the starting composition was such that 2% of the hydrocarbon was thiophene and, for a 5:1 H_2/hydrocarbon ratio, the integrated expression is

$$t - t_o = 4.34 \times 10^{-4}\{(1.804 + .00919\ P_{Tf})^2 + 6.508(\ln P_{Tf}) + .03316(P_{Tf}) - 38.594\}\ V$$

Half-Life of Reaction

For half of the thiophene to have disappeared, P_{Tf} = 43.1 mm Hg and

$$t_{1/2} = 7.51 \times 10^{-3}V \qquad \text{minute-gm. catalyst}$$

where V is the reactor and recirculation system volume, in cubic centimeters..

Estimation of Diffusional Resistance

In order for the rate-controlling step to be reaction or adsorption, diffusional resistance must be at a minimum. This is indicated by a small difference between bulk and surface compositions.

The mass transfer coefficient, K_m, is estimated from the "j-factor" (31):

$$j_D = \left(\frac{K_m\rho}{G}\right)\left(\frac{\mu}{\rho D_{eff}}\right)^{2/3}$$

which is a function of Reynolds number:

$$R_e = \left(\frac{d_p G}{\mu}\right).$$

Here,

K_m = mass transfor coefficient, cm/sec

$\mu = 1.33 \times 10^{-4}$ gm/cm sec @ 528°K (see below)

Deff = .354 cm^2/sec @ 528°K (see below)

and ρ is estimated as the density of hydrogen at 528°K and 1000 psia (48) equal to $3.42 \times 10^{-3} gm/cm^3$.

The mass flux, G, is determined by the circulation rate. Assuming that the pump operates at 100°C, the density is $5.57 \times 10^{-3}/cm^3$ and G becomes 4.61×10^{-4}gm/cm^2 sec with the Lapp model LS-20 pump. For 1/8" diameter particles, the Reynolds number is equal to 1.1. From an extrapolation of the plot of j_D as a function of Reynolds number[31]

$$j_D = 6.0$$

so

$$K_m = \left(\frac{\rho Deff}{\mu}\right)^{2/3} \frac{G}{\rho} j_D$$

or 3.53 cm/sec.

The rate at which thiophene is transported from the bulk phase to the surface is equal to the reaction rate. At the starting composition, the most rapid rate of disappearance occurs. If a stagnant film is present, the concentrations (and thus, the reaction rate) will be less. Under these conditions, the rate of reaction is evaluated as 3.08×10^{-4} gm moles/gm cat-min. The concentration gradient due to diffusion through the surface layer is:

$$K_m\, a_m(C_{bulk} - C_{surface}) = -r_T$$

where a_m = 180 m^2/gm catalyst for HDS-3A, yielding a concentration gradient from bulk phase to surface of 9.96×10^{-13}gm moles/cm^3, which is negligible.

Temperature Gradient within the Catalyst

The heat of reaction for

$$\text{thiophene} + 4H_2 \rightarrow \text{butane} + H_2S$$

is, from heats of formation[49], [53], [54], -6.81 kcal/gm mole. Supposing no heat could be conducted away from the catalyst during the reaction, the adiabatic temperature rise would be, during the half-life, 24.7°C under design conditions.

Clearly, heat effects must be examined. As an approximation, considering the heat to be generated uniformly throughout the catalyst:

$$\frac{1}{r^2}\frac{\partial}{\partial r}(r^2 q_r) = S'''$$

yields, on integration,

$$T - T_o = \frac{S'''}{6K}(R^2 - r^2)$$

With a starting temperature of 250°C and a thermal conductivity of .68 x 10^{-3}cal/cm sec °C[58], a heat generation rate of, from above, 1.47 x 10^{-3}cal/sec-gm catalyst, the temperature at the center of a catalyst particle is calculated to be 250.25°C.

It may be concluded that the temperature gradient within a catalyst particle is insignificant.

APPENDIX II

Physical Property Prediction And Design Validation

Viscosity

From the Handbook of Chemistry and Physics, 44th ed.(1962), values for viscosity of hydrogen and n-pentane are tabulated in table II-1. Viscosities for 250°C are predicted by extrapolation using Chapman-Enskog theory[38] in the form

$$\mu_{250} = (\mu_T)\ (523/T)^{1/2}\ \Omega_{\mu,T}/\Omega_{\mu,250°C}$$

where T is the measurement temperature in degrees Kelvin, μ is the viscosity, and $\Omega_{\mu,T}$ is the collision integral value at temperature T [61]. Predicted viscosities of the pure compounds are also tabulated in table II-1.

Mixture viscosity is predicted by the method of Wilke as outlined in Bird, Stewart and Lightfoot[38]:

$$\mu_{mix} = \sum_i (X_i\mu_i/(\sum_j X_j\Phi_{ij}))$$

where $\Phi_{11} = \Phi_{22} = 1$ and

$$\Phi_{ij} = \frac{1}{\sqrt{8}}\left(1 + \frac{M_i}{M_j}\right)^{-1/2}\left(1 + (\mu_i/\mu_j)^{1/2}(M_j/M_i)^{1/4}\right)^2$$

For a 5:1 H_2/hydrocarbon ratio, the mixture viscosity at 250°C is 143.0 micropoise.

Heat Capacity

Heat capacities for hydrogen and n-pentane at 250°C are computed by evaluating polynomials in temperature. For hydrogen, C_p = 6.46

cal/gm mol °C, and for n-pentane, C_p = 45.13 cal/gm mol °C.

Bulk Diffusivity

The Chapman-Enskog formula for bulk diffusivities[32] relates diffusivities for two components to temperature, molecular weight, pressure, and Lennard-Jones potential parameters. Where the parameters are not tabulated, they are computed by[32]

$$\sigma = 1.18\, V_b^{1/3}$$

$$\frac{k_B T}{\xi} = 1.30T/T_c$$

where V_b is the molar volume at normal boiling point, cm³/g mole, and T_c is the critical temperature. Molar volume may be estimated with Kopp's law by adding increments due to atomic contributions[62]. Predicted bulk diffusivities are tabulated in table II-2.

Knudsen Diffusivity

Molecular, or Knudsen, diffusivity is estimated by[32]

$$(D_K)_A = 9.70 \times 10^{3}(a)\left(\frac{T}{M_A}\right)^{1/2}$$

where a is the pore radius in centimeters, M_A is the molecular weight, and T is in degrees K. Values for selected compounds are tabulated in table II-2, and are seen to be about two orders of magnitude less than the corresponding bulk diffusivities. For the pore radius, Wheeler's expression,

$$a = \frac{2v_g}{S_g}$$

is used, with v_g representing the void volume per gram of catalyst and S_g being the specific surface area. Properties of American Cyanamid HDS3A catalyst are summarized in table II-3.

Combined and Effective Diffusivities

The combined diffusivity is a combination of bulk and Knudsen diffusivities, adjusted to account for stoichiometry:

$$D_A = \frac{1}{(1 - \propto y_a)/D_{AB} + 1/(D_K)_A}$$

where

$$\propto = 1 + N_A/N_B$$

and N_A and N_B are stiochiometric coefficients representing flow in (A) and out (B) of the catalyst. For the net reaction under consideration, five molecules (thiophene plus four hydrogens) flow in and two molecules (H_2S and butane) flow out. For the maximum design condition of .0167 mole fraction of reactant or product, combined diffusivities are as summarized in table II-2.

Satterfield, in a review of literature on the parallel-pore model,(59) recommends a tortuosity factor, δ, of 2 to 6 for a similar nickel-on-alumina catalyst to obtain the effective diffusivity:

$$D_{eff} = \epsilon_A D_A/\delta$$

Computed values are summarized in table II-2.

Surface Diffusion

The effects of surface diffusion are estimated from Sladek's work (60), which relates heat of adsorption, temperature, and bond type. Schneider and Smith(60) quote heats of adsorption of hydrocarbons on various substrates at from 3 to 5 kcal/g mole. This gives a range of

$$.005 < D_s < .01$$

which is two orders of magnitude less than the combined bulk + Knudsen diffusivity. Thus, surface diffusivity is ignored for hydrocarbon species under design conditions.

Dew Point Calculation

A mixture such as thiophene and n-pentane in hydrogen is highly non-ideal, and accurate phase equilibrium prediction is difficult. An estimation method based on work of Lenoir[63] provides an estimate of dew point. Using as an approximate composition 2% thiophene in n-pentane and an unknown amount of hydrogen, the effective boiling point of the heavy components is estimated at 99°F. The light component EBP is taken as -393°F, which leads to a convergence pressure of 10,000 psi at 150°F. At that temperature, equilibrium K-values are .030 for thiophene, .095 for n-pentane, and 16. for hydrogen. At the dew point,

$$\Sigma x_i = \Sigma(y_i/K_i) = 1.0$$

and

$$\left[\frac{.02}{.030} + \frac{.98}{.095}\right]x + \frac{(1-x)}{16} = 1.0$$

or x = .086, so a hydrogen-to-hydrocarbon ratio of higher than about 12:1 is necessary to remain above the dew point of the mixture at 150 degrees Fahrenheit.

Effectiveness Factor

The catalyst effectiveness factor is calculated by the method of Roberts and Satterfield (123). Using a modified Thiele modulus,

$$\phi_m = L(k/D_A)^{1/2}$$

where L is the volume-to-surface ratio in centimeters, k is the experimentally-observed reaction rate constant, in (gm mole-seconds)$^{-1}$, and D_A is the effective diffusivity in cm^2/second, experimental data were used to obtain a value of ϕ_m equal to 9.4 x 10^{-11} (dimensionless). Roberts' relation between effectiveness factor, η, and Thiele modulus, ϕ_m, was obtained by numerical integration using Langmuir-Hinshelwood kinetic expressions for single reactant models where adsorption of reactants and/or products is significant. The relationships are presented as plots of logarithm η as a function of logarithm ϕ_m. The value for the catalyst used in this study was off-scale to the left, corresponding to an effectiveness factor of unity.

Blank Runs

To demonstrate that thiophene does not react with iron or glass packing, mass 84/72 peak height ratio is regressed against elapsed time. For iron packing, runs 25, 26, and 27 (Appendix VII data) yielded no significant relationship between elapsed time and change in peak height ratio, which would indicate reaction. Runs 29 and 30, conducted over glass packing, yield no significant relationship either. Run 30 is almost significant; however, dropping one data point yields another, almost significant relationship indicating that thiophene is being produced rather than consumed. (This is thermodynamically prohibited.) It is concluded that thiophene does not react to significant extent over iron or glass packing in this study.

TABLE II-1

VISCOSITY AT 250°C, centipoise

	temp	$\mu x10^6$	Ω_T	Ω_{250}	$\mu x10^6_{250}$
Hydrogen	229°C	126p	0.798	0.793	130.1 poise
n-Pentane	100°C	84.1	1.518	1.302	116.1 poise

TABLE II-2

DIFFUSIVITIES AT 250°C, cm^2/sec

	$D_{AB}x10^2$	$(D_K)\cdot a$	D_A	D_{eff}
Thiophene	3.16	1.61	1.60	.354
Butane	2.48	1.94	1.92	.424
Butenes (ave)	2.38	1.97	1.95	.431
H_2S	5.07	2.53	2.52	.557

TABLE II-3

PROPERTIES OF HDS-3A CATALYST

Apparent bulk density, lb/ft^3	40.
Compacted bulk density, lb/ft^3	43.
Average diameter, in (cm)	.07 (.18)
Average length, in (cm)	.18 (.46)
Pore volume v_g, cm^3/gm	.6
Surface area, m^2/gm	180.
Void fraction	.774

TABLE II-4

THIOPHENE RUNS WITHOUT CATALYST

Run	# of Points	a	b	R^2	F	(F*)
25	5	-.000555	.558	.185	0.68	(10.13)
26	6	-.000581	.534	.257	1.39	(7.71)
27	9	-.000453	.516	.122	0.97	(5.59)
29	5	-.000219	.631	.049	0.16	(10.13)
30	7	-.000867	.449	.552	6.16	(6.61)
30 without 86 minute data	5	+.000525	.500	.730	8.11	(10.13)

Equation: $h_{84}/h_{72} = a + b(\text{time})$

R^2 is correlation coefficient

F* is critical F-statistic

APPENDIX III

Reaction Equilibrium Constants

At equilibrium the free energy of a reaction system

$$aA + bB \rightleftarrows rR + sS$$

is at a minimum, and can be expressed in terms of ratios of gas-phase mole fractions, fugacity coefficients, and system pressure expressed most often as an equilibrium constant:

$$-\frac{\Delta G^o}{T} = R\ \ln(K) \qquad \text{(III-1)}$$

The system free energy can also be expressed in terms of component free energies and enthalpies:

$$\frac{\Delta G^o}{RT} = \frac{\Delta G_o^o - \Delta H_o^o}{RT_o} + \frac{\Delta H_o^o}{RT} + \frac{1}{RT}\int_{T_o}^{T} \Delta C_p^o dT - \frac{1}{R}\int_{T_o}^{T} \frac{\Delta C_p^o}{T}\, dT \qquad \text{(III-2)}$$

where ΔH is the enthalpy difference between reactants and products, R is a gas constant, ΔC_p is a heat capacity difference between products and reactants at constant pressure, and T is the temperature. Subscript o denotes a standard state, and superscript o denotes pure component properties.

Heat Capacity Expressions

One method for developing heat capacity expressions is that of Rihani and Doraiswamy[55], in which contributions of various functional groups in a molecule are summed to give coefficients of the equation for that molecule. Multiplying each coefficient by the stoichiometric coefficient associated with that particular compound, and subtracting reactant values from product values, yields the coefficients used in equation III-2. Reid and Sherwood[55] recommend this method for hydrocarbons, to include thiophene. However, the method is not suitable for hydrogen or hydrogen sulfide; coefficients for these two materials were obtained from Himmelblau[64].

Absolute Enthalpies and Free Energies at Standard State

The absolute enthalpy and absolute free energy of a compound at a standard state are, respectively, its heat of formation and free energy of formation. Values of ΔH_f^o and ΔG_f^o are tabulated for many compounds (see, for example, API Project 44, or the short tabulations of Smith & Van Ness[65] or Hougen, Watson, and Ragatz[49]), but for some compounds it is necessary to resort to empirical means. The method used here is that of Souders, Mathews, and Hurd[56], which involves summing contributions due to various functional groups within a molecule.

Evaluation of Reactions

Prediction of the equilibrium composition resulting from a given reaction may be accomplished by proper substitution of stoichiometric coefficients, enthalpies, free energies and heat capacities into equation III-2. The reactions considered, stoichiometry, and results are outlined below and summarized in figure III-1.

Thiophene Disappearance

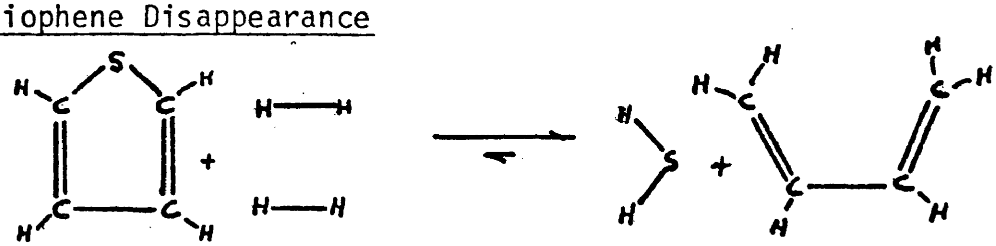

At 523°K, K equals 2.1×10^{11}, so the reaction favors products almost irreversibly.

Butadiene Disappearance

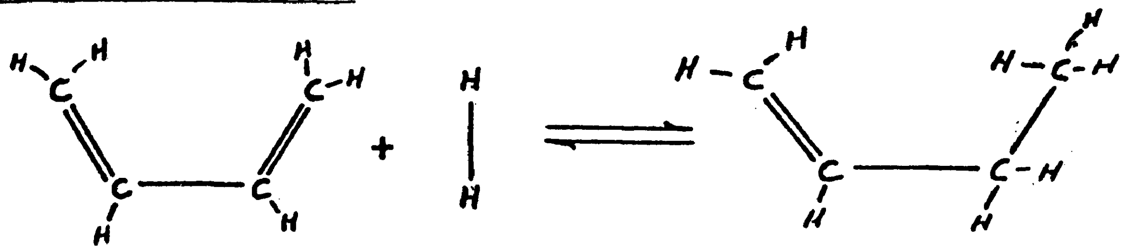

At 523°K, K equals 0.134. Noting that K may be expanded as

$$K = \left[\frac{y_{1Butene}}{y_{Butadiene}\, y_{H_2}}\right]\left[\frac{\Phi_{1Butene}}{\Phi_{Butadiene}\, \Phi_{H_2}}\right] \frac{1}{p}$$

it can be seen that higher pressure favors the product. At 500 psia,

$$[\gamma][\Phi] = 66.9$$

It must be noted here that since butadiene is being made irreversibly and, as will be seen later, 1-butenes are being used irreversibly, the equilibrium composition of 1-butene/butadiene mixtures can be of use only to show the thermodynamic possibility of thiophene-to-butane reaction schemes.

1-Butene - trans-2-Butene Isomerization

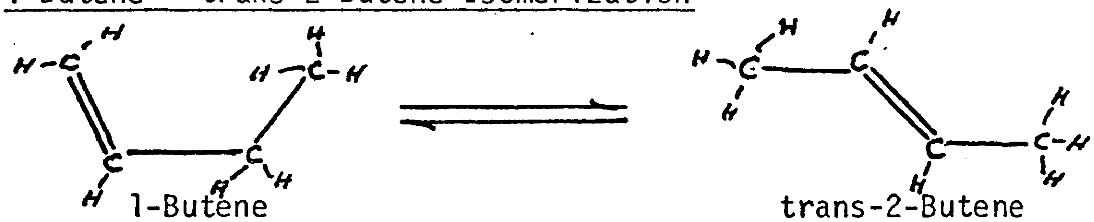

Equilibrium concentrations are the same order of magnitude (K = 3.87) at 523°K.

1-Butene - cis-2-Butene Isomerization

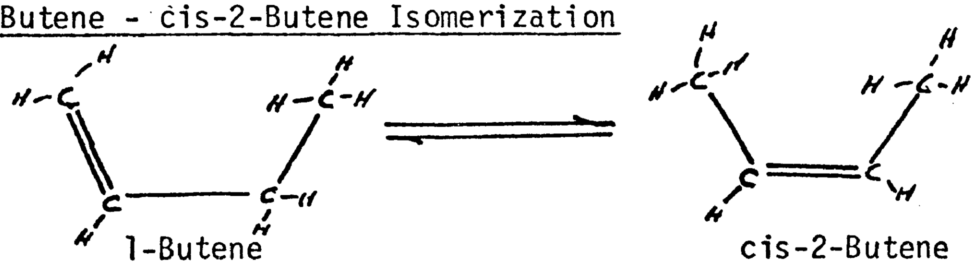

At 523°K, K equals 2.79, indicating that both isomers should be present in about the same order-of-magnitude concentration at equilibrium.

cis-2-Butene - trans-2-Butene Isomerization

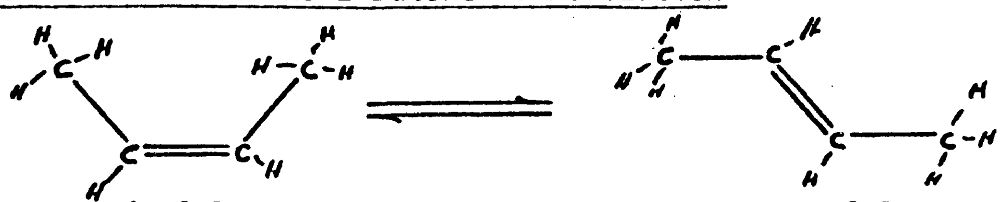

cis-2-Butene trams-2-Butene

K equals 1.55 at 523°K; equilibrium concentrations should be close-to-equal.

1-Butene to n-Butane

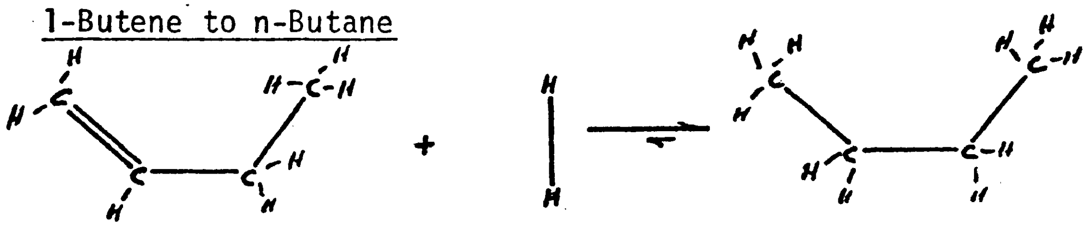

1-Butene Hydrogen n-Butane

At 523°K, K equals 3.7 x 10^{18}, which irreversibly favors n-Butane.

trans-2-Butene to Butane

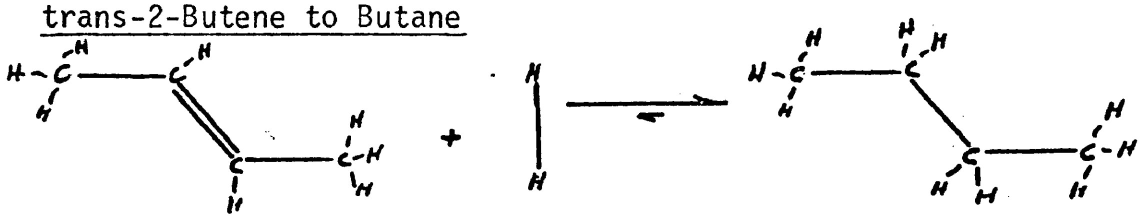

trans-2-Butene Hydrogen n-Butane

K equals 2.53 x 10^{17}(irreversible in favor of n-Butane) at 523°K.

cis-2-Butene to Butane

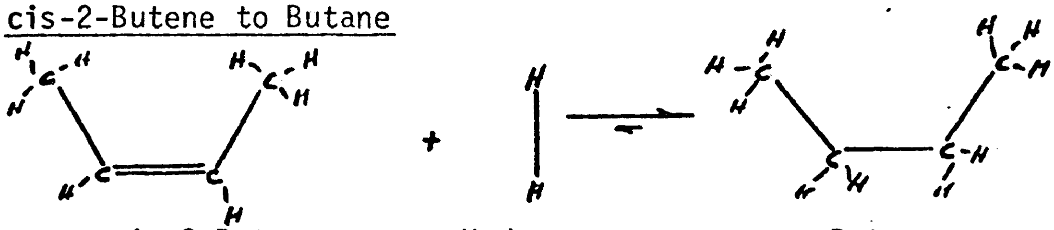

cis-2-Butene Hydrogen n-Butane

K equals 1.65 x 10^{18} (irreversible in favor of n-Butane) at 523°K.

n-Pentane Cracking

Reaction equilibrium constants are computed for two cracking reactions: n-pentane cracking to ethylene, propylene and hydrogen;

and the cracking of n-pentane to methane and 1-butene. For the first reaction, K is 2.92; for the second, K equals 0.68. Thermodynamically, cracking is possible.

However, no cracking is observed in these experiments. Plots of mass 72 peak height, presented earlier, do not decline with elapsed time. No cracking has been noted in previous studies conducted by Kieran and Kemball (80), or by Roberts and Satterfield (4, 25). Kolboe and Amberg (6) noted no cracking at 288°C over a variety of catalyst types.

APPENDIX IV

Significance Tests

Introduction

Table VII-1 lists the operating conditions used during experimental runs. Operating conditions were decided upon so as to condition the data well (enable more accurate determination of kinetic parameters) and to enable identification of effects due to mixing, concentration change, and diluent.

The method of experimental run comparison consists of calculating the variance associated with each experimental run or group of runs (defined as the difference between predicted and actual rate, squared, divided by the number of data points in the sample minus one), and testing for equality among different treatments. Table IV-1 lists the calculated variances for each run, for the two acceptable models. (One data point, the first in run 37, was discarded as an outlier.)

Comparison- Hydrogen Sulfide Levels

Table 3 lists F-statistics for the various models found to have statistical significance. Since no model was found which gave, for all data, a significant fit, had positive adsorption coefficients, and had activation energies of the proper signs, it is concluded that there is a significant difference between low-H_2S and high-H_2S data.

Mixing Effects

During run 14, the recirculation rate was adjusted to approximately 90% of the usual flowrate. Any departure from the usual degree of mixing would result in an apparent deviation from the reaction rate experienced under normal conditions. The result would be an increased sum-square-error due to inadequate agreement with the regression model. By inspection, run 14 variance is seen to fall within or below the range of variances experienced in other runs. In comparison of run 14 variance with the variance of the remaining data using Bartlett's test (ref.67, chapter 11), run 14 is determined not to be significantly different for either of the two low-sulfide models. The chi-squared statistics both lie below the critical value of $\chi^2_{.05}(1) = 6.314$.

Catalyst Activity

Linck(29) and Thomas (72) indicate that no significant change in catalyst activity should be expected. If an activity change is present, there should be a trend in variances listed in table IV-1 such that they decrease with increasing run number, reach a minimum, then rise again. This trend would be due to the model representing some average activity, with positive deviation (squared) during early runs and negative deviations (squared) during later runs. As can be seen by inspection, except for run 32, variances exhibit a declining trend with increasing run number. This decrease is due to a gradually decreasing mass spectrum background, which is suspected to be due to the weathering of residues in the thermal conductivity vacuum gauge in the intermediate pressure section of the sampling system, which was acquired from a previous project. The effect is somewhat random, and hindered chemical analysis only slightly. Lack of a minimum is sufficient to reject any assumption of declining catalyst activity.

High Diluent Effect

The effect of a two-fold increase in n-pentane content is tested by the same statistical method as is used to test for mixing effects. The results for model five (1.435) are sufficiently far enough below the critical chi-squared value of 6.314, indicating that no significant difference exists between high- and normal-concentration runs as represented by the mathematical models.

Packing Effect

No effects of changing from iron to glass packing are present, as shown in the Blank Runs section of Appendix II.

Conclusions

No significant effects are caused by either mixing, catalyst activity decline, n-pentane concentration, or packing type. A trend of variance declining with run number is believed to be caused by weathering of residue in the inlet system. A significant difference exists between low H_2S and high H_2S runs.

TABLE IV-1

EXPERIMENTAL RUN VARIANCES

Run #	# of Points	Model 5 (low)	Model 5 (high)
9	3	-	11.420
10	4	-	3.028
11	5	7.028	-
14	3	4.018	-
16	4	3.547	-
32	4	6.417	-
34	4	-	.1852
37*	5	2.291	-

* The first data point in run 37 (56 minutes), rate of 18.59, was discarded as an outlier.

APPENDIX V

Programs for Data Reduction and Interpretation

The following program is written for the Texas Instruments SR-52 programmable calculator, and is used to convert peak height ratios, initial concentrations, and catalyst information to gas phase and surface concentrations.

Data analysis is accomplished on the SR-52 with portions of the Statistics Library, Program Manual ST-1, available from Texas Instruments. Programs ST1-01 (Basic Statistics for One or Two Variables), ST1-08 (Linear Regression), and ST1-12-1 & 2 (Multiple Linear Regression) have been particularly useful.

T 1748

TITLE RAW DATA CONVERSION PAGE 1 OF 4

A				
LOAD	NEW PEAKS			

B				

STEP	PROCEDURE	ENTER	PRESS			DISPLAY
1.	LOAD SIDES A & B. (ASSUMES INITIALIZATION					
	CARD ALREADY HAS BEEN RUN.)					
2.	INITIALIZE.		A			1.
3.	ENTER TIHOPHENE INITIAL CONCENTRATION.		RUN			2.
4.	ENTER H_2S INITIAL CONCENTRATION.		RUN			3.
5.	ENTER n-PENTANE CONCENTRATION.		RUN			4.
6.	ENTER REACTOR VOLUME (ml).		RUN			5.
7.	ENTER CATALYST WEIGHT (gm).		RUN			0.
8.	ENTER MASS 84/72 PEAK HEIGHT RATIO.		RUN			1.
9.	ENTER MASS 34/72 PEAK HEIGHT RATIO.		RUN			2.
10.	ENTER MASS 58/72 PEAK HEIGHT RATIO.		RUN			3.
11.	ENTER MASS 56/72 PEAK HEIGHT RATIO.		RUN			C_4 - CONCENTRATION
12.	COMPUTE REMAINING CONCENTRATIONS		RUN			C_b "
			RUN			C_T "
			RUN			C_S "
			RUN			$C_{S,ADS}$ "
			RUN			$C_{T,ADS}$ + OTHER. "
13.	TO RUN ADDITIONAL DATA, ENTER MASS 84/72					
	PEAK HEIGHT RATIO, PRESS B, GO TO STEP 9 ABOVE.					

RAW DATA CONVERSION PAGE 6 OF 7

RAMMER DATE

Coding Form

T 1748

93

CODE	KEY	COMMENTS	LOC	CODE	KEY	COMMENTS	LOC	CODE	KEY	COMMENTS
	LBL				1	84/72			1	
	A				2				0	
	1		040 152		1				HLT	
	HLT				HLT				RCL	
	STO				STO		080 192		1	
	1	C_{TO}			1	34/72			3	
	4				1				x	
	2		045 157		2				RCL	
	HLT				HLT				0	
	STO				STO		085 197		8	
	1	C_{50}			1	58/72			+	
	5				3				RCL	
	3		050 162		+/−				1	
	HLT				X				2	
	STO				RCL		090 202		X	
	1	C_5			1				RCL	
	6				8				0	
	4		055 167		+				7	
	HLT				3				+	
	STO				HLT		095 207		RCL	
	1	VOL, ml			STO				1	
	7				1	56/72			1	
	5		060 172		0				X	
	HLT	GM CATALYST			X				RCL	
	X				RCL		100 212		0	
	1				1				6	
	8				9				+	
	0		065 177		−				RCL	
	=				RCL				0	
	INV				0		105 217		5	
	PROD				0				=	
	1	SURFACE			=				X	
	7	FACTOR	070 182		X				RCL	
	0				RCL				1	
	HLT				1		110 222		6	
	LBL				6				=	
	B				=					
	STO		075 187		STO	C_4−				

TEXAS INSTRUMENTS
INCORPORATED

LABELS	
A	LOAD
B	NEW PEAKS
C	
D	
E	
A′	
B′	
C′	
D′	
E′	

REGISTERS	
00	
01	
02	
03	
04	
05	
06	
07	
08	
09	
10	
11	
12	SEE FINAL SHEET
13	
14	
15	
16	
17	
18	
19	

FLAGS
0
1
2
3
4

T 1748

TITLE *RAW DATA CONVERSION* PAGE 3 OF 4

◄A◄				

◄B◄				

STEP	PROCEDURE	ENTER	PRESS			DISPLAY
	GENERAL EQUATION:					

$$C_i = \left[b_{0,i} + b_{84,i}(h_{84}/h_{72}) + b_{58,i}(h_{58}/h_{72}) + b_{56,i}(h_{56}/h_{72}) + b_{34,i}(h_{34}/h_{72})\right] C_5$$

FOR i = THIOPHENE, BUTANE, BUTENES, OR H_2S.

RAMMER ______ DATE ______

T 1748

Coding Form

95

CODE	KEY	COMMENTS	LOC	CODE	KEY	COMMENTS	LOC	CODE	KEY	COMMENTS
	STO	C_b			0				4	
	1				1				−	
	3		040 152		+				RCL	
	HLT				RCL				1	
	RCL				0		080 192		3	
	1				9				−	
	2				=				RCL	
	X		045 157		X				1	
	RCL				RCL				2	
	0				1		085 197		−	
	4				6				RCL	
	+				=				1	
	RCL		050 162		STO	C_S			0	
	1				1				=	
	1				1		090 202		X	
	X				HLT				RCL	$C_{T,ADS}$
	RCL				+/−				1	$+C_{4^=,ADS}$
	0		055 167		+				7	$+C_{4,ADS}$
	3				RCL				=	
	+				1		095 207		HLT	
	RCL				3					
	0				+					
	2		060 172		RCL					
	=				1					
	X				0		100 212			
	RCL				+					
	1				RCL					
	6		065 177		1					
	=				5					
	STO	C_T			=		105 217			
	1				X					
	2				RCL					
	HLT		070 182		1	$C_{S,ADS}$				
	RCL				7					
	1				=		110 222			
	1				HLT					
	X				RCL					
	RCL		075 187		1					

TEXAS INSTRUMENTS INCORPORATED

LABELS

A
B
C
D
E
A′
B′
C′
D′
E′

REGISTERS

00 b_0, BUTENES
01 b_{34}, H_2S
02 b_0, THIO
03 b_{34}, THIO
04 b_{84}, THIO
05 b_0, BUTANE
06 b_{34}, BUTANE
07 b_{84}, BUTANE
08 b_{58}, BUTANE
09 b_0, H_2S
10 $56/72 \rightarrow C_{4^=}$
11 $34/72 \rightarrow C_S$
12 $84/72 \rightarrow C_T$
13 $58/72 \rightarrow C_b$
14 $C_{T,0}$
15 $C_{S,0}$
16 C_5
17 SURF FACTOR
18 b_{58}, $C_{4^=}$
19 b_{56}, $C_{4^=}$

FLAGS

0
1
2
3
4

APPENDIX VI

Calibration

Calibration of Total Pressure Gauge

Calibration of the WIANCKO 1000 psig pressure gauge, serial number 30357, used to measure total pressure in the reactor circuit, was accomplished with a dead weight tester. A total of 30 data points taken at seven different pressure levels were used to determine the calibration curve by weighted linear regression analysis. The equation is:

$$\text{Pressure (psig)} = 7.0323 \times \text{(zero suppress rdg.)} + \text{constant} \quad \text{(VI-1)}$$

By balancing the recorder and nulling the meter at a zero suppression reading of zero while the reactor circuit is under a vacuum, the constant becomes zero and the pressure reading is in psia. Pressure can be estimated to within ±0.02 psi if recorder drift is not present. Sanborn recorder channel "D" was used, with a gauge factor of 500.00. Data are listed in table VI-1.

Gas Addition Inlet

Hydrogen sulfide is supplied to the reactor circuit in measured amounts via the gas addition inlet diagrammed in figure VI-1. Valve 1 is supplied as an integral part of the lecture bottle containing the hydrogen sulfide, and attaches to the base of valve 2 with a 1/8" threaded connection and lead gasket. Valves 2 and 3 are needle valves constructed of stainless steel. The pressure transducer, a CEC

TABLE VI-1

TOTAL PRESSURE GAUGE CALIBRATION

PSI	Gauge Readings
805	102.00, 102.00, 102.25, 102.00
705	87.00 (6 times)
605	72.25, 72.50 (5 times)
505	58.75, 59.00 (5 times)
405	46.00, (4 times), 46.25
305	33.75 (twice)

Model 4-015, serial number 1252, 0-500 psia stainless steel strain gauge transducer, is connected with the other inlet components with 1/4" stainless steel tubing and Swagelok fittings. An electrical signal proportional to pressure is read on a Sanborn four channel recorder on channel "D".

Metering Procedure

Charging-- A lecture bottle of hydrogen sulfide is screwed onto the base of valve 2, compressing the lead gasket. Valves 2 and 3 are opened, and the entire reactor circuit and inlet pumped out by the vacuum pump. Valves 2 and 3 are closed, and valve 1 opened. Recorder channel "D" is switched to "ATTN x1", the zero suppression knob turned to zero, and the "Resistance Balance" control adjusted to null the meter.

Metering-- Valve 2 is opened and the inlet filled with H_2S, then closed. The zero suppression knob is adjusted so as to null the meter, and the reading noted. Valve 3 is used to meter H_2S into the reactor circuit slowly. The zero suppress knob is turned to the desired final reading and valve 3 used to bring the recorder pen back to the previous position. The difference in zero suppression settings and the temperature (in degrees Kelvin) is substituted into the equation

$$\text{gram moles gas} = \frac{43.98 \times 10^{-4}}{T°K} \left(ZS_2/z_2 - ZS_1/z_1\right) \qquad \text{(VI-1)}$$

to give the amount of hydrogen sulfide added to the reactor circuit. Here, z is the compressibility factor. The pressure needed to calculate z is determined by: P(psia) = .7745 (zero supp. rdg.) + 0.0. (VI-2)

The compressibility is obtained from generalized charts[69], tables[52], or from an equation of state.

Calibration of Gas Addition Inlet

Calibration of the gas addition inlet is accomplished by substituting a gas burette (diagrammed in figure VI-) in place of the gas cylinder and valve #1. The inlet is pressured up with nitrogen through valve #3 from the reactor circuit. The three-way valve is opened so that the gas burette and tubing up to valve 2 are vented to the atmosphere, and the liquid level in the burette is noted. The three-way valve is now set to allow gas from valve 2 to flow into the burette without venting. The pressure reading is noted, and gas is metered into the burette with valve 2. The leveling bulb is adjusted so that its liquid level and that in the burette are equal. The new pressure reading and the volume of gas contained in the burette are then noted.

For the gas inlet, which is bounded by valves 1 and 2, assuming an ideal gas,

$$(\partial n/\partial P)_{V,T} = V_{sys}/RT \qquad \text{(VI-3)}$$

and, integrated,

$$\Delta n = (V_{sys}/RT)\Delta P \qquad \text{(VI-4)}$$

For the gas burette equipment,

$$(\partial n/\partial V)_{T,P} = P_{atm}/RT \qquad \text{(VI-5)}$$

or

$$\Delta n = (P_{atm}/RT)\Delta V \qquad \text{(VI-6)}$$

Since gas is metered from the inlet system into the burette,

$$V_{sys}\Delta P_{sys} = P_{atm}\Delta V \qquad \text{(VI-7)}$$

The change in volume is directly convertible to the number of moles of gas by

$$\Delta n = P_{atm}\Delta V/RT, \qquad (VI\text{-}8)$$

so

$$\Delta n = V_{sys}\Delta P_{sys}/RT. \qquad (VI\text{-}9)$$

A total of 17 data points were taken (two were rejected due to errors in procedure) over the approximately 250 psi design pressure range, using the above procedure. Nitrogen gas was used, as it approximates an ideal gas. The data obtained (see table VI-2) defined the constant

$$V_{sys}/R = 43.981 \pm .930 \text{ moles°K/division}. \qquad (VI\text{-}10)$$

The pressure reading is obtained by setting the recorder null meter to zero with the resistance balance control, with the zero suppression control at zero, metering gas into the reactor circuit, and using the zero suppress control to re-null the meter. The new zero suppress reading is used to predict the number of moles of ideal gas added according to:

$$\Delta n \text{ moles} = (43.981 \times 10^{-4})(\text{zero suppress reading})/(T°K) \quad (VI\text{-}11)$$

where z is the compressibility factor for the gas, equal to one for nitrogen. For a non-ideal gas, such as hydrogen sulfide, the above development with compressibility factor included yields

$$\Delta n = (V_{sys}/R)(1/T)[(ZS_2/z_2)-(ZS_1/z_1)+a(z_1^{-1}-z_2^{-1}) \qquad (VI\text{-}12)$$

where "a" is the zero suppression reading at the base pressure where the meter is nulled. If the base pressure is zero psia, this factor is zero, and:

$$\Delta n = (V_{sys}/R)(1/T)(ZS_2/z_2-ZS_1/z_1). \qquad (VI\text{-}13)$$

TABLE VI-2

CALIBRATION DATA: GAS ADDITION INLET

Conditions: Atmospheric Pressure 620.2 mm Hg
Temperature 25.6°C

Recorder: Sanborn Channel "D", Gauge factor 750.00

Transducer: CEC 500 PSIA Model 4-015, Serial #1252

Run #	Moles x 10^4	Zero Suppress Change	V_{sys}/R
1	8.753	59.5	43.959×10^{-4}
	10.436	69.1	45.119×10^{-4}
	7.357	57.8	38.026×10^{-4}
	9.238	61.9	44.586×10^{-4}
2	8.339	56.0	44.487×10^{-4}
	8.589	57.3	44.781×10^{-4}
	10.519	70.4	44.639×10^{-4}
	9.820	65.8	44.585×10^{-4}
	6.075	41.0	44.266×10^{-4}
3	7.523	50.8	44.242×10^{-4}
	9.421	63.1	44.604×10^{-4}
	2.780	18.9	43.943×10^{-4}
	6.302	42.7	44.092×10^{-4}
	7.939	53.7	44.167×10^{-4}
	10.552	71.3	44.213×10^{-4}

Mean Value = $(43.981 \pm .9298) \times 10^{-4}$ moles°K/division

Variance = 2.81838×10^{-8}

Reactor Circuit Volume Determination

The volume of the reactor circuit was determined by disconnecting the gas addition inlet at valve #3 (Figure VI-3) and attaching the gas burette equipment shown in Figure VI-1 (a 1000 ml burette was substituted for the original 50 ml burette). Procedure consisted of monitoring pressure with the total pressure transducer and noting both reactor circuit pressure and volume of gas in the burette before and after bleeding pressurized nitrogen from the reactor circuit into the burette. A total of ten data points were obtained. Procedural error and leakage through an inadequately-lubricated fitting caused four points to be discarded. The six remaining points are listed in table VI-3. The volume bounded by valves 3, 5, 8, 9 and 11 in Figure 1 is 290.8 $\pm$4.6 cm^3. Addition of the 15.0 ml glass sample bulb above valve 5 increases the volume to 306 cm^3 (for calculation of initial reactant concentrations). For runs 28-37, the volume is 246 cm^3 plus sample bulb volume.

Mass Spectrometer Calibration

The mass spectrometer used for chemical composition determination is a modified Consolidated Electrodynamics Corporation CEC 23-130 donated by Marathon Oil Company. Calibration was accomplished by injecting samples of thiophene, normal pentane, hydrogen sulfide, and a mixture of butanes. The resulting data were checked against published data available from the National Bureau of Standards. A mass spectrum is characterized by a) peak heights at various mass numbers relative to the highest, or base, peak (as percent of base

TABLE VI-3

REACTOR CIRCUIT VOLUME DETERMINATION
(Iron Packing)

	Volume(ml)	Start Press.(z.s.)	End Press.(z.s.)	Volume
1	630	21.25	17.50	284.
2	651	17.50	13.75	294.
3	699	13.75	9.75	296.
4	639	9.75	6.00	288.
5	522	22.00	19.00	294.
6	555	19.00	15.75	289.
(Glass Packing)				
1	813	54.50	48.50	227
2	810	48.25	42.25	227
3	825	42.25	36.50	240

corrected atmospheric pressure 615 mm Hg peak), and b) by height of base peak relative to that of normal butane at the same pressure (as ratio).

A mass spectrum, for each compound, is obtained by valving a small amount of gaseous compound (or vaporizing a small amount of liquid) into the heated inlet (see Figure 2). Sample pressure is reduced to 150 microns or below in the "holding volume" portion of the inlet, using the procedures outlined above. The sample is introduced to the gold leak, an internal throttling orifice, the output recorder is started, and mass scanning is initiated immediately afterward. Three scans are obtained over an elapsed time of approximately one minute.

Compounds with different molecular weights and/or structure diffuse through the gold leak at different rates. Thus a change in relative peak height with time indicates contributions by more than one compound. A peak resulting from several compounds will register larger than that of a pure compound, and will be unsuitable for calibration purposes unless the contaminants and the composition of the mixture are accurately known.

Raw Data Conversion-Pure Compounds

Raw data are obtained by measuring peak height at corresponding mass number for each of the three scans. The data are output as recorder traces at six different attenuations; the two greatest peak height traces at each mass number are measured for a total of six tabulations at most per mass number. These tabulated data are converted to relative peak height by first subtracting peak height of the background spectrum at corresponding mass numbers, then dividing each by the height of the highest, or base, peak. The result is three doubly-replicated measurements at different times, which are used to compute a mean peak height, variance, and 95% confidence interval at each mass number where a peak appeared.

<u>Time Effects in Mixture Composition Determination</u>

If the reservoir from which flow into the spectrometer takes place is relatively large, even if flow is molecular (Knudsen) in nature, its composition and pressure are not appreciably affected by a small rate of withdrawal and the analysis of the withdrawn material will differ from that in the reservoir by a constant amount approximately proportional to the square root of each compound's molecular weight. In practice, reservoir formed by the inlet system may or may not exhibit composition change with time during sampling. Varying diffusion rates could result in depletion of the faster-diffusing species with time, resulting in increasing proportions of higher molecular weight material as time passes.

Table VI-4 contains triply-replicated data for four different samples from the same blank run. Each set of three scans was obtained over an elapsed time of 45.6 seconds. No clear trend of increasing mass-84 to mass-72 peak height ratio within samples can be seen. Ratios are shown to be reproducible to within about 3%, which is comparable to the reproducibility observed in pure-compound data. Thus, flow through the gold leak orifice is either viscous in nature (79), or the reservoir is of sufficient volume that no fractionation is observed.

Variance in data is assumed to be caused by normally-distributed peak height due to instrument noise and by change in peak height with time due to composition change resulting from differing diffusion rates through the gold leak. Instrument noise is considered the same for any and all mass numbers, so any additional variance is attributed to composition change.

Detection of Difference with API Data

To test significant differences in relative peak height between experimentally-obtained pure compound data and reference data, a test on correlated data (44) was used. This tests the hypothesis that at each mass number, experimental and reference data are equal, with test statistic

$$t(n-1) = \frac{(X_{exp}-X_{ref})}{s/n^{1/2}} \tag{VI-14}$$

where n is the number of peaks experimentally measured at a mass number (here, up to six) and s is the square-root of the variance associated with the experimental data. Results are summarized in Tables VI-5 through VI-7. Raw data may be found in Tables VII-4 through VII-6.

Mixture Calibration

Calibration was accomplished by using known amounts of thiophene, pentane, butane, and hydrogen sulfide. Compressibility factors for hydrogen sulfide and butane were computed from the pressure series Virial equation of state, using second Virial coefficient data

TABLE VI-4

COMPOSITION - TIME DATA

Run 15 n-Pentane + Thiophene, furnace off, temperature variable

Time	h_{84}/h_{72}	Mean	Range	%
036.5a	.2337			
036.5b	.2339	.2339 ± .0003	.004 x 10^{-8}	.12
036.5c	.2341			
070.4a	.2061			
070.4b	.1985	.2040 ± .0080	.009 x 10^{-5}	4.3
070.4c	.2073			
133.6a	.2920			
133.6b	.3010	.2975 ± .0081	.009 x 10^{-5}	3.0
133.6c	.2994			
175.5a	.2658			
175.5b	.2715	.2708 ± .0079	.009 x 10^{-5}	3.4
175.5c	.2751			

Temperatures varied from 4° to 15°C above room temperature.

Initial Concentrations

$C_T = 4.363 \times 10^{-3}$ moles/liter

$C_S = 0$

$C_5 = 8.648 \times 10^{-2}$ moles/liter

TABLE VI-5

MASS SPECTRAL DATA COMPARISON

Run Date: 11/16/74 Compound: Thiophene

Mass	Mean Response	API Value	Variance	t-test	% dev.
26	.0586	.0555	4.85×10^{-6}	.7267	3.9
27	.0231	.0164	9.42×10^{-6}	2.118	13.9
39	.3520	.2860	1.86×10^{-4}	4.763 *	4.0
43	.0463	.0023	6.78×10^{-5}	5.343 *	18.7
45	.5586	.5690	2.31×10^{-4}	.6849	2.8
57	.0925	.1290	5.38×10^{-5}	6.205 *	8.0
58	.6384	.6480	2.37×10^{-4}	1.521	2.8
69	.0545	.0724	2.77×10^{-6}	9.377 *	3.0
84	1.0	1.0	---	---	---
85	.0558	.0505	1.95×10^{-5}	.9067	8.3

* - Reject

TABLE VI-6

MASS SPECTRAL DATA COMPARISON

Run Date: 11/20/74 Compound: Hydrogen Sulfide

Mass	Mean Response	API Value	Variance	t-test	% dev.
33	.4073	.420	6.6×10^{-5}	1.56	2.1
34	1.0	1.0	---	---	---
35	.0267	.0250	2.30×10^{-6}	1.12	6.0
36	.0441	.042	6.04×10^{-6}	.855	5.8

* = Reject

TABLE VI-7

MASS SPECTRAL DATA COMPARISON

Run Date: 11/20/74 Compound: Butane

Mass	Mean Response	API Value	Variance	t-test	% dev.
25	.0056	.0046	2.30×10^{-8}	.66	2.8
25.5	.0043	.0036	6.67×10^{-9}	8.57 *	2.0
26	.0605	.0617	2.40×10^{-7}	2.45	.9
27	.3568	.3710	3.67×10^{-5}	2.35	2.0
29	.4449	.4420	1.53×10^{-4}	.23	4.4
30	.0104	.0098	2.42×10^{-7}	1.22	5.0
36	.0013	.0008	1.00×10^{-8}	5.00 *	19.0
37	.0105	.0101	2.31×10^{-7}	.83	4.8
38	.0186	.0189	2.71×10^{-7}	.58	2.9
39	.1129	.1250	2.95×10^{-6}	7.04 *	1.6
40	.953	.0163	2.50×10^{-7}	2.00	3.4
41	.2796	.2780	4.04×10^{-6}	.80	.8
42	.1194	.1220	3.24×10^{-6}	1.44	1.6
43	1.0	1.0	---	---	---
44	.0392	.0333	7.05×10^{-4}	8.78 *	1.8
49	.0044	.0040	1.33×10^{-4}	3.16 *	3.0
50	.0131	.0129	5.84×10^{-4}	.36	4.5
51	.0102	.0105	5.22×10^{-4}	.60	5.1
52	.0024	.0026	2.27×10^{-8}	1.33	6.6
53	.0068	.0074	3.79×10^{-8}	3.09 *	3.0
54	.0019	.0019	6.67×10^{-9}	0	4.8
55	.0092	.0093	1.90×10^{-7}	.23	5.0

MASS SPECTRAL DATA COMPARISON -- Continued

Mass	Mean Response	API Value	Variance	t-test	% dev.
56	.0073	.0072	2.03×10^{-7}	.22	5.8
57	.0250	.0242	2.95×10^{-7}	1.47	2.3
58	.1096	.1230	2.86×10^{-6}	7.92 *	1.8
59	.0052	.0054	1.367×10^{-8}	1.71	2.4

from the Texas A&M University Thermodynamic Research Center (122). The amount of H_2S or butane added was computed with equation VI-1; thiophene/n-pentane mixture was measured by weight.

Thiophene/n-C_5 Calibration

Tables VII-1 and VII-2 contain data used in calibrating for thiophene concentration. A total of 35 data points were taken during five experimental runs with varying hydrogen sulfide concentration. The relationship between mass 84/72 peak height ratio and thiophene/n-C_5 concentration ratio is:

$$C_T = (0.0840 \pm .0040)(h_{84}/h_{72})C_5,\ \text{high } H_2S, \quad \text{(VI-15)}$$

and

$$C_T = (0.0968 \pm .0044)(h_{84}/h_{72})C_5,\ \text{low } H_2S. \quad \text{(VI-16)}$$

The reason for the difference is not known, but is suspected to be due to H_2S interaction with the rhenium filament in the mass spectrometer.

Hydrogen Sulfide Calibration

Tables VII-1 and 2 contain data used for the hydrogen sulfide calibration. A total of twelve data points were used from the experimental runs with glass packing but without catalyst. The relationship between mass 34/72 peak height ratio and H_2S/nC_5 concentration ratio is

$$C_S/C_5 = (.0510 +/- .0016)(h_{34}/h_{72}) - .0087 \quad \text{(VI-17)}$$

with significance F(1,10) = 6485. and correlation coefficient .998. The constant term is not statistically significant.

Butane Calibration

The thiophene and hydrogen sulfide calibrations are straightforward, due to the fact that, at mass 84, only thiophene gives a peak, and at 34, only H_2S gives a peak of significant size. However, butane and the butenes are not so simple. The derivation in the main body of the text shows mathematically that the mass 58/72 peak height ratio is made up not only of a butane contribution, but also of contributions from thiophene and pentane. Butenes, having molecular weights of 56, do not interfere.

The butane calibration was based on twenty one data points from three experimental runs without catalyst. The relationship between peak height ratios and concentration ratios is

$$C_4/C_5 = .2506 \frac{h_{58}}{h_{72}} - .1624 \frac{h_{84}}{h_{72}} - .0015 \qquad \text{(VI-18)}$$

The constant term, which statistically could be zero, is retained since it represents the pentane contribution to mass 58 peak height. The multiple correlation coefficient for this relationship is .879, with significance

$$F(1,19) = 137.4.$$

Effect of Adsorption on Mass Spectrometer Calibration

All concentration data are computed from calibrations based on data from runs 25-30 and 35. During all of these runs (except for 35), no catalyst was present. The surface area presented by both iron and glass packing is on the order of half of one percent of the surface area of the catalyst (.15 m^2 for glass heads, 26 m^2 for .13 grams of catalyst), so the amount of thiophene or H_2S adsorbed during calibration runs compared to the amount during runs with catalyst is negligible. Adsorption bonds on the steel reactor parts are weak (4.95 kcal/gm mole at 25°C (123)), further reducing the amount adsorbed.

The material sampled for analysis by mass spectrometry is representative of the vapor phase mixture composition only. Langmuir-Hinshelwood kinetic models, discussed before, are formulated in terms of vapor phase compositions, so the concentration data obtained in this study are applicable.

n-Pentane Mass 72 Peak Height

Table VII-7 contains data on the ratio of mass 72 peak height to mass 43 peak height. This ratio, according to tabulated data, should be .0531. For eight data points it averaged .0802 $\pm$.0032 (significantly different). The reason for this is not known, but could be due to an impurity in the n-pentane or due to use of a rhenium filament in the mass spectrometer. The .0802 value is used for the butene measurements, and determination of the other components is based on calibration against mixtures of known spectrum with pure compounds.

Likewise, the ratio of mass 56 peak height to mass 43 peak height is observed (Table VII-7) to be .0225 $\pm$.0010, significantly different from the tabulated value of .0173. This value is used in the butene calibration also.

APPENDIX VII

DATA

TABLE VII-1

INITIAL CONDITIONS SUMMARY

Run	Initial Concentration $\times 10^{3}$, gm moles/ℓ			Reactor	Catalyst	Pressure, PSIA		Reaction	Remarks
	Thiophene	H_2S	n-Pentane	Volume, ml	Weight, gm	Cold	Hot	Temp., °C	
09	2.59	17.11	51.35	291.	.1472	422.	605.	275.	High H_2S concentration, iron packing
10	2.15	15.96	42.71	291.	.1472	422.	598.	275.	High H_2S concentration, iron packing
11	2.58	0	51.07	291.	.1472	422.	607.	275.	Iron packing
14	2.58	0	51.12	291.	.1472	422.	601.	275.	Iron packing, low circulation rate
16	6.24	0	124.06	291.	.1472	422.	601.	275.	High n-Pentane concentration, iron packing
18	2.53	0	50.14	291.	.1472	422.	577.	256.	Low temperature, iron packing
19	2.49	17.52	49.27	291.	.1472	422.	598.	256.	Low temperature, high H_2S conc., iron packing
25	2.48	0	49.26	231.	0	422.	605.	275.	Calibration: thiophene, butane; iron packing
26	2.39	19.93	47.21	231.	0	422.	601.	275.	Calibration: thiophene, butane; iron packing
27	2.39	18.33	46.71	231.	0	422.	610.	275.	Calibration: thiophene; iron packing
29	2.21	22.68	43.82	231.	0	422.	598.	275.	Calibration: thiophene, H_2S; glass packing
30	2.41	0	47.67	231.	0	422.	591.	275.	Calibration: thiophene, butane; glass packing
32	2.74	0	54.01	231.	.1282	422.	582.	275.	Glass packing
34	2.44	22.68	48.33	231.	.1282	422.	614.	275.	High H_2S concentration; glass packing
37	3.72	0	73.91	231.	.1199	422.	594.	275.	Glass packing

TABLE VII-2

COMPOSITION CALIBRATION DATA

	Elapsed Time, Minutes	Peak Height Ratio 84/72	58/72	56/72	34/72
Run 25	056.0	.600	.4208		
	074.0	.452	.3210		
	101.0	.483	.3410		
	146.1	.448	.3136		
	170.0	.505	.3427		
	202.5	.465	.3199		
	223.0	.567	.3302		
	325.0	.588	.3759		
Run 26	057.5	.5641	.3622	Not Used	Not Used
	085.0	.5643	.4222		
	108.5	.6622	.4013		
	132.5	.5392	.3532		
	162.5	.6707	.4685		
	190.0	.6297	.4200		
Run 27	057.5	.4871	.3520		
	082.5	.6518	.5229		
	110.0	.5560	.4854		
	136.5	.4826	.3620		

	Elapsed Time, Minutes	Peak Height Ratio 84/72	58/72	56/72	34/72
Run 27 (cont'd)	136.5	.6307	.4883		
	165.0	.5837	.3950		
	165.0	.5944	.4225		Not Used
	190.0	.5921	.4311		
	190.0	.6271	.4480		
Run 29	076.0	.6346	.4790		9.980
	104.0	.5887	.4852		10.75
	104.0	.5863	.4701		9.96
	130.5	.5990	.4732	Not Used	10.79
	130.5	.6273	.5269		10.34
Run 30	062.0	.523	.499		
	086.0	.492	.460		
	086.0	.497	.465		
	109.0	.570	.479		Not Used
	109.0	.567	.488		
	130.0	.559	.501		
	154.0	.575	.493		

TABLE VII-3

COMPOSITION-TIME DATA

	Elapsed Time, Minutes	Peak Height Ratio 84/72	58/72	56/72	34/72	Reactor Composition, gm mol/ℓ x 10^3 Butenes	Butane	Thiophene	H_2S	Surface Concentration gm mol/ m^2cat x 10^6 Thiophene + C_4	H_2S	Thiophene Rx Rate, gm mole per Min. gm cat x 10^5	% Closure C	S
Run 09	045.9	.4071	.2763	.2772	5.3277	0.0169	0.0857	1.7561	13.9631	8.0262	H_2S surface concentration unknown, due to reaction with iron packing.	-	71.8	
	072.0	.3991	.2805	.2821	4.4704	0.0839	0.2065	1.7216	11.7163	6.3443		-	77.7	
	095.6	.3707	.2917	.2873	3.5916	0.1534	0.5874	1.5991	09.4130	2.7457		- 6.23	90.3	
	128.6	.2674	.2374	.2963	3.7862	0.2914	0.7500	1.1535	09.9231	4.3361		-10.76	84.8	
	149.8	.1851	.2072	.3006	3.7399	0.3584	1.0477	.7985	09.8017	4.2306		-10.76	85.1	
Run 10	045.8	.5890	.3778	.2590	8.5009	- .2164	- .1040	2.1130	18.5282	3.9668		-	83.2	
	069.0	.4843	.3286	.2971	6.8571	0.2333	0.0956	1.7374	14.9454	0.9635		- 9.64	95.9	
	094.9	.3718	.2902	.3021	6.1574	0.2987	0.4648	1.3338	13.4204	0.6227		- 7.84	97.4	
	124.2	.2911	.2810	.2823	5.0127	0.0720	0.9259	1.0443	10.9254	1.2270		- 6.47	94.8	
	151.3	.2236	.2279	.3008	4.4347	0.2962	0.8258	0.8021	09.6657	2.5229		- 5.44	89.3	
	178.0	.2121	.2316	.2789	4.0103	0.0426	0.9451	0.7609	08.7407	4.4487		-	81.2	
Run 11	053.0	.4447	.3668	.3093	.4121	0.4382	0.9315	2.1985	01.0741	-10.89		-	138.	
	076.0	.3079	.2875	.2863	.3677	0.1397	1.0512	1.5222	00.9584	- 1.505		-11.32	125.3	
	098.7	.2645	.2668	.2923	.3109	0.2275	1.1462	1.3076	00.8103	- 1.156		- 6.79	104.1	
	124.0	.2056	.2392	.2841	.3160	0.1209	1.2814	1.0164	00.8236	1.7252		- 4.76	93.9	
	147.0	.1861	.2321	.2853	.2423	0.1392	1.3523	0.9200	00.6315	1.8052		- 3.31	93.6	
	171.9	.1662	.2312	.2872	.1931	0.1657	1.5058	0.8217	00.5033	0.9099		- 2.86	96.8	

TABLE VII-3 (cont'd)

COMPOSITION-TIME DATA

	Elapsed Time, Minutes	Peak Height Ratio 84/72	58/72	56/72	34/72	Reactor Composition, gm mol/ℓ x 10^3 Butenes	Butane	Thiophene	H_2S	Surface Concentration gm mol/ m^{2}cat x 10^6 Thiophene + C_4	H_2S	Thiophene Rx Rate, gm mole per Min. gm cat x 10^5	% Closure C	S
Run 14	060.0	.2964	.2515	.2844	.0389	0.1222	0.6865	1.4667	00.1015	3.3319	H_2S surface concentration unknown, due to reaction with iron packing.	-	88.2	
	093.0	.1952	.2314	.2962	.0587	0.2901	1.2690	0.9659	00.1531	0.5921		- 7.84	97.9	
	124.0	.1452	.2124	.2814	.0584	0.0902	1.4415	0.7180	00.1524	3.6143		- 3.93	87.2	
	152.0	.1164	.1964	.2827	.0582	0.1120	1.4748	0.5760	00.1518	4.3683		- 3.06	84.6	
Run 16	073.0	.1507	.1712	.2893	.0375	0.2092	0.8673	0.7457	00.0978	8.3053		- 1.74	95.3	
	099.5	.1350	.1788	.2746	.0401	0.0043	1.0950	0.6680	00.1046	8.7086		- 2.58	95.1	
	128.8	.1091	.1798	.2808	.0727	0.0897	1.3228	0.5399	00.1897	6.8777		- 3.59	96.1	
	160.6	.0695	.1726	.2686	.0830	- .0771	1.5592	0.3439	00.2165	8.2642		- 4.22	95.3	
Run 18	059.0	.3610	.2907	.2492	.0543	- .3664	0.6399	1.7522	00.1390	5.5233		- 8.10	80.1	
	096.0	.2863	.1603	.3092	.1031	0.4775	- .3902	1.3897	00.2638	11.546		- 8.10	58.4	
	125.0	.1896	.2268	.3123	.1301	0.5039	1.2326	0.9203	00.3329	- 1.402		- 8.10	105.0	
	156.5	.1236	.2036	.3091	.0982	0.4660	1.4785	0.5999	00.2513	- .1687		- 5.24	100.6	
	187.1	.0931	.1828	.2810	.0966	0.0900	1.4655	0.4519	00.2472	5.7250		- 2.75	79.4	
Run 19	060.7	.4199	.2779	.2553	3.0483	- .2758	- .0004	1.7398	07.6649	11.232		- 6.78	58.9	
	103.3	.3460	.2669	.2757	4.1026	- .0016	0.4550	1.4320	10.3160	6.581		- 6.78	75.9	
	131.0	.2459	.2230	.2623	3.8262	- .1699	0.7138	1.0177	09.6210	10.134		- 5.52	62.9	
	163.1	.1989	.1906	.2749	3.9890	- .0054	0.6898	0.8232	10.0303	10.608		- 4.27	61.2	
	194.0	.1503	.1902	.2699	3.9540	- .0611	1.0737	0.6220	09.9423	9.3327		- 4.27	65.9	

TABLE VII-3 (cont'd)

COMPOSITION-TIME DATA

	Elapsed Time, Minutes	84/72	Peak Height Ratio 58/72	56/72	34/72	Reactor Composition, gm mol/ℓ x 10^3 Butenes	Butane	Thiophene	H_2S	Surface Concentration gm mol/ m^2 cat x 10^6 Thiophene + C_4	H_2S	Thiophene Rx Rate, gm mole per Min. gm cat x 10^{-5}	% Closure C	S
Run 32	057.5	.2489	.2431	.3676	0.1938	1.3461	1.0283	1.3014	00.5342	- 9.4368	18.4204	-	134.4	32.8
	086.0	.1326	.1813	.2773	0.2810	0.0433	1.2120	0.6933	00.7746	7.8534	4.8110	- 9.65	71.4	82.5
	110.0	.0924	.1791	.2846	0.3317	0.1504	1.5347	0.4832	00.9143	5.6536	7.7158	- 5.23	79.4	71.9
	140.0	.0599	.1635	.2847	0.3548	0.1559	1.6087	0.3132	00.9781	6.5606	7.8724	- 3.92	76.1	71.3
	140.0	.0603	.1620	.2816	0.3432	0.1110	1.5848	0.3153	00.9461	7.2273	7.5050	- 3.92	73.7	72.6
Run 34	053.0	.3378	.2777	.2792	7.6411	0.0417	0.6415	1.3714	18.8474	3.8396	45.2179	- 6.80	84.3	82.0
	085.0	.3012	.2808	.2992	7.6646	0.3111	0.8451	1.2229	18.9055	0.5917	49.3729	-	97.6	80.4
	085.0	.2834	.2683	.2958	7.4546	0.2607	0.9068	1.1505	18.3876	0.7241	55.1491	-	97.0	78.1
	112.5	.2293	.2293	.2933	7.5507	0.2369	0.9068	0.9309	18.6246	3.6389	52.0601	- 6.80	85.1	79.3
	139.0	.1604	.2110	.3004	7.4904	0.3338	1.2259	0.6512	18.4758	2.2747	57.7134	- 6.80	90.7	77.0
	165.0	.1310	.2009	.3001	7.4041	0.3322	1.3343	0.5319	18.2630	2.4006	60.9133	- 6.80	90.2	75.8
Run 37	056.0	.2209	.2238	.2798	.1767	0.0944	1.3856	1.5803	00.6665	7.1485	8.7078	-18.59	82.0	78.1
	080.0	.1727	.1878	.2756	.2375	0.0230	1.2974	1.2355	00.8958	12.5482	4.5446	- 7.37	68.5	88.6
	080.0	.1742	.1938	.2948	.2347	0.0405	1.3904	1.2462	00.8853	7.3536	9.7373	- 7.37	81.5	75.5
	106.0	.1465	.1953	.2770	.3033	0.0484	1.7506	1.0480	01.1439	9.4310	7.0114	- 5.37	76.3	82.4
	130.0	.1229	.1899	.2765	.3477	0.0403	1.9338	0.8792	01.3115	9.3641	7.0930	- 4.69	76.5	82.2
	130.0	.1375	.1759	.2831	.3409	0.1770	1.4994	0.9837	01.2858	11.4333	4.1807	- 4.69	71.3	89.5

TABLE VII-4

NORMALIZED PURE COMPOUND DATA: THIOPHENE

Run Date: 11/16/74

MASS	RESPONSES						
	SCAN 1		SCAN 2		SCAN 3		API
26	.0575	.0559	.0573	.0621	.0592	.0598	.0555
27	.0198	.0189	.0235	.0260	.0241	.0261	.0164
39	.3304	.3473	.3593	.3710	.3483	.3358	.2860
43	.0356	.0364	.0472	.0523	.0530	.0530	.0023
45	.5489	.5589	.5660	.5838	.5542	.5399	.5690
57	.0779	.0943	.0966	.0978	.0934	.0951	.1290
58	.6216	.6330	.6369	.6635	.6368	-	.6480
69	.0533	.0531	.0527	.0565	.0553	.0561	.0724
84	1.0	1.0	1.0	1.0	1.0	1.0	1.0
85	.0547	.0552	.0567	.0613	.0587	.0483	.0505

TABLE VII-5

NORMALIZED PURE COMPOUND DATA: HYDROGEN SULFIDE

Run Date: 11/20/74

MASS	RESPONSES						
	SCAN 1		SCAN 2		SCAN 3		API
33	.4120	.3916	.4104	.4127	.4053	.4118	.420
34	1.0	1.0	1.0	1.0	1.0	1.0	1.0
35	.0259	.0253	.0261	.0291	.0258	.0281	.025
36	.0431	.0464	.0436	.0455	.0421	.0439	.042

TABLE VII-6

NORMALIZED PURE COMPOUND DATA: BUTANE

Run Date: 11/20/74

MASS	RESPONSES						
	SCAN 1		SCAN 2		SCAN 3		API
25	.0057	.0057	.0056	.0055	.0055	.0053	.0046
25.5	.0044	.0044	.0043	.0042	.0044	.0043	.0036
26	.0609	.0602	.0606	.0599	.0612	.0602	.0617
27	.3542	.3542	.3539	.3539	.3676	-	.3710
29	.4503	.4264	.4501	-	.4527	-	.4420
30	.0130	.0111	.0099	.0107	.0098	.0105	.0098
36	.0014	-	.0013	-	.0012	-	.0008
37	.0101	.0110	.0100	.0105	.0104	.0112	.0101
38	.0181	.0191	.0179	.0188	.0183	.0191	.0189
39	.1130	.1108	.1138	.1109	.1152	.1134	.1250
40	.0149	.0161	.0149	.0156	.0149	.0155	.0163
41	.2778	.2824	.2790	.2775	.2816	.2790	.2780
42	.1192	.1183	.1195	.1168	.1211	.1217	.1220
43	1.0	1.0	1.0	1.0	1.0	1.0	1.0
44	.0397	.0394	.0395	.0382	.0397	.0384	.0333
49	.0045	.0045	.0043	.0042	.0045	.0044	.0040
50	.0126	.0139	.0126	.0131	.0127	.0136	.0129
51	.0099	.0110	.0097	.0103	.0097	.0103	.0105
52	.0025	.0027	.0023	.0023	.0024	.0024	.0026
53	.0070	.0070	.0069	.0068	.0066	.0065	.0074

TABLE VII-6 (cont'd)

BUTANE (continued)

MASS	RESPONSES						
	SCAN 1		SCAN 2		SCAN 3		API
54	.0018	.0020	.0019	.0019	.0018	.0018	.0019
55	.0089	.0097	.0088	.0092	.0089	.0098	.0093
56	.0070	.0070	.0071	.0069	.0074	.0081	.0072
57	.0244	.0258	.0244	.0250	.0248	.0253	.0242
58	.1101	.1078	.1106	.1080	.1117	-	.0123
59	.0053	.0053	.0052	.0051	.0052	.0050	.0054

TABLE VII-7

n-PENTANE DATA (RUN #35)

Mass 72/43 Peak Height Ratio	Time	Mass 56/43 Peak Height Ratio
.0806	047.0	.0217
.0796	072.0	.0232
.0773	072.0	.0223
.0805	095.0	.0232
.0791	095.0	.0225
.0829	122.5	.0223
.0817	150.5	.0225
.0802	150.5	.0219
.0802	Average	.0225

NOMENCLATURE

a coefficient in thiophene calibration

later, $1/\bar{C}_m K_A$, later, $1/K$, later, pore radius.

A $1/\bar{C}_m K_B$

a_m surface area of catalyst

b $1/\bar{C}_m$, later, K_T/K

B $L/\bar{C}_m$ for component B

b.p.s. base peak sensitivity

C_A concentration of component A, gm moles/liter

C_p heat capacity, cal/gm mole-^oC

$\bar{C}_m$ concentration of vacant sites, gm moles/gm catalyst.

C_0 concentration of all other components, gm moles/liter

C_o initial concentration, gm moles/liter

C_T Thiophene concentration, gm moles/liter

C_S hydrogen sulfide concentration, gm moles/liter

$\bar{C}_v$ concentration of vacant sites, gm moles/gm catalyst

C_4 butane concentration, gm moles/liter

C_4^- butene concentration, gm moles/liter

C_5 n-pentane concentration, gm moles/liter

c $(K_S-K_5)/K$

d_A molecular diameter of A, cm

D_{ij} diffusivity of i in j, cm^2/sec

frac.pk.ht. fractional peak height referenced to base peak.

G mass flux, gm/cm^2

ΔG_f^o Gibbs free energy of formation

h_j peak height at mass j

$-\Delta H$ Arrhenius activation energy, cal/gm mole

ΔH_f^o enthalpy of formation

j_D factor for mass transfer calculations

k overall rate constant, l/gm catalyst-minutes

k_{ai} adsorption rate constant for component i

K_{AC},etc adsorption equilibrium constant for component C in terms of concentration of component A, l/gm mole

k_{di} desorption rate constant for component i

K_i adsorption equilibrium constant for component I,l/gm mole

k_m mass transfer coefficient, cm/sec

k_o Arrhenius frequency factor,l/gm catalyst-min.

L volume-to-surface ratio

mw_A molecular weight of A

m exponent for number of adsorptio- sites in Langmuir-Hinshelwood kinetic expression

n1,n2.. integer constants

n ratio of number of sites for monolayer coverage by B to that for species A. Later, number of data points.

N_i stoichiometric coefficient for species I

Δn change in number of gram moles

P_i partial pressure of species i

pk.ht. peak height

q_r heat generation rate, cal/gram-sec

r rate of adsorption, desorption, or reaction

R gas constant

s^2 variance

S_g specific surface area, m^2/gm catalyst

T temperature, degrees C or K

t time, minutes

v_A volume of species A adsorbed, cm^3/gram catalyst

v_m volume of adsorbed gas equivalent to one monolayer

v_g void volume, cm^3/gm catalyst

V volume, liters or cubic centimeters

x_i mole fraction of species i

z compressibility factor, dimensionless

ZS "zero suppress" control reading, units

$[\gamma]$ mole fractions of products divided by reactants

η effectiveness factor, dimensionless

μ viscosity, centipoise

ξ Lennard-Jones parameter

σ Lennard-Jones parameter

μ viscosity parameter defined in appendix II

$[\Phi]$ fugacity coefficients of products divided by reactants

ϕ_m modified Thiele modulus, dimensionless

Ω collision integral

SUPERSCRIPTS

n1,n2 integer powers

bar adsorbed species

o standard state

SUBSCRIPTS

T thiophene

H hydrogen

4 butane

4- butene

5 n-pentane

S hydrogen sulfide

o initial value

j atomic mass number

i component i

LITERATURE CITED

1. Schuman, S. C., and H. Shalit, "Hydrodesulfurization," Catalyst Reviews 4, 245-317 (1970).

2. Schuit, G. C. A., and B. C. Gates, "Chemistry & Engineering of Catalytic Hydrodesulfurization," AIChE J. 19(3), p. 417-38 (1973).

3. Desikan, P., and C. H. Amberg, "Catalytic Hydrodesulfurization of Thiophene. IV. The Methylthiophenes," Can. J. Chem. 41(8), 1966-71 (1963).

4. Satterfield, Charles N., and G. W. Roberts, "Kinetics of Thiophene Hydrogenolysis on a Cobalt Molybdate Catalyst," AIChE J. 14(1), 159-64 (1968).

5. Takashi Watanabe, Etsuro Echigoya, and Kiyoshi Morikawa, "Kinetic Study of Catalytic Hydrodesulfurization of Benzene-Thiophene System," Sekiyu Gakkai Shi (10(12), 882-5 (1967). (Chem. Abstracts)

6. Kolboe, S., and C. H. Amberg, "Catalytic Hydrodesulfurization of Thiophene. VI. Comparisons Over Molybdenum Disulfide, Cobalt Molybdate, and Chromia Catalysts," Can.J.Chem. 44(22) 2623-30 (1966).

7. Desikan, P., and C. H. Amberg, "Catalytic Hydrodesulfurization of Thiophene. V. Hydrothiophenes. Selective Poisoning and Acidity of the Catalyst Surface," Can.J.Chem. 42(4), 843-50 (1964).

8. Mann, R.S., "Catalytic Hydrodesulfurization of Thiophene", Indian J. Technol 3(2), 53-6 (1965), (Chem Abstracts)

9. Hagenbach, Germain, Philippe Courty, and Bernard Delmon, "Catalytic Activity of Molybdenum and Cobalt in the Form of Sulfides in Various Reactions Involving Hydrotreatment in the Presence of Hydrogen Sulfide", C.R.Acad.Sci.Ser.C. 271(4), 783-6 (1970) (Chem Abstracts)

10. Delmon, B., G.Hagenbach, and P.Courty, "Catalytic Activity of Cobalt and Molybdenum Sulfide in Hydrogenolysis of Thiophene, Hydrogenation of Cyclohexene, and Isomerization of Cyclohexane", J.Catal. 23(2), 295-8 (1971)

11. Owens, P.J., and C.H.Amberg, "Hydrodesulfurization of Thiophene, II. Reactions Over a Chromia Catalyst", Can.J.Chem. 40, 941-6 (1962)

12. Safaev, A.S., A.V. Abdukadyrov, and S.A.Sultanov, Katal. Prerab. Uglevodorodn. Syr'ya #2, 24-7 (1967)(Chem Abstracts)

13. Katsuhiko Wakabayaski and Yoshio Orito, "Hydrodesulfurization of Organic Compounds Containing Sulfur. III. Relation Between The Pretreating Conditions of the Hydrodesulfurization Catalyst and Catalytic Activity", Kogyo Kagaku Zasshi 74(7), 1320-3 (1971)(Chem.Abs)

14. Seitaro Namba and Takamasa Aonuma, "Thiophene Hydrogenolysis Over a Desulfurization Catalyst. III. Active Center of Cobalt Molybdenum - Aluminum Oxide Catalyst in Thiophene Hydrogenolysis", Kogo Kagaku Zasshi 74(11), 2402-3 (1971)(Chem Abstracts)

15. Seitaro Namba, T. Aonuma, and T. Shiba, "Effect of Pre-Sulfurization of The Catalyst on the Hydrogenolysis of Thiophene", Kogyo Kagaku Zasshi 73(2), 272-5 (1970)(Chem Abstracts)

16. Kalechits, I.V., and Yuan-Keng Ying, "Kinetics of Simultaneous Hydrogenation of Olefin and Hydrogenolysis of Thiophene Over $CoMoO_4$-Al_2O_3 Catalyst", Zhur. Fiz. Khim.35, 501-8 (1961)(Chem.Abst)

17. Seitaro Namba and Takamasa Aonuma, "Thiophene Hydrogenolysis Over a Desulfurization Catalyst IV. Kinetic Study of Thiophene Hydrogenolysis Over Cobalt Molybdenum-Alumina Catalyst", Kogo Kagaku Zasshi 74(12), 2475-8 (1971)(Chem Abstracts)

18. Owens, P.J., and C.H.Amberg, "Hydrodesulfurization of Thiophene. III. Adsorptions of the Reactants and Products on Chromia", Can.J.Chem. 40, 947-56 (1962)

19. Fiezkhanov, F.A., G.M.Panchenkov, and I.M.Kolesnokov, Izv. Vysshikh Uchebn. Zavedenii, Nift i Gaz 7(9), 69-71 (1964)(Chem.Abst)

20. Fiezkhanov, F.A., G.M.Panchenov, and I.M.Kolesnokov, Zh.Fiz.Khim. 39(7), 1647-52 (1965)(Chem Abstracts)

21. Fiezkhanov, F.A., and O.M.Zolotukhina, Khim. Seraorgan., Soderzhahch. v Neft. i Nefteprod. 9, 310-16 (1972)(Chem Abstracts)

22. Safaev, A.S., A.V.Abdukadyrov, and S.A.Sultanov, Katal.Prerab. Uglevodorodn.Syr'a #1, 34-8 (1967)(Chem Abstracts)

23. Tarama, K., S.Teranishi, K.Hattori, and M.Higashi, "Hydrodesulfurization I. Hydrogenolysis of Thiophene in Benzene by a V_2O_3-MoO_2 Catalyst", Nenryo Kyokaishi 42, 42-51 (1963)(Chem Abstracts)

24. Lewis, W.E. and J.D.Paynter, "Effectiveness Factors in Batch Reactors", Chem. Eng. Sci. 26(9), 1357-60 (1971)

25. Roberts, George W., D.Sc. Thesis, Massachusetts Institute of Technology (1965)

26. Luft, Gerhard, R.Roemer, and H.Roeder, "Loop Reactors for Kinetic Measurements", Chem.Ing.Tech. 45(9-10), 596-602 (1973)

27. Simons, J.,"Mixing Studies in a Well-Stirred Gas-Solid Catalytic Reactor", Master of Science Thesis, Notre Dame Univ., Ind. (1963)

28. Berty, J.M., J.O.Hambrick, T.R.Malone, & D.S.Ullock,"Reactor for Vapor-Phase Catalytic Studies", Amer. Inst. Chem. Engrs. 64th Nat'l. Meet. preprint #42E, New Orleans, La. (1969)

29. Linck, Keith R., "A Study of the Hydrodenitrification of 2,6-Lutidine (A Preliminary Study of Nitrogen Removal from Shale Oil)", PhD Thesis, Colorado School of Mines, Golden, Colo. (1974)

30. Smith, J.M., Chemical Engineering Kinetics, 2nd Ed., McGraw-Hill, New York 477 (1970)

31. Ibid, p363-4

32. Ibid, p404-6

33. Ibid, chapts 9 and 10

34. Ibid, p432

35. Butt, J.B., H.Bliss, and C.A.Walker, "Rates of Reaction in a Recycling System--Dehydration of Ethanol and Diethyl/Ether over Alumina", in A.I.Ch.E. Journal 8:1, 42-7 (1962)

36. Korbach, P.F., and W.E.Stewart, "Kinetic and Equilibrium Studies of Benzene Hydrogenation in Batch Recycle Reactor, in I&EC Fundamentals 3:1, 24-7 (1964)

37. Bird, R.B., W.E.Stewart, and E.N.Lightfoot, Transport Phenomena, Wiley, New York, 508-13 (1960)

38. Ibid, p23-4

39. American Petroleum Institute, Mass Spectral Data, API Research Project 44, Nos. 67-71, 158, 454, 500

40. Lapidus, Leon, Digital Computation for Chemical Engineers, McGraw-Hill, New York, 335-7, 360-2 (1962)

41. Kittrell, J.R., "Mathematical Modeling of Chemical Reactions", in Advances in Chemical Engineering, vol. 8, Academic Press, New York, 98-183 (1970)

42. Ibid, p114-15

43. Johnson, Norman L., and F.C.Leone, Statistics and Experimental Design in Engineering and the Physical Sciences, vol. I, Wiley, New York, 382 (1964)

44. Ibid, p219-29

45. Draper, N.R., and H.Smith, Applied Regression Analysis, Wiley, New York, 270-2 (1966)

46. Prausnitz, J.M., C.A.Eckert, R.V.Orye, and J.P.O'Connell, "Computer Calculations for Multicomponent Vapor-Liquid Equilibria, Prentice-Hall, Englewood Cliffs, N.J., 165-6 (1967)

47. Daniel, Cuthbert, and Fred S. Wood, Fitting Equations to Data, Wiley, New York, 86-7 (1971)

48. Barron, Randall, Cryogenic Systems, McGraw-Hill, New York (1966)

49. Hougen, O.A., K.M.Watson and R.A.Ragatz, Chemical Process Principles, vol. I, Wiley, New York, 299 (1943, 1954)

50. Ibid, p512

51. Ibid, vol. II, p994

52. Hougen, O.A., and K.M.Watson, Chemical Process Principles, vol. III, Wiley, New York (1947)

53. Hodgman, Charles D., Ed., Handbook of Chemistry and Physics, 44th ed., Chemical Rubber Publishing Co., Cleveland (1963)

54. Reid, Robert C., and Thomas K. Sherwood, The Properties of Gases and Liquids, 2nd ed., McGraw-Hill, New York (1966)

55. Ibid, p182-6

56. Ibid, p236-42

57. Ibid, p586-611

58. Satterfield, C.N., Mass Transfer in Heterogeneous Catalysis, M.I.T.Press, Cambridge, Mass., 170 (1970)

59. Ibid, p33-41, 157

60. Ibid, p47-54

61. Hirschfelder, J.O., C.F.Curtis, and R.B.Bird, Molecular Theory of Gases and Liquids, Wiley, New York, 1110-12 (1954)

62. Satterfield, C.N., and T.K.Sherwood, The Role of Diffusion in Catalysis, Addison-Wesley, Reading, Mass., 9 (1963)

63. Van Winkle, Matthew, Distillation, McGraw-Hill, New York, 88-104 (1967)

64. Himmelblau, D.M., Basic Principles and Calculations in Chemical Engineering, Prentice-Hall, Englewood Cliffs, N.J., 418-19 (1962)

65. Smith, J.M., and H.C.Van Ness, Introduction to Chemical Engineering Thermodynamics, McGraw-Hill, New York, 416-7(1959)

66. Churchill, Stuart W., The Interpretation and Use of Rate Data, McGraw-Hill, New York, 306-9 (1974)

67. Walpole, Ronald E., and Raymond H. Myers, Probability and Statistics for Engineers and Scientists, Macmillan, New York, chapts 8 and 9 (1972)

68. Hunter, W.G., and J.R.Kittrell, Statistical Methodology for Chemical Reaction Modeling, A.I.Ch.E. Today Series, New York, sec. II (1967)

69. Hougen, O.A., K.M.Watson, & R.A.Ragatz, Chemical Process Principles Charts, 3rd ed., Wiley, New York (1964)

70. American Cyanamid Co., Refining Chemicals Dept., "Aero HDS Hydrogen Treating Catalysts", Bound Brook, N.J. (1969)

71. Bennett, Carl A., and Norman L. Franklin, Statistical Analysis in Chemistry and the Chemical Industry, Wiley, New York, 197-200 (1954)

72. Thomas, Charles L., Catalytic Processes and Proven Processes, Academic Press, New York, 166,169 (1970)

73. Obolentsev, R.D., A.R.Kuzyev, and G.M.Mikheev, "Kinetics of the Catalytic Hydrogenolysis of Organic Compounds of Bivalent S, IV", Khim. Seraorgan., Soderzhahch. v Neft. i Nefteprod., Akad. Nauk SSSR, Bashkirsk. Filial 6, 331-7 (1964)(Chem Abstracts)

74. Consolidated Electrodynamics Corporation, CEC Model 21-130 Mass Spectrometer Operation and Maintenance Manual, CEC, Pasadena (1961)

75. Carnahan, Brice, H.A.Luther, and James O. Wilkes, Applied Numerical Analysis, Wiley, New York, 290-1 (1969)

76. Garin, Francois, & Francois G. Gault, "The Mechanisms of Hydrogenolysis and Isomerization of Hydrocarbons on Metals. VIII. Isomerization of 13_C Labeled Pentanes on a 10% Pt-Al_2O_3 Catalyst," JACS 97(16), 4466-76 (1975).

77. Union Carbide Corp., Isotherm Data Sheet #203, Hydrogen Sulfide Adsorption (undated).

78. Barnard, G. P., Modern Mass Spectrometry, Institute of Physics, London, 1953, p 192-230.

79. Ibid, p 112.

80. Kieran, P., and C. Kemball, "Catalytic Reactions of Ethyl

Mercaptan on Disulfides of Molybdenum and Tungsten," Jour. Catal. 4, 380-393 (1965).

81. Young, D. M. and A. D. Crowell, Physical Adsorption of Gases, Buttersworth, London (1962), p 378-80.

82. Tomskine, F. C., and D. M. Young, Trans. Faraday Soc. 47(88), (1951), in ref. (81) above.

83. Lipsch, J. M. J. G., "The $CoO-MoO_3-Al_2O_3$ Catalyst," reprinted from the PhD Thesis by Climax Molybdenum Co., Ltd., Villers House, 41/47 Strand, London, England, undated.

84. Mitchell, P. C. H., "The Chemistry of Some Hydrodesulfurization Catalysts Containing Molybdenum," Climax Molybdenum Co., Ltd., (1967).

85. Ashley, J. H., and P. C. H. Mitchell, "Cobalt-Molybdenum-Alumina Hydrodesulfurization Catalysts. Part 1. A Spectroscopic and Magnetic Study of the Fresh Catalyst and Model Compounds," Jour. Chem. Soc. (A), 1968, reprinted by Climax Molybdenum Co., Ltd.

86. Ashley, J. H., and P. C. H. Mitchell, "Cobalt-Molybdenum-Alumina Hydrodesulfurization Catalysts. Part II. Incorporation of Cobalt (II) and Molybdenum (VI) into γ-Alumina," Jour. Chem. Soc. (A), 1969, reprinted by Climax Molybdenum Co., Ltd.

87. Lipsch, J. M. J. G., and Schuit, G. C. A., "The $CoO-MoO_3-Al_2O_3$ Catalyst. I. Cobalt Molybdate and the Cobalt Oxide Molybdenum Oxide System," Jour. Catal. 15, 163-173 (1969).

88. Lipsch, J. M. J. G., and Schuit, G. C. A., "The $CoO-MoO_3-Al_2O_3$ Catalyst. II. The Structure of the Catalyst," Jour. Catal. 15, 174-178 (1969).

89. Lipsch, J. M. J. G., and Schuit, G. C. A., "The $CoO-MoO_3-Al_2O_3$ Catalyst. III. Catalytic Properties," Jour. Catal. 15, 179-189 (1969).

90. Amberg, C. H., "Molybdenum in Hydrodesulfurization Catalysts," Climax 1st International Conf. on Chemistry in Uses of Molybdenum, Univ. of Reading, England (Sept. 1963).

91. Griffith, R. H., J. D. F. Marsh and W. B. S. Newling, "The Catalytic Decomposition of Simple Heterocyclic Compounds. II. Reaction Kinetics and Mechanism," Proc. Royal Soc. (A), 137, p 194-201, 1949.

92. Hoog, H., J. Inst. Petroleum, 1950, 36, p 738, quoted in #84 above.

93. Komarewsky, V. I. and E. A. Knaggs, "Hydrogenolysis of Thiophene Over Vanadium Oxide," I&EC, 43(6), 1414-18 (1951).

94. Pease, R. H., W. B. Kreighton, "Removal of Thiophene from Benzene by Catalytic Hydrogenation," I&EC 25 , p 1012-13 (Sept. 1933).

95. Owens, P. J., and C. H. Amberg, "Thiophene Desulfurization by a Microreactor Technique," Advances in Chemistry Series #33, 182-198,(1961).

96. Van Looy, H., and G. Limodo, Comp. Rend. Congr. Intern. Chem. Ind. 31e, Liege (1958); Ind. Chem. Belge., Suppl. 1, 645 (1959).(Quoted in several references above)

97. Kirsh, F. W., H. Heinemann, and D. H. Stevenson, I&EC, 49, 646 (1957).

98. Ozimek, Barbara, and Bohdan Radomyski, "Kinetics of Thiophene Hydrogenolysis on a Cobalt-Molybdenum Catalyst," Chem. Stosow, 1975, 19(1), 97-112 (Polish), reviewed in Chem. Abstracts 83:177857Z.

99. Samigov, K. A., U. B. Khakimov, and G. Sh. Talipov, "Study of The Interaction of Thiophene with The Surface of γ-Aluminum Oxide," Tezisy Dokl. Vses. Semin. "Primen. Opt. Spertrosk. Adsorbtsii Katal, 3rd," 1974, p 24-5 (Russian) in Chem. Abstracts 85:52129y.

100. Dollimore, David, A. Galwey, G. Rickett, "Adsorption and Reactivity of Some Sulfur-Containing Compounds on a Mixed-Oxide Cobalt-Molybdate Type Catalyst," J. Chem. Phys., Phys. Chem., Biol. 1975, 72(9), 1059-64 (English), Chem. Abstracts 84:35784x.

101. Mikovsky, R. J., A. J. Silvestri, and H. Heinemann, "On the Mechanism of Thiophene Desulfurization," J. Catal. 34, 324-326 (1974).

102. Kolboe, S., Can. J. Chem. 47, 352 (1969).

103. Griffith, R. H., "Advances in Catalysis (1)," p 106-12, (1948), Academic Press.

104. Wakabayayashi, Katsuhiko; Abe, Hiromitsu; Orito, Yoshio; Kogyo Kagaku Zasshi, 1971, 74(7), 1317-19 (Japanese), reviewed in Chem. Abstracts 75:98375x.

105. Wakabayashi, Katsuhiko; Orito, Yoshio; Kogyo Kagaku Zasshi, 1974, 74(7), 1320-3 (Japanese), in Chem. Abstracts 75:98379b.

106. Abidov, B., Yunusou, M. P., Tezisy Dokl. Nauchn. Sess. Khm. Teknol. Org. Soedin. Sery Sernistyky Neftei, 13th (1974), p. 313 (Russian) in Chem. Abstracts 85:176344j.

107. Mann, R. S., J. Chem. Soc. (1964), 1531.

108. Satterfield, C. N., M. Modell, and J. F. Mayer, "In teractions Between Catalytic Hydrodesulfurization of Thiophene and Hydrodenitritication of Pyridene," AIChEJ 21(6), 1100-07, 1975.

109. Morooka, S., and C. E. Hamrin, "Desulfurization of Model Coal Sulfur Compounds by Coal Mineral Matter and a Cobalt-Molybdate Catalyst-I., Thiophene," Chem. Engr. Sci. 32, p. 125-33 (1977).

110. Kittrell, J. R., W. G. Hunter, and C. C. Watson, "Non-Linear Least Squares Analysis of Catalytic Rate Models," AIChEJ 11(6), p. 1051-57 (1965).

111. Boag, I. F., D. W. Bacon, and J. Downie, "The Analysis of Data From Recirculation Reactors," Can. J. Chem. Angr. 54 (Feb./Mar.), p. 107-10 (1976).

112. Pirjamali, M., H. Liubjerg, J. Villadsen, Chem. Eng. Sci. 1973, 28 (1), p. 328-32, "Correction Procedure for Interparticle Gradients in a Laboratory Catalytic Recirculation Reactor."

113. Siddiqui, R. A., and C. H. Amberg, unpublished work, 1962, mentioned in Amberg, C. H., chapt. 30 of The Solid-Gas Interface, E. A. Flood (ed.), Marcel Dekker, Inc., New York, p. 889 (1967).

114. Massoth, F. E., and S. W. Cowley, "A Stirred Flow Microbalance Reactor for Catalyst Studies," ISEC Fund. 15 (3), 218-23 (1976).

115. Tamaru, Kenzi, "Adsorption Measurements During Surface Catalysis," Advances in Catalysis (15), 65-90 (1964), Academic Press, New York.

116. Noto, Y., K. Fukuda, T. Onishe, and K. Tamaru, "Mechanism and Selectivity of Formic Acid Decomposition Over Metal Oxides. A Dynamic Treatment of Chemisorbed Sieves During the Course of the Reaction," IV. Intl. Cong. on Catalysis, Moscow (1968), preprint 37.

117. Hsu, S. M., and R. L. Kabel, "A Batch Reactor to Study Concomitant Adsorption and Heterogeneous Catalysis," J. Catal. 33, 74-82 (1974).

118. Semenchenko, V. K., N. V. Luznetsova, I. V. Israilov, "Surface Phenomena in Solutions in the Presence of Chemical Reactions. III. Characteristics of the Surface Layer with Volume Concentrations," Zh. Fiz. Khm. 48 (5), p. 1272-4 (1974), Russian, in Chem. Abstracts 81:111686v.

119. Myers, A. L. and J. M. Prausnitz, "Thermodynamics of Mixed-Gas Adsorption," AIChEJ 11 (1), p. 121-7 (1965).

120. Baker, B. G., "Configurational Entropy of Adsorption of Large Atoms," Jour. Chem. Phys. 45(7), 2694-7 (1966).

121. Welsch, R. J., and J. B. Butt, "Monte Carlo Simulation of The Hydrogenolysis of Thiophene with Cobalt-Molybdate Catalyst," Chem. Eng. Comm. 1, 155 (1973).

122. Thermodynamic Research Center Data Project, Texas A&M University, p. 14-2-h, Dec. 31, 1973, and P. 23-2-(1/200)-h, Oct. 31, 1970.

123. Roberts, G. W. and C. N. Satterfield, "Effectiveness Factor for Porous Catalysts," I&EC Fundamentals 4(3), p. 288-93 (1965).

124. Kaminski, M. and Z. Szklarska-Smialowska, "Adsorption of Thiophene Derivatives on Steel in Sulfuric Acid Solutions," Corrosion Science 13(7), p. 557-65 (1973).

125. Carberry, James J., Chemical and Catalytic Reaction Engineering, McGraw-Hill, New York (1976), p. 388-92.